New insights in the biosynthesis and metabolism of carnitine

van Vlies, N.

Publication date
2007
Document Version
Final published version

New insights in the biosynthesis and metabolism of carnitine

Naomi van Vlies

2007

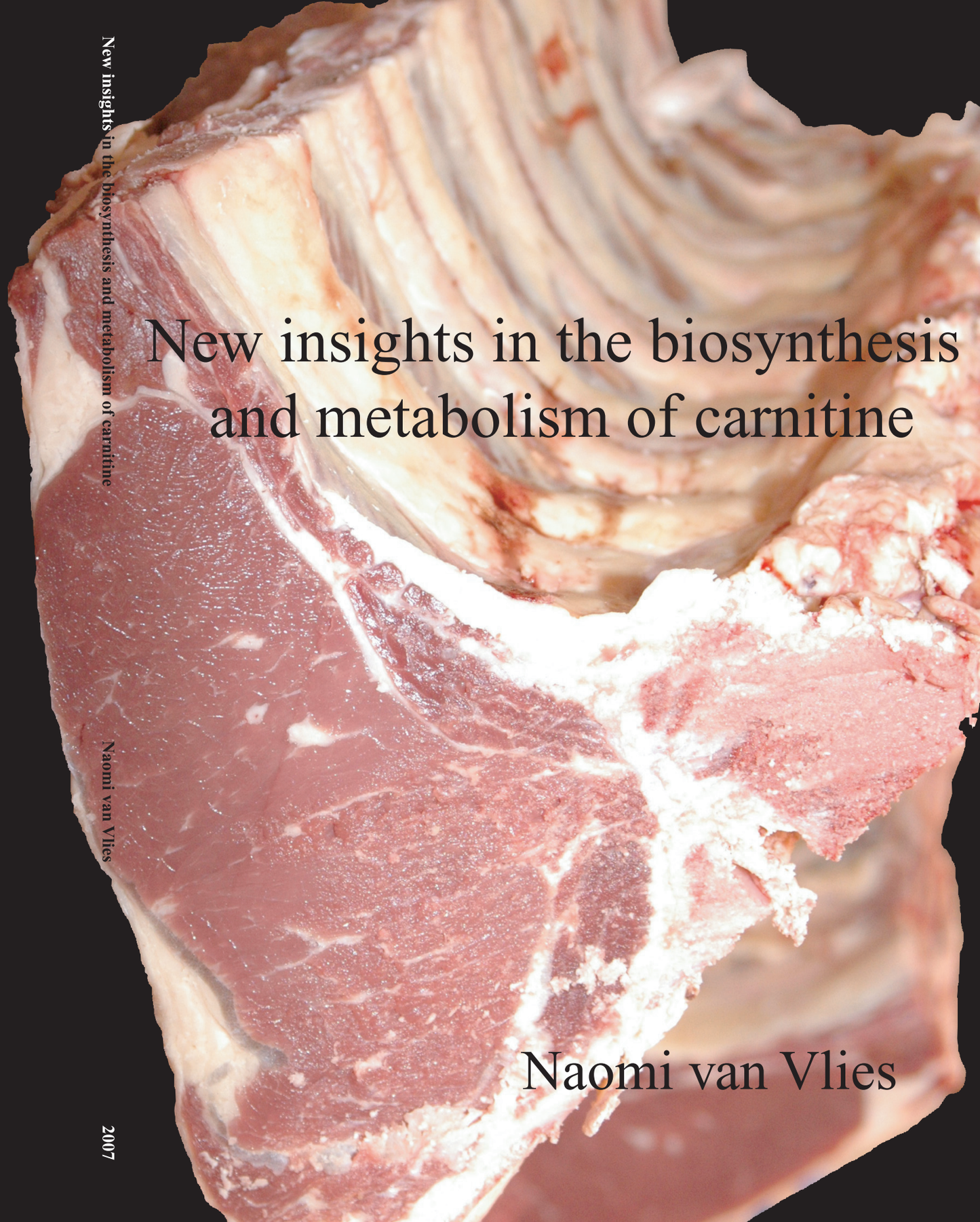

New insights in the biosynthesis and metabolism of carnitine

Naomi van Vlies

New insights in the biosynthesis and metabolism of carnitine

New insights in the biosynthesis and metabolism of carnitine

ACADEMISCH PROEFSCHRIFT

ter verkrijging van de graad van doctor
aan de Universiteit van Amsterdam
op gezag van de Rector Magnificus
Prof. Dr. J.W. Zwemmer
ten overstaan van een door het
college voor promoties ingestelde commissie,
in het openbaar te verdedigen
in de Aula der Universiteit

op dinsdag 22 mei 2007, te 14.00 uur

door

Naomi van Vlies

geboren te Amsterdam

Promotiecommissie:

promotor:	Prof. Dr. R.J.A. Wanders
co-promotor:	Dr. F.M.Vaz
overige leden:	Prof. Dr. C.J.F. van Noorden
	Prof. Dr. J. Glatz
	Prof. Dr. R.P.J. Oude Elferink
	Prof. Dr. F.A. Wijburg
	Dr. S. Kersten
	Dr. B. Distel

Faculteit der Geneeskunde

The work described in this thesis was carried out at the laboratory of Genetic Metabolic Diseases, Departments of Clinical Chemistry and Pediatrics, Academic Medical Center, University of Amsterdam, The Netherlands.

Table of contents

Abbreviations

γ-BB	4-trimethylaminobutyric acid
γ-BBD	4-trimethylaminobutyric acid dioxygenase
CACT	carnitine/acyl-carnitine transporter
CAT	carnitine acetyltransferase.
CHO	Chinese hamster ovary
CoASH	coenzyme A
CPTI	carnitine palmitoyl transferase I
CPTII	carnitine palmitoyl transferase II
DMSO	dimethylsulfoxide
DTNB	dithiobisnitrobenzoic acid
EDTA	ethylenediaminetetraacetic acid
ETF	electron-transferring flavoprotein
GABA	4-aminobutyric acid
HPLC	high performance liquid chromatography
HTML	3-hydroxy-6-N-trimethyllysine
IgG	immunoglobulin G
JVS	juvenile visceral steatosis
LCAD	long-chain acyl-CoA dehydrogenase
LCHAD	long-chain 3-hydroxyl-acyl-CoA dehydrogenase
LCHYD	long-chain enoyl-CoA hydratase
LCT	long-chain-3-keto-acyl-CoA thiolase
MCAD	medium-chain acyl-CoA dehydrogenase
MCT	medium-chain-3-keto-acyl-CoA thiolase
MOPS	3-N-morpholinopropanesulfonic acid
MS	mass spectrometry
NEM	N-ethylmaleimide
ORF	open reading frame
PBS	phosphate buffered saline
PCR	polymerase chain reaction
PMSF	phenylmethyl sulfonyl fluoride
PPARα	peroxisome proliferator activated receptor α
SCAD	short-chain acyl-CoA dehydrogenase
SCHAD	short-chain 3-hydroxyl-acyl-CoA dehydrogenase
SCHYD	short-chain enoyl-CoA hydratase
SCT	short-chain 3-keto-acyl-CoA thiolase
SDS-PAGE	sodium dodecyl sulfate polyacrylamide gel electrophoresis
SEM	sucrose-EDTA-MOPS
TMABA	4-trimethylaminobutyraldehyde
TMABA-DH	4-trimethylaminobutyraldehyde dehydrogenase
TML	6-N-trimethyllysine
TMLD	6-N-trimethyllysine dioxigenase
VLCAD	very long-chain acyl-CoA dehydrogenase

Chapter 1

Introduction

Carnitine

Functions of carnitine

Carnitine (3-hydroxy-4-N,N,N-trimethylaminobutyrate) plays an essential role in fatty acid metabolism. While medium- and short-chain fatty acids enter the mitochondrial matrix, where β-oxidation takes place, as free acids, long-chain acyl-CoAs must first be converted into their corresponding carnitine-esters in order to cross the inner mitochondrial membrane [1, 2]. Apart from its involvement in the transport of long-chain fatty acids, carnitine is also used to transport peroxisomal β-oxidation products to the mitochondria, to excrete accumulating acyl-groups and to modulate the level of free CoA [3-5].

The carnitine biosynthesis pathway

Carnitine is present in most animals, as well as in several plants and microorganisms. Mammals acquire carnitine both from the diet (meat, fish and dairy products) and through endogenous synthesis [5]. Carnitine is ultimately synthesized from the amino acids lysine and methionine. In some proteins (*i.e.* calmodulin, histones, myosin and actin), lysine residues are trimethylated on the 6-amino group by specific methyltransferases, which use S-adenosyl methionine as methyl donor [6]. After lysosomal degradation of these proteins, free 6-N-trimethyllysine (TML) becomes available for carnitine biosynthesis (figure 1). First, TML is hydroxylated by the enzyme TML-dioxygenase (TMLD) to 3-hydroxy-6-N-trimethyllysine (HTML). HTML is subsequently cleaved by a specific aldolase to yield 4-trimethylaminobutyraldehyde (TMABA), which is oxidized by TMABA-dehydrogenase (TMABA-DH) to 4-trimethylaminobutyric acid (γ-butyrobetaine, γ-BB). Finally, γ-BB is hydroxylated to carnitine by γ-BB dioxygenase (γ-BBD) [5, 7, 8].

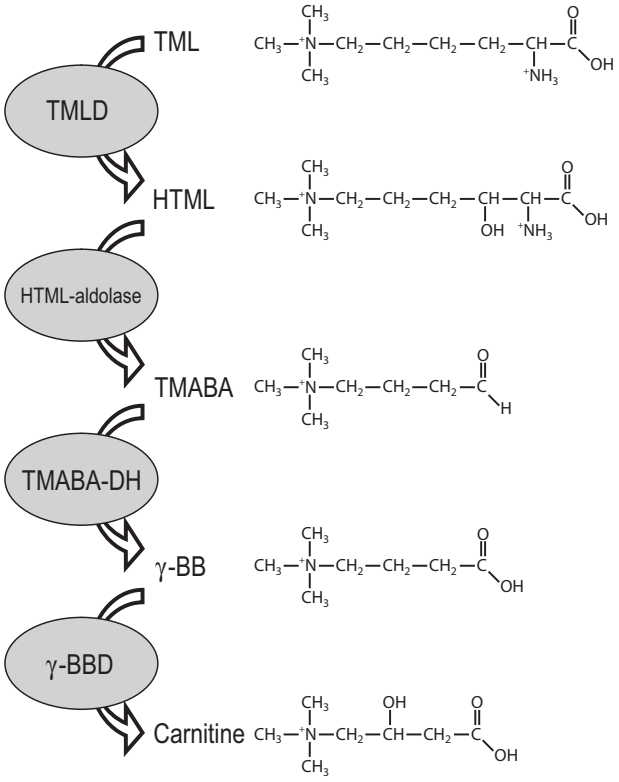

Figure 1. The carnitine biosynthesis pathway. 6-N-trimethyllysine (TML) is hydroxylated by TML-dioxygenase (TMLD) to 3-hydroxy-6-N-trimethyllysine (HTML), which is converted to 4-trimethylaminobutyraldehyde (TMABA) by HTML-aldolase. TMABA-dehydrogenase (TMABA-DH) oxidizes TMABA to 4-trimethylaminobutyric acid (γ-butyrobetaine, γ-BB), which is hydroxylated to carnitine by γ-BB dioxygenase (γ-BBD) [5].

Carnitine biosynthesis in rat

Tissues demonstrate differences both in enzyme activity and in the capacity to transport carnitine biosynthesis metabolites. In rat, the activity of the first three enzymes of the carnitine biosynthesis pathway can be detected in all investigated tissues, but liver and kidney contain the highest enzyme activities [9-12]. The last enzyme, γ-BBD, is expressed only in liver and testis, making these the only tissues capable of complete carnitine synthesis in the rat [10, 13-15]. In contrast to normal rats, however, no labeled carnitine was found in either liver, plasma, heart or skeletal muscle of hepatectomized rats which were given labeled γ-BB. This suggests that the carnitine synthesized in testis is used in this tissue only and that this does not contribute significantly to systemic carnitine stores [16].

When rats receive exogenous TML, the majority is taken up by the kidneys and converted into γ-BB, which is subsequently released into the circulation, taken up by the liver and converted into carnitine [17]. In contrast to kidney, most tissues take up TML and HTML very poorly [17, 18]. Therefore, Rebouche [19] proposed that, in the rat, part of the intracellular TML is converted to γ-BB in the tissue of origin and the remainder is released into the circulation to be metabolized by the kidneys. Because the metabolism of exogenously administered TML most likely differs profoundly from that of TML produced within tissues and the metabolism of endogenous TML is difficult to investigate in model systems, it remains unclear what amount of TML is converted into γ-BB by the kidneys and how much is converted in the tissue of origin.

Because γ-BBD is not expressed in extrahepatic tissues (except testis) the γ-BB produced in these tissues must be transferred to the liver for conversion into carnitine. At least two hepatic transport systems for γ-BB exist. Christiansen and Bremer have reported a low-affinity γ-BB transporter (K_m value of approximately 500 μM) in rat hepatocytes. This transporter was shown to have a 10-fold higher K_m value for carnitine (5.6 mM) than for γ-BB, but γ-BB transport could be inhibited by carnitine [20]. A high-affinity γ-BB transporter (K_m value of approximately 5 μM), however, was described by Berardi *et al*. [21]. They also showed that γ-BB transport was stimulated by sodium and chloride ions and transport could be inhibited by propionyl-carnitine, but surprisingly not by carnitine or acetyl-carnitine.

After conversion of γ-BB into carnitine, carnitine is released into the circulation mostly as acetyl-carnitine by a yet unknown mechanism [22]. Extra-hepatic tissues take up carnitine from the plasma via the Na^+-dependent carnitine transporter OCTN2. This transporter also mediates the intestinal uptake and renal reabsorption of both γ-BB and carnitine [5].

Carnitine biosynthesis in man

In man, all tissues contain the first three enzymes of the carnitine biosynthesis pathway and, as in rat, the highest activity is found in liver and kidney [23]. In contrast to rat, however, γ-BBD activity is detected in liver but also in brain (at approximately 50% of the activity as found in liver) and kidney, which shows even more γ-BBD activity (4-fold) than liver [23-25]. While γ-BBD activity is not found in rat, guinea pig and mouse kidney, it is present in the kidneys of hamsters, rabbits, dogs, cats, humans and several monkeys) [19]. It remains unclear what causes the difference in γ-BBD expression between rat, man and other mammals.

When humans ingest TML, in contrast to rat, most is excreted unchanged in the urine and only a small part is converted into carnitine [26, 27]. Intracellular TML is therefore believed to be converted in the tissue of origin into γ-BB, which is then released into the circulation, taken up by the kidneys as well as liver (and brain), and converted into carnitine. Tissues that do not express γ-BBD take up carnitine from the plasma via OCTN2 [5]. The body carnitine content is mainly regulated by renal carnitine reabsorption. The efficiency of carnitine

reabsorption depends on carnitine intake. When carnitine intake is low, carnitine is reabsorbed more efficiently [28], possibly by upregulation of OCTN2. Defects in OCTN2 lead to primary carnitine deficiency [29], which is described in a following section.

Mitochondrial β-Oxidation

Mitochondrial fatty acid transport; the carnitine shuttle

Fatty acid oxidation is very important in cellular energy homeostasis, especially during fasting or when the energy demand is increased (during exercise or stress). Before long-chain fatty acids can be metabolized by the mitochondrial β-oxidation system, they must be transported into the mitochondrial matrix [30, 31]. Long-chain fatty acids are activated outside the mitochondria by one of the many long-chain acyl-CoA synthetases [32]. Acyl-CoAs cannot cross the inner mitochondrial membrane but must first be trans-esterified to carnitine by Carnitine Palmitoyl Transferase I (CPTI), on the mitochondrial outer membrane (figure 2). Subsequently, the resulting acyl-carnitines are transported across the mitochondrial inner membrane by the Carnitine/Acyl-Carnitine Transporter (CACT). Finally, Carnitine Palmitoyl Transferase II (CPTII) reconverts the acyl-carnitines into their CoA-esters and the acyl-CoAs can enter the β-oxidation pathway. Carnitine is transported back into the cytosol either as free carnitine to import another acyl-group or it can be converted into a new acyl-carnitine by CPTII or Carnitine Acetyl Transferase (CAT) and can be exported from the mitochondrial matrix, out of the cell, followed by excretion from the body via either urine or bile [1, 2].

Mitochondrial β-oxidation

Once in the mitochondria, acyl-CoAs are degraded into acetyl-CoA via a 4-step pathway called β-oxidation (figure 3), with multiple enzymes for each of the four steps. First, an acyl-CoA-ester is dehydrogenated to yield a trans-2-enoyl-CoA. This is followed by hydratation of the double bond. In the third step the resulting 3-hydroxy-acyl-CoA is dehydrogenated to 3-keto-acyl-CoA. Finally, thiolytic cleavage of the 3-keto-acyl-CoA produces a 2-carbon chain-shortened acyl-CoA and acetyl-CoA. The electrons generated in the first and third reaction are fed into the respiratory chain via the ETF/ETF dehydrogenase system and NAD^+, respectively. The produced acetyl-CoA can enter the Krebs cycle or can be used for ketone body formation in the liver or kidney [30, 31].

Mitochondrial β-oxidation enzymes

For each β-oxidation step multiple chain-length specific enzymes exist (figure 2). The first reaction is catalyzed either by short-chain acyl-CoA dehydrogenase (SCAD, for C4 and C6 acyl-CoAs), medium-chain acyl-CoA dehydrogenase (MCAD, for C4 to C12 acyl-CoAs), long-chain acyl-CoA dehydrogenase (LCAD), which has activity towards C8 to C20 acyl-CoAs, or very long-chain acyl-CoA dehydrogenase (VLCAD, for C12 to C24 acyl-CoAs) [30]. The precise role of LCAD in mitochondrial β-oxidation, however, is unclear. Apart from straight-chain substrates LCAD has been shown to handle branched-chain fatty acids (such as 2,6-dimethylheptanoyl-CoA, 2-methyldecanoyl-CoA, 2-methylpentadecanoyl-CoA and 2-methyl-hexadecanoyl-CoA) and certain polyunsaturated acyl-CoAs (such as docosahexaenoic acid, arachidonic acid, 4,7,10-cis-hexadecatrienoic acid, 5-cis-tetradecenoic acid, and 4-cis-decenoic acid) [33-35].

For both the second and the third step there are only two separate enzymes. Short-chain enoyl-CoA hydratase (SCHYD), also called crotonase, and short-chain 3-hydroxy-acyl-CoA dehydrogenase (SCHAD) have activity towards fatty acids with chain-lengths up to 10 carbon atoms. Long-chain enoyl-CoA hydratase (LCHYD) and long-chain 3-hydroxyl-acyl-CoA

dehydrogenase (LCHAD) handle fatty acids with 8 or more carbon atoms [30, 31, 36]. There are three 3-keto-acyl-CoA thiolases: the long-chain- (LCT), medium-chain- (MCT) and the short-chain 3-keto-acyl-CoA thiolase (SCT) [30, 31].

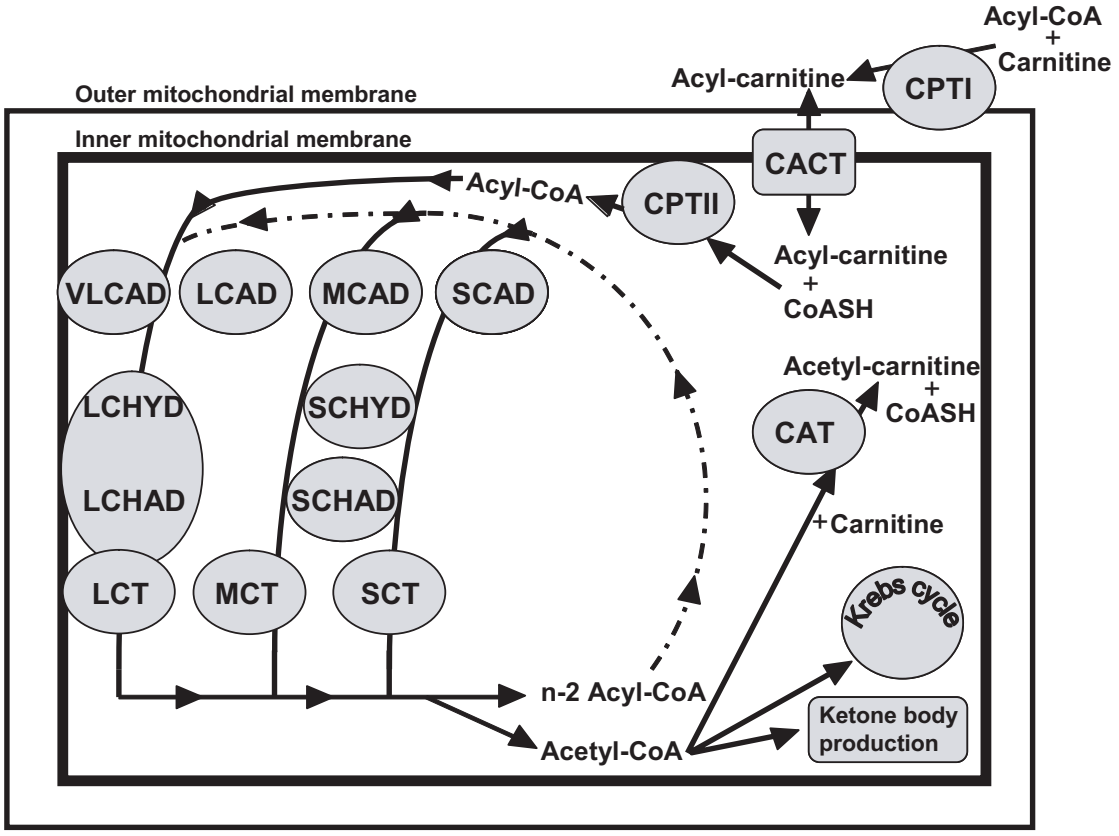

Figure 2. Mitochondrial fatty acid transport and β-oxidation.
Long-chain acyls-CoAs are converted into a carnitine-ester by carnitine palmitoyl transferase I (CPTI) and transported over the mitochondrial inner membrane by the carnitine/acyl-carnitine transporter (CACT). Carnitine palmitoyl transferase II (CPTII) reconverts the acyl-carnitines into their CoA-esters, which can enter the β-oxidation pathway. Carnitine is transported back into the cytosol either as free carnitine or it can be converted into a new acyl-carnitine by CPTII or carnitine acetyl transferase (CAT) to exported the acyl-group from the mitochondrial matrix.
The first step of the β-oxidation pathway is catalyzed either by very long-chain acyl-CoA dehydrogenase (VLCAD), medium-chain acyl-CoA dehydrogenase (MCAD) or short-chain acyl-CoA dehydrogenase (SCAD). The precise role of long-chain acyl-CoA dehydrogenase (LCAD) is still unclear. The next reaction is catalyzed by either short-chain enoyl-CoA hydratase (SCHYD) or long-chain enoyl-CoA hydratase (LCHYD), which together with long-chain 3-hydroxyl-acyl-CoA dehydrogenase (LCHAD) constitutes the α-subunit of the mitochondrial trifuncional protein. The β-subunit of this enzyme complex contains the long-chain-3-keto-acyl-CoA thiolase (LCT) activity. The third reaction is catalized by LCHAD or short-chain 3-hydroxyl-acyl-CoA dehydrogenase (SCHAD). Finally, a 2-carbon chain-shortened acyl-CoA and an acetyl-CoA are produced by either LCT, medium-chain-3-keto-acyl-CoA thiolase (MCT) or short-chain 3-keto-acyl-CoA thiolase (SCT) and the new acyl-CoA can enter another round of β-oxidation [30, 31].

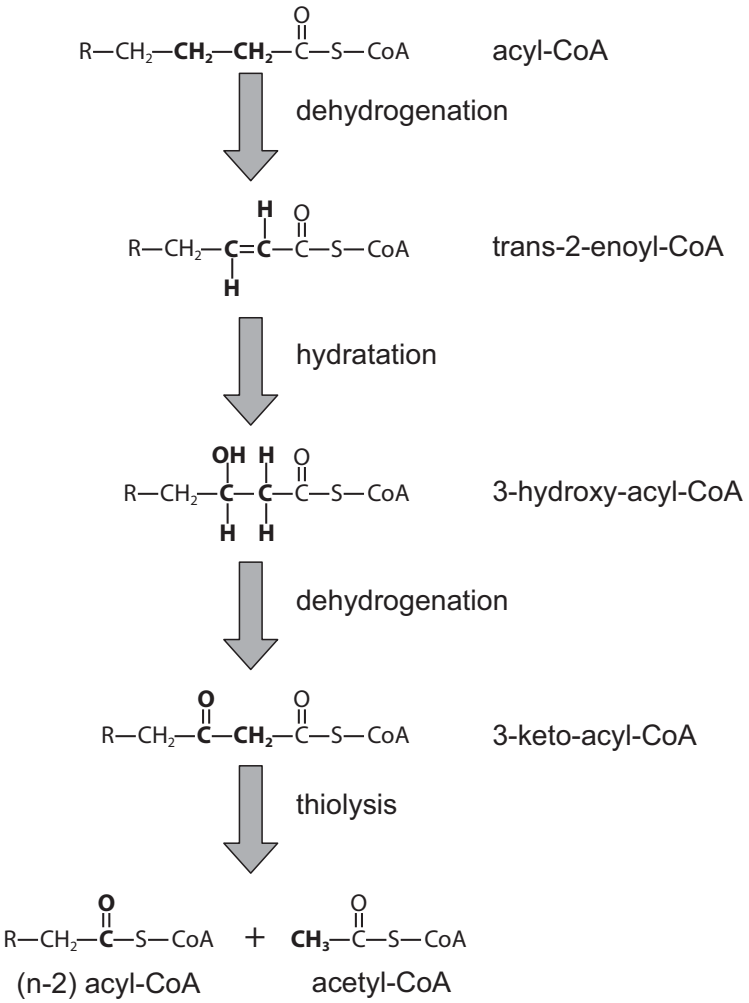

Figure 3. The mitochondrial β-oxidation pathway.
An acyl-CoA-ester is dehydrogenated to yield a trans-2-enoyl-CoA, which is followed by hydratation of the double bond. Next, the resulting 3-hydroxy-acyl-CoA is dehydrogenated to 3-keto-acyl-CoA and subsequent thiolytic cleavage produces a 2-carbon chain-shortened acyl-CoA and acetyl-CoA [30, 31].

Carnitine metabolism and β-oxidation: mouse models of human disease

Numerous human genetic deficiencies affecting the different enzymes and transporters of the β-oxidation pathway have been described [31]. The precise pathogenesis of some of these disorders is still mostly unclear. Recently, several mouse models for human mitochondrial β-oxidation defects have been developed, which can be used to elucidate the disease mechanisms which underlie these defects.

Primary carnitine deficiency and the OCTN2-/- mouse model.
Human primary carnitine deficiency is caused by mutations in the gene coding for the plasma membrane carnitine transporter OCTN2. As a result, dietary carnitine is taken up poorly and urinary carnitine is not reabsorbed by the kidney which leads to severely decreased levels of carnitine in plasma and tissues. Patients typically present in infancy with episodic hypoketotic hypoglycemic encephalopathy, progressive cardiomyopathy and failure to thrive [29].
In 1988, Koizumi and colleagues [37] described a C3H.OH strain of mice in which microvesicular fatty infiltration of viscera was inherited in an autosomal recessive manner. These mice also displayed severe lipid accumulation in the liver, hypoglycemia, hyperammonemia, cardiac hypertrophy, growth retardation and systemic carnitine deficiency. These symptoms were shown to be caused by diminished intestinal carnitine absorption and renal reabsorption, due to a missense mutation in the OCTN2 gene [38, 39]. Because both the

affected gene as well as the symptoms in this mouse are similar to that of human patients, this mouse is used as a model for human systemic carnitine deficiency [29].

VLCAD-deficiency and the (V)LCAD-/- mouse model.
Human VLCAD deficiency is a severe condition involving cardiomyopathy, fasting hypoketotic hypoglycemia, Reye-like disease and even sudden unexpected death [31].
In the late 1990s two mouse models for human VLCAD deficiency were developed. In contrast to the human disease, murine VLCAD deficiency is characterized by relatively mild symptoms: mild hepatic steatosis, mild cardiac fatty change in response to fasting and cold intolerance [40]. In 1998, Kurtz *et al*. [41] created an LCAD-deficient mouse, which does show symptoms similar to human VLCAD deficiency (fasting- and cold intolerance, hypoketotic hypoglycemia, fatty changes in liver and heart and unprovoked sudden death). Therefore, this mouse is used as a model for human VLCAD deficiency.
To date, no human LCAD-deficient patients have been described. Several cases of LCAD deficiency were described before 1992, but these patients were later shown to be VLCAD-deficient [31]. The absence of LCAD-deficient subjects indicates that, in humans, LCAD is either of minor significance or vitally important in the mitochondrial β-oxidation. LCAD-deficient subjects either experience no or very mild symptoms (like VLCAD-deficient mice) and are therefore not recognized or LCAD deficiency could be embryonically lethal. The latter possibility seems more likely, since there is a substantial gestational loss of LCAD-/-) and +/- pups in the LCAD mouse model [41].

Regulation of carnitine metabolism

Various substances, including carnitine biosynthesis metabolites, hormones and hyperlipidemic drugs, have been shown to have an effect on carnitine homeostasis, but the precise mechanisms that lead to these changes are still mostly unknown.
The γ-BBD activity in rat liver was modified by administration of both carnitine and γ-BB [42]. γ-BBD activity in carnitine-fed animals was decreased, while the activity was increased in rats on a γ-BB-supplemented diet. Thyroid hormone was also shown to influence γ-BBD. Thyroid hormone administration increased γ-BBD mRNA levels and enzyme activity in the rat and doubled liver carnitine content [43, 44].
The hepatic carnitine concentration was also increased in rats with a MtT-F4 tumor, which secretes large quantities of prolactin, growth hormone and ACTH. Which of these hormones is responsible for the chance in liver carnitine content or via which mechanism this elevation occurs is unknown [45].
Several observations indicate that sex hormones also influence carnitine metabolism. Male rats had higher plasma, cardiac and skeletal muscle carnitine levels than females, but female rats had a higher carnitine concentration in liver [46]. In humans, males were reported to have higher plasma, but not skeletal muscle, carnitine levels, as compared to females [47-49].
Insulin has different effects on carnitine metabolism in liver and skeletal muscle. Carnitine uptake in skeletal is stimulated by insulin via increased expression of OCTN2 [50]. In liver, however, the carnitine level is increased by glucagon or by a decrease in the insulin concentration [51].

PPARα and carnitine metabolism

Peroxisome Proliferator Activated Receptor α (PPARα) is a ligand-dependent transcription factor involved in the regulation of energy metabolism. PPARα heterodimerizes with a Retinoid X Receptor and binds to specific response elements to stimulate expression of target

genes. PPARα is expressed in tissues with a high rate of fatty acid oxidation (such as liver, heart, skeletal muscle, kidney and brown adipose tissue) [52]. Most aspects of fatty acid metabolism are regulated by PPARα; cellular uptake of fatty acids (via fatty acid translocase and the fatty acid transport proteins), activation of fatty acids (acyl-CoA synthetases), peroxisomal β-oxidation (straight-chain acyl-CoA oxidase, D-bifunctional protein, L-bifunctional protein, peroxisomal 3-ketoacyl-CoA thiolase B and sterol carrier protein X), mitochondrial β-oxidation (CPTI, CPTII, VLCAD, LCAD, MCAD, SCAD and 3-keto-acyl-CoA thiolase), ketogenesis (hydroxymethylglutaryl-CoA synthase), ω-oxidation (cytochrome P450 4A) and lipoprotein metabolism (lipoprotein lipase and several apolipoprotiens) [52-54]. PPARα also influences carnitine metabolism. Clofibrate (a synthetic PPARα ligand) fed rats and phytol-treated mice (a natural PPARα ligand) have elevated hepatic carnitine levels compared to control animals [54, 55]. When mice or rats are fasted, liver carnitine levels also rise [51, 56]. No elevation of the hepatic carnitine concentration is observed, however, upon fasting or in phytol-fed PPARα -/- mice, which indicates that this effect is mediated via PPARα [54, 56].

Outline of this thesis

Most studies of carnitine biosynthesis have been performed in the rat. Very little is known about murine carnitine biosynthesis, even though this animal is frequently used as a model system to study fatty acid metabolism and deficiencies therein. In order to study carnitine metabolism, we first developed assays to measure the activity of the carnitine biosynthesis enzymes (chapter 2) as well as other enzyme activities involved in carnitine metabolism (chapter 3) and a method to determine the concentration of carnitine metabolites in tissues (chapter 4). These assays were used to investigate the metabolism of carnitine in two mouse models for human β-oxidation disorders (chapters 4 and 5) and to study the regulation of carnitine homeostasis by PPARα, using the PPARα-/- mouse (chapter 6).
Very little research has been performed concerning the transport of carnitine metabolites, although this is a very important aspect of carnitine biosynthesis and metabolism. Therefore, we aimed to identify proteins involved in carnitine metabolite transport into the cell and between different cellular compartments. In chapter 7 we show that TMLD is a mitochondrial matrix enzyme and provide evidence that suggests the existence of a mitochondrial TML/HTML transporter. In chapter 5 we describe the identification and characterization of a liver γ-BB transporter.

References

[1] J.D. McGarry, N.F. Brown. The mitochondrial carnitine palmitoyltransferase system. From concept to molecular analysis, Eur. J. Biochem. 244 (1997) 1-14
[2] R.R. Ramsay, R.D. Gandour, F.R. van der Leij. Molecular enzymology of carnitine transfer and transport, Biochim. Biophys. Acta 1546 (2001) 21-43.
[3] P. Rinaldo. Fatty acid transport and mitochondrial oxidation disorders, Semin. Liver Dis. 21 (2001) 489-500
[4] M.J. Bennett, P. Rinaldo, A.W. Strauss. Inborn errors of mitochondrial fatty acid oxidation, Crit. Rev. Clin. Lab. Sci. 37 (2000) 1-44
[5] F.M. Vaz, R.J. Wanders. Carnitine biosynthesis in mammals, Biochem. J. 361 (2002) 417-429
[6] W.K. Paik, S. Kim. Protein methylation, Science 174 (1971) 114-119.
[7] J. LaBadie, W.A. Dunn, N.N. Aronson, Jr. Hepatic synthesis of carnitine from protein-bound trimethyl-lysine. Lysosomal digestion of methyl-lysine-labelled asialo-fetuin, Biochem. J. 160 (1976) 85-95.
[8] R.A. Cox, C.L. Hoppel. Biosynthesis of carnitine and 4-N-trimethylaminobutyrate from 6- N-trimethyl-lysine, Biochem. J. 136 (1973) 1083-1090

[9] V. Tanphaichitr, H.P. Broquist. Site of carnitine biosynthesis in the rat, J. Nutr. 104 (1974) 1669-1673.
[10] H.T. Haigler, H.P. Broquist. Carnitine synthesis in rat tissue slices, Biochem. Biophys. Res. Commun. 56 (1974) 676-681.
[11] R.A. Cox, C.L. Hoppel. Carnitine biosynthesis in rat liver slices, Biochim. Biophys. Acta 362 (1974) 403-413.
[12] R.A. Cox, C.L. Hoppel. Carnitine and trimethylaminobutyrate synthesis in rat tissues, Biochem. J. 142 (1974) 699-701.
[13] J.D. Erfle. Hydroxylation of gamma-butyrobetaine by rat and ovine tissues, Biochem. Biophys. Res. Commun. 64 (1975) 553-557
[14] S. Englard, H.H. Carnicero. gamma-Butyrobetaine hydroxylation to carnitine in mammalian kidney, Arch. Biochem. Biophys. 190 (1978) 361-364
[15] A.L. Carter, T.O. Abney, H. Braver, A.H. Chuang. Localization of gamma-butyrobetaine hydroxylase in the rat testis, Biol. Reprod. 37 (1987) 68-72.
[16] T. Bohmer. Conversion of butyrobetaine to carnitine in the rat in vivo, Biochim. Biophys. Acta 343 (1974) 551-557.
[17] A.L. Carter, R. Frenkel. The role of the kidney in the biosynthesis of carnitine in the rat, J. Biol. Chem. 254 (1979) 10670-10674
[18] B.J. Zaspel, K.J. Sheridan, L.M. Henderson. Transport and metabolism of carnitine precursors in various organs of the rat, Biochim. Biophys. Acta 631 (1980) 192-202
[19] C.J. Rebouche. Sites and regulation of carnitine biosynthesis in mammals, Fed. Proc. 41 (1982) 2848-2852
[20] R.Z. Christiansen, J. Bremer. Active transport of butyrobetaine and carnitine into isolated liver cells, Biochim. Biophys. Acta 448 (1976) 562-577.
[21] S. Berardi, B. Stieger, S. Wachter, B. O'Neill, S. Krahenbuhl. Characterization of a sodium-dependent transport system for butyrobetaine into rat liver plasma membrane vesicles, Hepat. 28 (1998) 521-525.
[22] A. Sandor, J. Cseko, G. Kispal, I. Alkonyi. Surplus acylcarnitines in the plasma of starved rats derive from the liver, J. Biol. Chem. 265 (1990) 22313-22316.
[23] C.J. Rebouche, A.G. Engel. Tissue distribution of carnitine biosynthetic enzymes in man, Biochim. Biophys. Acta 630 (1980) 22-29
[24] G. Lindstedt, S. Lindstedt, I. Nordin. Gamma-butyrobetaine hydroxylase in human kidney, Scan. J. Clin. Lab. Invest. 42 (1982) 477-485
[25] S. Englard. Hydroxylation of gamma-butyrobetaine to carnitine in human and monkey tissues, FEBS Lett. 102 (1979) 297-300
[26] B. Melegh, R. Hermann, I. Bock. Generation of hydroxytrimethyllysine from trimethyllysine limits the carnitine biosynthesis in premature infants, Acta Paediatr. 85 (1996) 345-350.
[27] F.M. Vaz, B. Melegh, J. Bene, D. Cuebas, D.A. Gage, A. Bootsma, P. Vreken, A.H. van Gennip, L.L. Bieber, R.J. Wanders. Analysis of carnitine biosynthesis metabolites in urine by HPLC- electrospray tandem mass spectrometry, Clin. Chem. 48 (2002) 826-834.
[28] C.J. Rebouche, K.A. Lombard, C.A. Chenard. Renal adaptation to dietary carnitine in humans, Am. J. Clin. Nutr. 58 (1993) 660-665.
[29] I. Tein. Carnitine transport: pathophysiology and metabolism of known molecular defects, J. Inherit. Metab. Dis. 26 (2003) 147-169
[30] K. Bartlett, S. Eaton. Mitochondrial beta-oxidation, Eur. J. Biochem. 271 (2004) 462-469
[31] P. Rinaldo, D. Matern, M.J. Bennett. Fatty acid oxidation disorders, Annu. Rev. Physiol. 64 (2002) 477-502
[32] P.A. Watkins. Fatty acid activation, Prog. Lipid. Res. 36 (1997) 55-83
[33] R.J. Wanders, S. Denis, J. Ruiter, L. Ijlst, G. Dacremont. 2,6-Dimethylheptanoyl-CoA is a specific substrate for long-chain acyl-CoA dehydrogenase (LCAD): evidence for a major role of LCAD in branched-chain fatty acid oxidation, Biochim. Biophys. Acta 1393 (1998) 35-40
[34] W. Le, A.S. Abbas, H. Sprecher, J. Vockley, H. Schulz. Long-chain acyl-CoA dehydrogenase is a key enzyme in the mitochondrial beta-oxidation of unsaturated fatty acids, Biochim. Biophys. Acta 1485 (2000) 121-128
[35] K.P. Battaile, M. McBurney, P.P. Van Veldhoven, J. Vockley. Human long chain, very long chain and medium chain acyl-CoA dehydrogenases are specific for the S-enantiomer of 2- methylpentadecanoyl-CoA, Biochim. Biophys. Acta 1390 (1998) 333-338
[36] Y. Uchida, K. Izai, T. Orii, T. Hashimoto. Novel fatty acid beta-oxidation enzymes in rat liver mitochondria. II. Purification and properties of enoyl-coenzyme A (CoA) hydratase/3-hydroxyacyl-CoA dehydrogenase/3-ketoacyl-CoA thiolase trifunctional protein, J. Biol. Chem. 267 (1992) 1034-1041

[37] T. Koizumi, H. Nikaido, J. Hayakawa, A. Nonomura, T. Yoneda. infantile disease with microvesicular fatty infiltration of viscera spontaneously occurring in the C3H-H-2(0) strain of mouse with similarities to Reye's syndrome., Lab. Anim. 22 (1988) 83-87
[38] M. Horiuchi, K. Kobayashi, S. Yamaguchi, N. Shimizu, T. Koizumi, Nikaido, H, J. Hayakawa, M. Kuwajima, T. Saheki. Primary defect of juvenile visceral steatosis (jvs) mouse with systemic carnitine deficiency is probably in renal carnitine transport system, Biochim. Biophys. Acta 1226 (1994) 25-30
[39] K. Lu, H. Nishimori, Y. Nakamura, K. Shima, M. Kuwajima. A missense mutation of mouse OCTN2, a sodium-dependent carnitine cotransporter, in the juvenile visceral steatosis mouse, Biochem. Biophys. Res. Commun. 252 (1998) 590-594
[40] A.M. Schuler, P.A. Wood. Mouse models for disorders of mitochondrial fatty acid beta-oxidation., ILAR J 43 (2002) 57-65
[41] D. Kurtz, P. Rinaldo, W. Rhead, L. Tian, D. Millington, J. Vockley, D. Hamm, A. Brix, J. Lindsey, C. Pinkert, W. O'Brien, P. Wood. Targeted disruption of mouse long-chain acyl-CoA dehydrogenase gene reveals crucial roles for fatty acid oxidation., Proc. Natl. Acad. Sci. U S A 95 (1998) 15592-15597
[42] C.J. Rebouche. Effect of dietary carnitine isomers and gamma-butyrobetaine on L- carnitine biosynthesis and metabolism in the rat, J. Nutr. 113 (1983) 1906-1913.
[43] S. Galland, B. Georges, F. Le Borgne, G. Conductier, J.V. Dias, J. Demarquoy. Thyroid hormone controls carnitine status through modifications of gamma-butyrobetaine hydroxylase activity and gene expression, Cell. Mol. Life Sci. 59 (2002) 540-545
[44] S.V. Pande, R. Parvin. Clofibrate enhancement of mitochondrial carnitine transport system of rat liver and augmentation of liver carnitine and gamma- butyrobetaine hydroxylase activity by thyroxine, Biochim. Biophys. Acta 617 (1980) 363-370
[45] R. Parvin, C. Gianoulakis, S.V. Pande, M. Chretien. Effect of pituitary tumor MtT-F4 on carnitine levels in the serum, liver and heart of rats, Life Sci. 29 (1981) 1047-1049.
[46] P.R. Borum. Variation in tissue carnitine concentrations with age and sex in the rat, Biochem. J. 176 (1978) 677-681.
[47] G. Cederblad. Plasma carnitine and body composition, Clin. Chim. Acta 67 (1976) 207-212.
[48] N. Takiyama, K. Matsumoto. Age-and sex-related differences of serum carnitine in a Japanese population, J. Am. Coll. Nutr. 17 (1998) 71-74.
[49] J.R. Opalka, F.N. Gellerich, S. Zierz. Age and sex dependency of carnitine concentration in human serum and skeletal muscle, Clin. Chem. 47 (2001) 2150-2153
[50] F.B. Stephens, D. Constantin-Teodosiu, D. Laithwaite, E.J. Simpson, P.L. Greenhaff. Insulin stimulates L-carnitine accumulation in human skeletal muscle, Faseb J. 20 (2006) 377-379
[51] J.D. McGarry, C. Robles-Valdes, D.W. Foster. Role of carnitine in hepatic ketogenesis, Proc. Natl. Acad. Sci. U S A 72 (1975) 4385-4388.
[52] J. Berger, D.E. Moller. The mechanisms of action of PPARs, Annu. Rev. Med. 53 (2002) 409-435
[53] P. Lefebvre, G. Chinetti, J.C. Fruchart, B. Staels. Sorting out the roles of PPAR alpha in energy metabolism and vascular homeostasis, J. Clin. Invest. 116 (2006) 571-580
[54] J. Gloerich, N. van Vlies, G.A. Jansen, S. Denis, J.P. Ruiter, M.A. van Werkhoven, M. Duran, F.M. Vaz, R.J. Wanders, S. Ferdinandusse. A phytol-enriched diet induces changes in fatty acid metabolism in mice both via PPARalpha-dependent and -independent pathways, J. Lipid Res. 46 (2005) 716-726
[55] H.S. Paul, C.E. Gleditsch, S.A. Adibi. Mechanism of increased hepatic concentration of carnitine by clofibrate, Am. J. Physiol. 251 (1986) E311-315.
[56] T. Hashimoto, W.S. Cook, C. Qi, A.V. Yeldandi, J.K. Reddy, M.S. Rao. Defect in peroxisome proliferator-activated receptor alpha-inducible fatty acid oxidation determines the severity of hepatic steatosis in response to fasting, J. Biol. Chem. 275 (2000) 28918-28928

Chapter 2

Measurement of carnitine biosynthesis enzyme activities by tandem mass spectrometry: differences between the mouse and the rat

N. van Vlies, R.J.A. Wanders, F.M. Vaz

Anal. Biochem. 354 (2006) 132-139

Abstract

Although the mouse frequently is used to study metabolism and deficiencies therein, little is known about carnitine biosynthesis in this animal. To this point, only laborious procedures have been described to measure the activity of carnitine biosynthesis enzymes using subcellular fractions as the enzyme source. We developed two simple tandem mass spectrometry-based methods to determine the activity of three carnitine biosynthesis enzymes (6-*N*-trimethyllysine dioxygenase, 4-trimethylaminobutyraldehyde dehydrogenase, and 4-trimethylaminobutyric acid dioxygenase) in total homogenates that can be prepared from frozen tissue. The new assays were used to characterize these enzymes in mouse liver homogenate. Because carnitine biosynthesis has been studied extensively in the rat, we compared the mouse tissue distribution of carnitine biosynthesis enzyme activities and levels of the biosynthesis metabolites with those in the rat to determine which tissues contribute to carnitine biosynthesis in these species. Surprisingly, large differences in enzyme activities were found between the rat and the mouse, whereas carnitine biosynthesis metabolite levels were very similar in both species, possibly due to the different kinetic properties of the first enzyme of carnitine biosynthesis. Also, muscle carnitine levels were found to vary considerably between these two species, suggesting that there is a metabolic dissimilarity between the mouse and the rat.

Introduction

Carnitine (3-hydroxy-4-N,N,N-trimethylaminobutyrate) is an essential substance in fatty acid metabolism because it enables the transport of activated long-chain fatty acids from the cytosol into the mitochondrial matrix, where β-oxidation takes place [1-2]. Carnitine is also involved in the transport of the peroxisomal β-oxidation products to mitochondria, modulation of the free coenzyme A (CoA) level, and excretion of toxic acyl groups [3-7].

Mammals acquire carnitine both from their diets and through endogenous synthesis [7]. Carnitine ultimately is synthesized from the amino acids lysine and methionine. In some proteins (calmodulin, histones, myosin, and actin), lysine residues are trimethylated on the 4-amino group by specific methyltransferases that use *S*-adenosyl methionine as the methyl donor [8]. After lysosomal degradation of these proteins, free 6-*N*-trimethyllysine (TML) becomes available for carnitine biosynthesis. First, TML is hydroxylated by the enzyme TML dioxygenase (TMLD, EC 1.14.11.8) to 3-hydroxy-6-*N*-trimethyllysine (HTML). HTML subsequently is cleaved by a specific aldolase to yield 4-trimethylaminobutyraldehyde (TMABA), which is oxidized by TMABA dehydrogenase (TMABA-DH, EC 1.2.1.47) to 4-trimethylaminobutyric acid (γ-butyrobetaine, γ-BB). Finally, γ-BB is hydroxylated to carnitine by γ-BB dioxygenase (γ-BBD, EC 1.14.11.1) [7, 9, 10].

The first and last enzyme of the carnitine biosynthesis, TMLD and γ-BBD, are very similar. Both enzymes are dioxygenases; hydroxylation of their substrate is coupled to the conversion of 2-oxoglutarate and molecular oxygen to succinate and carbon dioxide. Furthermore, both enzymes use Fe^{2+} as cofactor and require the presence of ascorbic acid for optimal activity [11-15]. In addition, the TMLD protein shows high homology to the γ-BBD protein and both appear to belong to a separate subfamily of the 2-oxoglutarate-dependent dioxygenases [7,16].

Several methods have been described to measure TMLD and γ-BBD activity, and in nearly all methods homogenates are prepared from fresh tissues followed by differential centrifugation to partially purify the enzyme activity. In most TMLD assays, hydroxylase activity is measured radiochemically. After incubation of the partially purified enzyme with radiolabeled TML and appropriate cofactors, the reaction mixture is deproteinized and the substrate ([^{3}H]-

TML or [^{14}C]-TML) is separated from the produced radiolabeled HTML by ion-exchange chromatography. The radioactivity in the HTML fraction is used as a measure for the TMLD activity [12, 13, 17]. An alternative radiochemical method has been described where upon hydroxylation, tritium is released as radioactive water, and after separation of the substrate and water by ion-exchange chromatography, the radioactivity in the water fraction is used to determine the TMLD activity [18]. The only nonradioactive TMLD assay has been described by Davis [19]. The produced HTML is quantified by virtue of an added internal standard, namely triethyllysine. In this procedure, the basic amino acid fraction is purified by ion-exchange/ion-exclusion chromatography. After lyophilization of the eluate and resuspension in an appropriate buffer, this mixture is derivatized with 1,2-benzenedicarboxaldehyde followed by HPLC analysis and fluorescent detection of the amount of produced HTML. Because the majority of these procedures employ either partially purified proteins or organellar fractions as an enzyme source, these assays can only be performed using a fresh tissue source. In addition, these methods employ elaborate purification procedures to allow separation and quantification of the produced HTML.

Like TMLD, γ-BBD activity can be determined using radiolabeled γ-BB [14, 15, 17, 20]. The most commonly used γ-BBD assay, however, makes use of a two-step procedure where in the first step carnitine is produced from unlabeled γ-BB, after which carnitine-acetyltransferase is used to convert carnitine and [^{14}C]-acetyl-CoA into [^{14}C]-acetyl-carnitine. After separation of [^{14}C]-acetyl-carnitine and [^{14}C]-acetyl-CoA by ion-exchange chromatography, the radioactivity in the acetyl-carnitine fraction is used to calculate the γ-BBD activity [21-23]. A disadvantage of this procedure is the necessity to determine the concentration of endogenous carnitine in each protein sample.

The third step of the carnitine biosynthesis is the conversion of TMABA into γ-BB, which is NAD^+ dependent. This property has been used to measure TMABA-DH activity by spectrophotometric or fluorometric determination of the amount of produced NADH [24]. The disadvantage of chromogenic assays is that they are very sensitive to matrix-dependent interference of the protein sample, and this can hamper accurate activity measurements in tissue homogenates by spectrophotometric, and especially fluorometric, means.

In this article, we present a straightforward, nonradioactive assay where both TMLD and γ-BBD activity can be determined simultaneously in crude homogenates by ion-pair HPLC-tandem mass spectrometry. Based on this method, we also have developed a novel assay to measure TMABA-DH activity by directly determining the amount of the product of this reaction, namely γ-BB. These assays were used to characterize kinetic and other properties of TMLD, TMABA-DH, and γ-BBD in mouse liver homogenate. We characterized the mouse enzymes because this animal is used frequently as a model system to study fatty acid metabolism and deficiencies therein, but very little is known about murine carnitine biosynthesis. Because carnitine biosynthesis has been studied extensively in the rat, we compared the mouse tissue distribution of the enzyme activities and the levels of the carnitine biosynthesis metabolites with those in the rat to determine which tissues contribute to carnitine biosynthesis in these species and to gain a better understanding of the intertissue relationships of carnitine biosynthesis.

Materials and methods

Chemicals

TML, γ-BB, and carnitine-acetyltransferase were obtained from Sigma. [$^2H_9$]-TML and [$^2H_3$]-γ-BB were synthesized as described previously [25]. [$^2H_9$]-HTML was prepared enzymatically by incubating [$^2H_9$]-TML with *Neurospora crassa* TMLD, which was expressed heterologously in *Saccharomyces cerevisiae* as described by Swiegers *et al*. [26].

The resulting mixture of [$^2H_9$]-HTML and [$^2H_9$]-TML was applied to Microcon YM 30 filters (Amicon), and the deproteinized filtrate was used as internal standard for TML and HTML. The [$^2H_9$]-carnitine internal standard was obtained from Herman J. ten Brink (VU University Medical Center, Amsterdam, The Netherlands). TMABA was synthesized as described by Vaz and co-workers [27]. [^{14}C]-Acetyl-CoA was purchased from Amersham Biosciences. Acetyl-CoA was obtained from Roche. The AG 1-X8 resin was obtained from Bio-Rad. All other reagents were of analytical grade.

Animals
Adult male 129/S1 mice were anesthetized and sacrificed by cervical dislocation. Tissues were collected, frozen immediately in liquid nitrogen, and stored at -80°C until further use. Adult male Wistar rats were anesthetized and sacrificed by decapitation. Tissues were collected, frozen immediately in liquid nitrogen, and stored at -80°C until further use. All experiments were approved by the local Ethical Committee.

Preparation of homogenates
Tissues were homogenized in 10 mM Mops buffer (pH 7.4) containing 0.9% (w/v) NaCl, 10% (w/v) glycerol, and 5 mM dithiothreitol (DTT). The protein concentration was determined by the method of Bradford [28] using bovine serum albumin (BSA) as standard.

TMLD and γ-BBD activity measurement
The reaction mixture (final volume 250 µl) consisted of 20 mM potassium phosphate buffer (pH 7.4) containing 50 mM KCl, 3 mM 2-oxoglutarate, 10 mM sodium ascorbate, 0.5 mM DTT, 0.5 mM ammonium iron sulfate, 2.5 mg/ml BSA, 0.01% (w/v) Triton X-100, 2 mM TML, and 200 µM [$^2H_3$]-γ-BB. The reaction was started by adding 50 µl of homogenate (final protein concentration 1 mg/ml unless indicated otherwise) to the reaction mixture, which was incubated for 20 min (unless indicated otherwise) at 37°C. To stop the hydroxylase reactions, $ZnCl_2$ was added to a final concentration of 1 mM and the reaction mixtures were placed on ice. The $ZnCl_2$ solution also contained the internal standards; 150 pmol [$^2H_9$]-HTML and 550 pmol [$^2H_9$]-carnitine per reaction. Subsequently, the reaction mixture was loaded onto a Microcon 30-kDa filter and centrifuged at 14,000 × *g* for 20 min at 4°C; this separates the metabolites (TML, HTML, γ-BB, and carnitine) from the enzymes and removes most of the proteins. Then 100 µl of the filtrate was derivatized with methylchloroformate, and the produced HTML and [$^2H_3$]-carnitine were quantified using ion-pair HPLC-tandem mass spectrometry as described previously [25].

TMABA-DH activity measurement
The reaction mixture (final volume 250 µl) consisted of a 0.1 M sodium pyrophosphate buffer (pH 9.0) containing 0.5 mM NAD^+ and 0.1 mM TMABA. The reaction was started by adding 100 µl of homogenate (final protein concentration 0.5 mg/ml unless indicated otherwise) to the reaction mixture, which was incubated for 10 min (unless indicated otherwise) at 25°C. The reaction was stopped by the addition of acetic acid to a final concentration of 350 µM, and the samples were placed on ice. Each aliquot of the acetic acid solution also contained 6.25 nmol [$^2H_3$]-γ-BB internal standard. The reaction mixture was centrifuged at 16,000 × *g* for 3 min at 4°C to remove protein precipitates before the mixture was loaded onto a Microcon 30-kDa filter and centrifuged at 14,000 × *g* for 20 min at 4°C; this separates the metabolites (TMABA and γ-BB) from most of the remaining proteins. Then 100 µl of filtrate was derivatized, and the produced γ-BB was quantified using ion-pair HPLC-tandem mass spectrometry as described previously [25].

Determination of K_m values
To establish K_m values for substrates and cofactors of the three enzymes, the concentration of the compounds of interest was varied while the concentration of the other substances was kept constant. For the determination of the K_m values for Fe^{2+}, endogenous Fe^{2+} was removed from the homogenate using a G25 gel filtration column (Amersham Biosciences).

Tissue carnitine biosynthesis metabolites
The concentration of carnitine biosynthesis metabolites in tissues was determined as described previously [29].

Results

Combined TMLD and γ-BBD assay
Most TMLD and γ-BBD activity assays use either partially purified proteins or organellar fractions as an enzyme source or employ elaborate purification procedures to allow separation of substrate and product. To develop a less laborious method, we investigated whether we could adapt our HPLC–tandem mass spectrometry procedure for the analysis of carnitine biosynthesis metabolites in body fluids [25] and tissues [29] to determine TMLD and γ-BBD activity in total homogenates.
In our initial experiments, we attempted to measure TMLD activity by direct determination of the amount of produced HTML. After incubation of mouse liver homogenate with the substrates and cofactor of TMLD and the addition of [$^2H_9$]-HTML as internal standard, the amount of produced HTML could be quantified readily by ion-pair HPLC-tandem mass spectrometry analysis (results not shown). Theoretically, the HTML produced by TMLD in the assay could be converted into TMABA and γ-BB (and in the liver into carnitine) by the action of endogenous HTML-aldolase and TMABA-DH (and γ-BBD in the liver), and this would lead to an underestimation of the TMLD activity. When liver homogenate was incubated with TML and the cofactors for TMLD, however, only HTML was detected. No γ-BB or carnitine was formed (results not shown). To exclude the possibility that part of the produced HTML was converted into TMABA (which is not measured), we added purified TMABA-DH [27] and NAD^+ to the incubation. Again no γ-BB or carnitine was formed (results not shown). This is possibly due to the shortage of a (yet unknown) cofactor(s) of the HTML-aldolase, which itself remains unidentified.
Using a similar setup as for the TMLD activity measurement, we tried to measure γ-BBD activity. Instead of unlabeled γ-BB, however, [$^2H_3$]-γ-BB was used as substrate. This enables the distinction between endogenous carnitine (present in the homogenate) and the carnitine formed in the assay, making the quantification of endogenous carnitine unnecessary (needed in the most commonly used γ-BBD assay [21-23]) and reducing the number of incubations by half. Using [$^2H_9$]-carnitine as internal standard, the produced [$^2H_3$]-carnitine could be quantified by HPLC-tandem mass spectrometry analysis (results not shown).
Because both TMLD and γ-BBD are 2-oxoglutarate-dependent dioxygenases and have the same cofactor requirements, we investigated whether it was possible to measure the activity of these enzymes simultaneously. To exclude the possibility that TML or γ-BB inhibits γ-BBD or TMLD, respectively, the effects of TML on γ-BBD and of γ-BB on TMLD were determined. This was done by incubating liver homogenate with the complete reaction mixture, containing both substrates, and incubating homogenate with assay mixtures containing only TML or γ-BB. As shown in table 1, 2 mM TML or 200 μM γ-BB had no effect on the activity of γ-BBD or TMLD, respectively, making possible the simultaneous determination of TMLD and γ-BBD activity. The accurate and instant termination of the

enzyme reactions, however, proved to be problematic. In initial experiments, the reactions were terminated by centrifugation through a Microcon 30-kDa filter, separating proteins from the substrates and products. This procedure, however, led to considerable variation between duplicate samples. Because it was shown previously that divalent cations, particularly Zn^{2+}, strongly inhibit TMLD and γ-BBD activity [18] and [30], we investigated whether we could use this property to stop the hydroxylase reactions. As shown in table 1, the addition of 1 mM $ZnCl_2$ completely inhibited the activity of γ-BBD and markedly diminished that of TMLD. The addition of Zn^{2+} together with immediate transfer of the sample into an ice/water bath (to inhibit TMLD activity completely), therefore, was used to terminate the hydroxylase reactions.

Table 1. TMLD and γ-BBD activity

	TMLD activity	γ-BBD activity
	pmol × min^{-1} × mg^{-1}	
Complete mixture	8.5 ± 0.9	130 ± 6.2
- TML	0	128 ± 9.3
- γ-butyrobetaine	8.3 ± 0.5	0
+ 1 mM $ZnCl_2$	0.2 ± 0.03	0
- 2-oxoglutarate	0	0
- Fe^{2+} [a]	1.7 ± 0.3	15.6 ± 3.1
- Ascorbic acid	2.1 ± 0.5	7.8 ± 1.2
- dithiotreitol	6.7 ± 0.4	109 ± 7.7
-bovine serum albumin	7.1 ± 0.6	125 ± 8.7
- KCl	8.5 ± 0.8	117 ± 8.2
- Triton-X-100	8.4 ± 0.8	130 ± 12.8

Values are means ± standard deviations of three incubations. Substances listed were either added to (+) or excluded from (−) the complete mixture (as described in Materials and methods). [a] A G25 gel filtration column was used to remove endogenous Fe^{2+} from the homogenate.

Characterization of the TMLD and γ-BBD assay in mouse liver homogenate

To find optimal assay conditions, linearity with time and homogenate protein concentration was examined. Both hydroxylase activities were linear with time for 20 min (figure 1A). TMLD and γ-BBD activities were also proportional to the amount of homogenate protein in the range of 0.5–2 mg/ml (figure 1B). Activity was not completely linear, however, between 0 and 0.5 mg/ml protein. An incubation time of 20 min and a protein concentration of 1 mg/ml were chosen as standard conditions for the combined TMLD/γ-BBD activity assay.

When components of the reaction mixture were excluded from the assay, the activities of both TMLD and γ-BBD were reduced considerably (table 1). The most pronounced reduction of activity was observed when ascorbic acid was absent from the reaction mixture, whereas removal of DTT caused a small decrease in hydroxylase activity. The addition of Triton-X-100 to the incubations did not alter enzyme activities, but it facilitated centrifugation of the reaction mixtures over the Microcon filters.

As expected, absence of the enzymes' specific substrate or 2-oxoglutarate resulted in complete loss of activity (table 1). Absence of the cofactor Fe^{2+}, however, did not completely abolish enzyme activity, even when endogenous Fe^{2+} was removed from the homogenate with a gel filtration column.

To determine K_m values for Fe^{2+}, 2-oxoglutarate, and the specific substrates of both enzymes, the concentrations of these substances were varied consecutively. Lineweaver–Burk double-reciprocal plots were used to calculate K_m values, which are shown in table 2.

When we compared the new γ-BBD assay with the most commonly used assay [21-23] using mouse liver homogenate, the means of the two methods were not significantly different based on the Student's *t* test (old method, 94 ± 16 pmol × min^{-1} × mg^{-1} (n = 5), and new method, 120 ± 16 pmol × min^{-1} × mg^{-1} (n = 6), (P = 0.59).

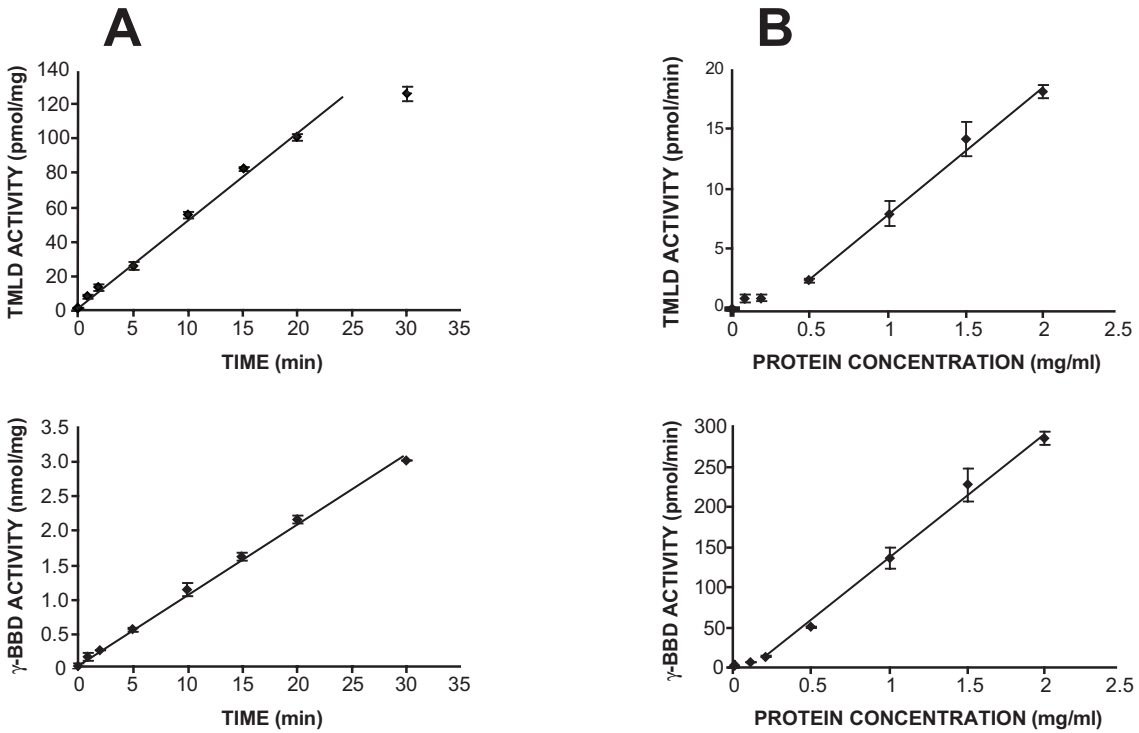

Figure. 1. Time and protein dependence of TMLD and γ-BBD activity in mouse liver homogenate. All measurements were performed in triplicate (mean ± standard deviation). (A) Time dependence. The final protein concentration was 1 mg/ml. (B) Protein dependence. The incubation time was 20 min.

Table 2. K_m values of TMLD and γ-BBD

	TMLD	γ-BBD
	(μM)	
TML	164	-
γ-butyrobetaine	-	40
2-oxoglutarate	605	63
Fe^{2+}	4.0	2.5

Values are means of three incubations.

Measurement and characterization of TMABA-DH in mouse liver homogenate

Initial attempts to measure TMABA-DH activity, by measuring the conversion of NAD^+ to NADH using a spectrophotometric or fluorometric method, failed due to high background activity in the liver homogenate. Because γ-BB can be measured using HPLC-tandem mass spectrometry, we determined the TMABA-DH activity by directly quantifying the γ-BB produced from TMABA using [$^2H_3$]-γ-BB as internal standard (results not shown). In theory, the γ-BB produced in the TMABA-DH assay could be converted into carnitine by the action of endogenous γ-BBD, leading to underestimation of the TMABA-DH activity. When liver homogenate was incubated with only γ-BB (without exogenous cofactors for γ-BBD), however, no carnitine was formed (results not shown), demonstrating that the amount of γ-BB formed is a good measure of TMABA-DH activity.

To find optimal assay conditions, linearity with time and homogenate protein concentration was examined. TMABA-DH activity was linear up to 20 min (figure 2A) and was proportional to the homogenate protein concentration in the range of 0-1 mg/ml (figure 2B). An incubation time of 10 min and a protein concentration of 0.5 mg/ml were chosen as standard conditions for the TMABA-DH activity assay.

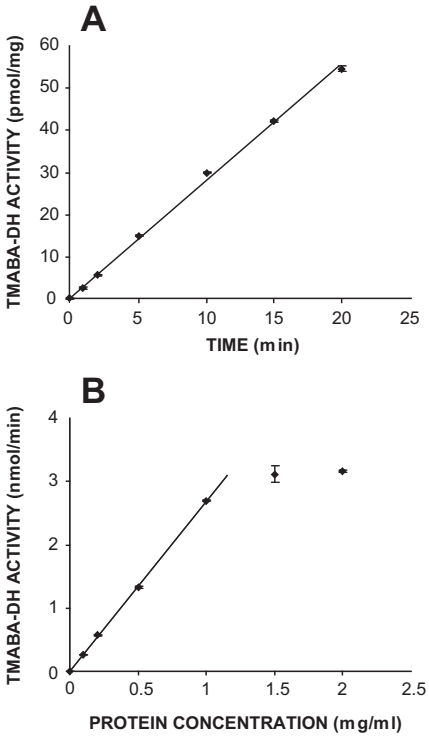

Figure 2. Time and protein dependence of TMABA-DH activity in mouse liver homogenate. All measurements were performed in triplicate (mean ± standard deviation). (A) Time dependence. The final protein concentration was 0.5 mg/ml. (B) Protein dependence. The incubation time was 10 min.

K_m values of TMABA-DH for TMABA and NAD^+ were determined using Lineweaver–Burk double-reciprocal plots and were 11 and 28 μM, respectively. These K_m values are similar to those determined for rat and human TMABA-DH [27].

Tissue distribution of carnitine biosynthesis enzymes in mouse tissues

To determine which organs play a role in carnitine biosynthesis, mouse liver, heart, kidney, skeletal muscle, brain, and testis were analyzed for TMLD, TMABA-DH, and γ-BBD activity. Testis was included because two previous articles have reported that this tissue contains γ-BBD activity in the rat [31,32]. The highest TMLD activity level was found in kidney and liver (table 3), whereas muscle and brain TMLD activity was barely detectable. TMABA-DH activity was present in all tissues, and the activity level was considerably higher than the TMLD activity level. High TMABA-DH activity levels were present in liver, kidney, and testis; intermediate activity levels were present in heart and brain; and the activity level in muscle was relatively low. The final enzyme of the carnitine biosynthetic pathway, γ-BBD, was detected only in mouse liver.

Tissue distribution of carnitine biosynthesis enzymes in rat tissues

Because differences between rodents in the tissue distribution of the carnitine biosynthesis enzymes have been reported previously [33], and because most research on carnitine biosynthesis is performed on the rat, we also used our new assays to investigate the activity of carnitine biosynthesis enzymes in tissues of this animal (table 3).

As in the mouse, the rat kidney contained the highest TMLD activity. In the rat, however, the kidney TMLD activity level is much higher than the levels of the other rat tissues (10-fold for liver and heart and 100-fold for muscle) and is much higher than the level of the mouse

kidney (nearly 40-fold). Rat tissues also contain considerably higher TMABA-DH activities than do the corresponding mouse tissues, especially heart and muscle. In contrast to TMLD and TMABA-DH activities, γ-BBD activity in rat liver was comparable to that in mouse liver. In agreement with previous results [31,32], rat testis did indeed contain γ-BBD activity; however, mouse testis did not.

Table 3. Activities of carnitine biosynthesis enzymes in mouse and rat tissues

		Mouse	Rat
		pmol × min $^{-1}$ × mg protein $^{-1}$	
TMLD	Liver	8.2 ± 0.6	59 ± 7
	Heart	3.2 ± 0.3	42 ± 18
	Kidney	13.4 ± 1.2	508 ± 81
	Muscle	0.5 ± 0.4	5 ± 4
	Brain	0.2 ± 0.1	10 ± 5
	Testis	1.1 ± 0.1	24 ± 3
TMABA-DH	Liver	2138 ± 103	6632 ± 1239
	Heart	179 ± 12	1765 ± 427
	Kidney	1445 ± 37	5753 ± 831
	Muscle	7.7 ± 1.3	583 ± 80
	Brain	298 ± 26	498 ± 88
	Testis	1698 ± 89	3014 ± 472
γ-BBD	Liver	120 ± 16	94 ± 25
	Heart	ND	ND
	Kidney	ND	ND
	Muscle	ND	ND
	Brain	ND	ND
	Testis	ND	8.2 ± 1.6

Values are mean ± standard deviation of three animals, each analyzed in duplicate. ND, not detectable.

Tissue distribution of carnitine biosynthesis metabolites in mouse and rat tissues

Because the large differences in carnitine biosynthesis enzyme activities between the mouse and the rat could be related to different tissue levels of carnitine biosynthesis metabolites, we measured the levels of these metabolites in mouse and rat tissues (table 4). Surprisingly, no major differences in tissue metabolite concentrations were found between the mouse and the rat. TML and γ-BB were in the same range in all tissues of both animals. HTML was barely detectable in rat heart and muscle but was clearly present in rat brain. Carnitine was much more abundant than the other biosynthesis metabolites. Although the carnitine levels differed among the various tissues within one species, carnitine levels in the same mouse and rat tissues corresponded well, with the exception of muscle. Compared with other tissues, mouse muscle contains relatively little carnitine. This is quite different in the rat, where muscle contains the second most carnitine (after heart).

Discussion

Two new tandem mass spectrometry-based assays were developed to determine the activity of the enzymes of the carnitine biosynthesis. In these assays, total homogenates can be used as an enzyme source, making the partial purification or subcellular fractionation of the homogenate and thus the need to use fresh tissues unnecessary. In the first assay, both TMLD and γ-BBD, the first and final enzymes of the carnitine biosynthesis, were measured together in a single reaction mixture. In the second assay, TMABA-DH activity was determined by

directly measuring the product of the reaction (γ-BB) instead of measuring the concomitant conversion of NAD^+ to NADH. In contrast to spectrophotometric or fluorometric TMABA-DH assays, this assay can be used for activity measurements in total homogenates because our method of detection is much less susceptible to matrix-dependent interference of the homogenate.

The new assays were used to characterize TMLD, TMABA-DH, and γ-BBD in mouse liver homogenate. Mouse liver TMLD and γ-BBD have a lower K_m for the cofactor Fe^{2+} than the K_m values found for the rat liver hydroxylases [15,34]. Also, the absence of Fe^{2+} from the reaction mixture did not cause a complete loss of activity. This residual activity could be the result of endogenous Fe^{2+}, which is so tightly bound to the enzymes that it could not be removed with a gel filtration column. This is in accordance with the low K_m value of both enzymes for Fe^{2+}.

Table 4. Levels of carnitine biosynthesis metabolites in mouse and rat tissues

		Mouse	Rat
		nmol/g wet weight	
TML	Liver	1.4 ± 0.2	1.5 ± 0.4
	Heart	2.5 ± 0.6	2.0 ± 0.4
	Kidney	2.1 ± 0.2	2.5 ± 0.1
	Muscle	3.0 ± 0.1	3.3 ± 1.2
	Brain	2.3 ± 0.2	0.9 ± 0.1
	Testis	1.8 ± 0.3	0.5 ± 0.1
HTML	Liver	ND	ND
	Heart	ND	0.23 ± 0.07
	Kidney	ND	ND
	Muscle	ND	0.27 ± 0.11
	Brain	ND	0.64 ± 0.14
	Testis	ND	ND
γ-butyrobetaine	Liver	10.1 ± 1.8	6.3 ± 1.5
	Heart	12.9 ± 1.2	16.7 ± 1.6
	Kidney	10.6 ± 1.9	14.7 ± 2.3
	Muscle	6.2 ± 1.0	11.4 ± 2.8
	Brain	8.1 ± 0.9	8.8 ± 3.1
	Testis	12.1 ± 1.4	5.9 ± 0.7
free carnitine	Liver	280 ± 58	304 ± 40
	Heart	805 ± 128	1287 ± 134
	Kidney	428 ± 95	647 ± 140
	Muscle	143 ± 26	774 ± 266
	Brain	89 ± 21	57 ± 6.7
	Testis	154 ± 34	159 ± 15

Values are mean ± standard deviation of three animals, each analyzed in duplicate. ND, not detectable

When we analyzed several mouse and rat tissues for carnitine biosynthesis enzyme activities, we found considerable differences in enzyme activities not only among the various tissues but also between the two species. Despite these differences, tissue concentrations of carnitine biosynthesis metabolites were similar in both species. The TMLD activity in mouse tissues (especially kidney) is substantially lower than that in rat tissues. The K_m of rat TMLD for TML, however, has been reported to be approximately 10-fold higher (1.6 mM [13] and 1.1 mM [16]) than that of the mouse enzyme (164 μM, as found in the current study). It is possible that the inverse relation between TMLD activity and affinity for TML results in

similar tissue levels in the rat and the mouse. In contrast, both the K_m for γ-BB and the activity of mouse liver γ-BBD are comparable to those of the rat liver enzyme (as found in the current study and [20]), as are the γ-BB levels.
HTML could not be detected in any of the studied mouse tissues, and it could be detected only in some rat tissues in low concentrations. This suggests that the enzyme responsible for the conversion of HTML into TMABA, HTML-aldolase, is very active in vivo and not rate limiting for the biosynthesis of carnitine. The TMABA-DH activity level was high when compared with the other enzymes in all mouse and rat tissues, with the exception of mouse muscle; therefore, TMABA-DH probably is also not rate limiting for carnitine biosynthesis. Because enzyme activities do not seem to correlate with the carnitine biosynthesis metabolite levels, it is likely that in the mouse the flux through the carnitine biosynthesis is regulated by the availability of TML rather than carnitine biosynthesis enzyme activity, as was proposed for the rat by Rebouche and co-workers [35] and Davis and Hoppel [36].
In contrast to the carnitine biosynthesis intermediates, free carnitine levels differed considerably among the various tissues within one species, whereas carnitine levels in the same mouse and rat tissues corresponded well, with the exception of muscle. Compared with other tissues, mouse muscle contains relatively little carnitine, whereas rat muscle contains the second most carnitine (after heart). All experimental animals received the same chow; therefore, this difference is not due to dietary composition and must reflect a metabolic dissimilarity.

Acknowledgments

The authors thank A. H. Bootsma and A. van Cruchten for technical assistance.

References

[1] J.D. McGarry, N.F. Brown. The mitochondrial carnitine palmitoyltransferase system: from concept to molecular analysis, Eur. J. Biochem. 244 (1997) 1–14.
[2] R.R. Ramsay, R.D. Gandour, F.R. van der Leij. Molecular enzymology of carnitine transfer and transport, Biochim. Biophys. Acta 1546 (2001) 21–43.
[3] P. Rinaldo. Fatty acid transport and mitochondrial oxidation disorders, Semin. Liver Dis. 21 (2001) 489–500.
[4] M.J. Bennett, P. Rinaldo, A.W. Strauss. Inborn errors of mitochondrial fatty acid oxidation, Crit. Rev. Clin. Lab. Sci. 37 (2000) 1–44.
[5] B.S. Jakobs, R.J. Wanders. Fatty acid β-oxidation in peroxisomes and mitochondria: the first unequivocal evidence for the involvement of carnitine in shuttling propionyl-CoA from peroxisomes to mitochondria, Biochem. Biophys. Res. Commun. 213 (1995) 1035–1041.
[6] N.M. Verhoeven, D.S. Roe, R.M. Kok, R.J. Wanders, C. Jakobs, C.R. Roe. Phytanic acid and pristanic acid are oxidized by sequential peroxisomal and mitochondrial reactions in cultured fibroblasts, J. Lipid Res. 39 (1998) 66–74.
[7] F.M. Vaz, R.J. Wanders. Carnitine biosynthesis in mammals, Biochem. J. 361 (2002) 417–429.
[8] W.K. Paik, S. Kim. Protein methylation, Science 174 (1971) 114–119.
[9] J. LaBadie, W.A. Dunn, N.N. Aronson Jr. Hepatic synthesis of carnitine from protein-bound trimethyl-lysine: lysosomal digestion of methyl-lysine-labelled asialo-fetuin, Biochem. J. 160 (1976) 85–95.
[10] R.A. Cox, C.L. Hoppel. Biosynthesis of carnitine and 4-N-trimethylaminobutyrate from 6-N-trimethyl-lysine, Biochem. J. 136 (1973) 1083–1090.
[11] B. Lindblad, G. Lindstedt, M. Tofft. The mechanism of α-ketoglutarate oxidation in coupled enzymatic oxygenations, J. Am. Chem. Soc. 91 (1969) 4604–4606.
[12] J.D. Hulse, S.R. Ellis, L.M. Henderson. Carnitine biosynthesis: β-hydroxylation of trimethyllysine by an α-ketoglutarate-dependent mitochondrial dioxygenase, J. Biol. Chem. 253 (1978) 1654–1659.
[13] D.S. Sachan, C.L. Hoppel. Carnitine biosynthesis: hydroxylation of N-6-trimethyl-lysine to 3-hydroxy-N-6-trimethyl-lysine, Biochem. J. 188 (1980) 529–534.

[14] G. Lindstedt, S. Lindstedt, M. Tofft. γ-Butyrobetaine hydroxylase from Pseudomonas sp AK 1, Biochemistry 9 (1970) 4336–4342.
[15] G. Lindstedt, S. Lindstedt. Cofactor requirements of γ-butyrobetaine hydroxylase from rat liver, J. Biol. Chem. 245 (1970) 4178–4186.
[16] F.M. Vaz, R. Ofman, K. Westinga, R.J. Wanders. Molecular and biochemical characterization of rat ε-N-trimethyllysine hydroxylase, the first enzyme of carnitine biosynthesis, J. Biol. Chem. 276 (2001) 33512–33517.
[17] C.J. Rebouche, A.G. Engel. Tissue distribution of carnitine biosynthetic enzymes in man, Biochim. Biophys. Acta 630 (1980) 22–29.
[18] R. Stein, S. Englard. The use of a tritium release assay to measure 6-N-trimethyl-l-lysine hydroxylase activity: synthesis of 6-N-[3-^{3}H]trimethyl-dl-lysine, Anal. Biochem. 116 (1981) 230–236.
[19] A.T. Davis. Assay for trimethyllysine hydroxylase by high-performance liquid chromatography, J. Chromatogr. 422 (1987) 253–256.
[20] G. Lindstedt. Hydroxylation of γ-butyrobetaine to carnitine in rat liver, Biochemistry 6 (1967) 1271–1282.
[21] G. Cederblad, S. Lindstedt. Metabolism of labeled carnitine in the rat, Arch. Biochem. Biophys. 175 (1976) 173–180.
[22] P.G. Barth, H.R. Scholte, J.A. Berden, J.M. Van der Klei-Van Moorsel, I.E. Luyt-Houwen, E.T. Van't Veer-Korthof, J.J. Van der Harten, M.A. Sobotka-Plojhar. An X-linked mitochondrial disease affecting cardiac muscle, skeletal muscle, and neutrophil leucocytes, J. Neurol. Sci. 62 (1983) 327–355.
[23] F.M. Vaz, S. van Gool, R. Ofman, L. Ijlst, R.J. Wanders. Carnitine biosynthesis: identification of the cDNA encoding human γ-butyrobetaine hydroxylase, Biochem. Biophys. Res. Commun. 250 (1998) 506–510.
[24] J.D. Hulse, L.M. Henderson. Carnitine biosynthesis: purification of 4-N′-trimethylaminobutyraldehyde dehydrogenase from beef liver, J. Biol. Chem. 255 (1980) 1146–1151.
[25] F.M. Vaz, B. Melegh, J. Bene, D. Cuebas, D.A. Gage, A. Bootsma, P. Vreken, A.H. van Gennip, L.L. Bieber, R.J. Wanders. Analysis of carnitine biosynthesis metabolites in urine by HPLC–electrospray tandem mass spectrometry, Clin. Chem. 48 (2002) 826–834.
[26] J.H. Swiegers, F.M. Vaz, I.S. Pretorius, R.J. Wanders, F.F. Bauer. Carnitine biosynthesis in Neurospora crassa: identification of a cDNA coding for ε-N-trimethyllysine hydroxylase and its functional expression in Saccharomyces cerevisiae, FEMS Microbiol. Lett. 210 (2002) 19–23.
[27] F.M. Vaz, S.W. Fouchier, R. Ofman, M. Sommer, R.J. Wanders. Molecular and biochemical characterization of rat γ-trimethylaminobutyraldehyde dehydrogenase and evidence for the involvement of human aldehyde dehydrogenase 9 in carnitine biosynthesis, J. Biol. Chem. 275 (2000) 7390–7394.
[28] M.M. Bradford. A rapid and sensitive method for the quantitation of microgram quantities of protein utilizing the principle of protein–dye binding, Anal. Biochem. 72 (1976) 248–254.
[29] N. van Vlies, L. Tian, H. Overmars, A.H. Bootsma, W. Kulik, R.J. Wanders, P.A. Wood, F.M. Vaz. Characterization of carnitine and fatty acid metabolism in the long-chain acyl-CoA dehydrogenase-deficient mouse, Biochem. J. 387 (2005) 185–193.
[30] D.S. Sachan, H.P. Broquist, Synthesis of carnitine from ε-N-trimethyllysine in post mitochondrial fractions of Neurospora crassa, Biochem. Biophys. Res. Commun. 96 (1980) 870–875.
[31] A.L. Carter, T.O. Abney, H. Braver, A.H. Chuang. Localization of γ-butyrobetaine hydroxylase in the rat testis, Biol. Reprod. 37 (1987) 68–72.
[32] H.T. Haigler, H.P. Broquist. Carnitine synthesis in rat tissue slices, Biochem. Biophys. Res. Commun. 56 (1974) 676–681.
[33] C.J. Rebouche. Sites and regulation of carnitine biosynthesis in mammals, Fed. Proc. 41 (1982) 2848–2852.
[34] R. Stein, S. Englard. Properties of rat 6-N-trimethyl-l-lysine hydroxylases: similarities among the kidney, liver, heart, and skeletal muscle activities, Arch. Biochem. Biophys. 217 (1982) 324–331.
[35] C.J. Rebouche, L.J. Lehman, L. Olson. ε-N-Trimethyllysine availability regulates the rate of carnitine biosynthesis in the growing rat, J. Nutr. 116 (1986) 751–759.
[36] A.T. Davis, C.L. Hoppel. Effect of starvation on the disposition of free and peptide-linked trimethyllysine in the rat, J. Nutr. 116 (1986) 760–767.

Chapter 3

An improved enzyme assay for carnitine palmitoyl transferase I in fibroblasts using tandem mass spectrometry

N. van Vlies, J.P. Ruiter, M. Doolaard, R.J.A. Wanders, F.M. Vaz

Mol. Genet. Metab. 90 (2007) 24-29

Abstract

Carnitine palmitoyl transferase I (CPTI), which converts acyl-CoA and carnitine into acyl-carnitine and free CoASH, is the rate limiting enzyme of hepatic mitochondrial β-oxidation. CPTI-deficiency is a severe disorder characterized by Reye-like attacks with hypoketotic hypoglycemia, hepatomegaly, elevated liver enzymes and hyperammonemia. We developed a simple tandem-MS-based assay to measure CPTI activity in human fibroblasts. Surprisingly, a large part of the palmitoyl–carnitine formed in our assay by CPTI was degraded into C14- to C2-acyl-carnitines. Degradation of the product of CPTI leads to underestimation of the CPTI activity. When we used potassium cyanide to inhibit enzymes downstream of CPTI and thereby degradation of the product, we measured four times more CPTI activity than the previous methods. This inhibition is essential for correct calculation of CPTI activity. In fibroblasts of CPTI-deficient patients, CPTI activity was not detectable and this assay can be used for the diagnosis of CPTI-deficiency.

Introduction

Before activated long-chain fatty acids can be catabolized by the mitochondrial β-oxidation system, they must be first transported into the mitochondrial matrix. Since acyl-CoAs cannot cross the inner mitochondrial membrane, acyl-CoAs are first converted into the corresponding acyl-carnitine ester by Carnitine Palmitoyl Transferase I (EC 2.3.1.21, CPTI), an integral mitochondrial outer membrane protein. Subsequently, the acyl-carnitines are transported across the mitochondrial inner membrane by the carnitine/acyl-carnitine transporter (CACT). Finally, the acyl-carnitines are reconverted into their CoA-esters by Carnitine Palmitoyl Transferase II (CPTII) and the acyl-CoAs can enter the β-oxidation pathway [1, 2].

In liver, the activity of CPTI largely controls the flux through the mitochondrial β-oxidation pathway [3]. Hepatic CPTI activity is regulated by the concentration of malonyl-CoA, the first metabolite of fatty acid synthesis, which is produced from acetyl-CoA by the enzyme acetyl-CoA carboxylase. When glucose is plentiful, malonyl-CoA is produced and used for lipogenesis. The newly formed fatty acids are protected from oxidation through inhibition of CPTI by the high level of malonyl-CoA. Inhibition of CPTI, and therefore β-oxidation, is relieved when glucose levels fall and the hepatic malonyl-CoA concentration decreases [4].

Three genetically distinct isoforms of CPTI have been identified [5–9]. CPTI-a is the main isoform in liver, kidney, lung, spleen, intestine, pancreas, ovary, lymphocytes, and fibroblasts. CPTI-b is predominantly expressed in skeletal muscle, heart, adipose tissue, and testis. In brain both CPTI-a and CPTI-c are found. Low levels of the latter isoform are also detected in intestine, ovary and, testis [1, 9–12].

To date, only deficiencies of the CPTI-a isoform have been described. Patients typically present in infancy with Reye-like attacks with hypoketotic hypoglycemia, hepatomegaly, elevated liver enzymes and hyperammonemia [13]. CPTI-deficient patients usually have elevated levels of free carnitine accompanied by the absence of medium- and long-chain acyl-carnitines in plasma and blood [14, 15]. Definite diagnosis of CPTI deficiency requires enzyme analysis followed by sequence analysis of the CPTI-a gene. Patient’s fibroblasts usually show 0–20% of control CPTI activity [13].

To date, one mass spectrometric method [16] and several radiometric methods [1, 11, 17, 18] have been described to measure CPTI activity. Unfortunately, these methods are rather laborious; samples are repeatedly extracted with butanol to separate the product, palmitoyl-carnitine, from the substrate, palmitoyl-CoA.

Here we report a novel, fast tandem-mass spectrometric (MS) assay without elaborate extraction procedures. Furthermore, we show that in most of the previously described

methods CPTI activity has been underestimated and that inhibition of the mitochondrial β-oxidation pathway is essential for reliable and accurate measurement of CPTI activity.

Materials and methods

Chemicals

[U-^{13}C]-Palmitate was purchased from Advance Research Chemicals, CoASH from Roche, digitonin from Boehringer Mannheim. Carnitine, malonyl-CoA and D/L-octanoyl-carnitine were purchased from Sigma. D-Decanoyl-carnitine was a kind gift from the late J.D. McGarry (University of Texas Southwestern Medical Center, USA). The [$^2H_3$]-C3, [$^2H_3$]-C8 and [$^2H_3$]-C16-acyl-carnitines internal standards were obtained from Dr. Herman J. ten Brink (VU Medical Hospital, The Netherlands). [U-^{13}C]-palmitoyl-CoA was synthesized as described by Rasmussen *et al*. [19]. All other reagents were of analytical grade.

CPTI activity measurement

Human skin fibroblasts were cultured as described before [20]. Cells were harvested by trypsinization and were washed twice with phosphate buffered saline. The cell pellet was resuspended in 0.5 ml phosphate buffered saline and the protein concentration was determined using bicinchoninic acid [21], with bovine serum albumin as standard. The cell suspension was diluted with phosphate buffered saline to a concentration of 0.5 mg/ml.

The reaction mixture (final volume 250 μl) consisted of 150 mM KCl, 25 mM Tris, 2 mM EDTA, 20 mM potassium phosphate, 1 mg/ml bovine serum albumin, 4.5 mM reduced glutathione, 5 mM KCN, 50 μg/ml digitonin, 0.5 mM carnitine and 25 μM [U-^{13}C]-palmitoyl-CoA, pH 7.0. Reactions were started by adding 50 μl of fibroblast suspension (final protein concentration of 0.1 mg/ml, unless indicated otherwise) to the reaction mixture, followed by an incubation period of 10 min (unless indicated otherwise) at 37°C. To stop the reaction, 800 μl of acetonitrile was added and the reaction mixtures were placed on ice. Subsequently, the reaction mixtures were centrifuged at 16,000 × g for 5 min at 4°C and the supernatant was collected. 100 pmol [$^2H_3$]-C3-acyl-carnitine, 100 pmol [$^2H_3$]-C8-acylcarnitine and 300 pmol [$^2H_3$]-C16-acyl-carnitine internal standard was added to the supernatant, which was subsequently evaporated under a stream of nitrogen. 100 μl of propylation reagent (a 4:1 (v/v) mixture of 1-propanol and acetylchloride) was added to the residue, vortexed and incubated at 65°C for 15 min. The propylation reagent was evaporated under a stream of nitrogen and the residue was taken up in 100 μl acetonitrile, which was stored at -20°C until analysis. On the day of analysis 70 μl of the acetonitrile solution was mixed with 30 μl of distilled water and the samples were analyzed using tandem-MS.

Tandem-MS analysis

Each sample was analyzed twice. In the first run, the complete acyl-carnitine spectrum was analyzed, as described [22], to verify that only [U-^{13}C]-C16-carnitine was formed during the incubation. In the second run, the scan range for parent ions of 85 *m*/*z* was narrowed to 440–460 *m*/*z*, to accurately measure the [$^2H_3$]-C16-acyl-carnitine internal standard (445*m*/*z*) and the produced [U-^{13}C]-C16-carnitine (458*m*/*z*).

The ratio of the peak-height of [U-^{13}C]-C16-carnitine to the peak-height of [$^2H_3$]-C16-acyl-carnitine internal standard was determined using MassLynx NT software version 4.0 (Waters (Micromass), Manchester, UK). This ratio was used to calculate the concentration of [U-^{13}C]-C16-carnitine in each sample.

Validation

To determine the variation of the tandem-MS analysis, several control samples were pooled and this sample was analyzed 10 times in the same analytical run. To determine the intra-assay (within day) variation, CPTI activity was measured in one control fibroblast cell line cultured in 10 different flasks of the same passage number. For practical reasons, measurements were performed sequentially on the same day. To determine inter-assay (between day) variation, the CPTI activity was measured in the same control fibroblast cell line during 5 consecutive weeks (different passage numbers).

The detection limit was established by analyzing mixtures of a fixed concentration of [$^{2}H_{3}$]-palmitoyl-carnitine internal standard with unlabelled palmitoyl-carnitine in decreasing concentrations, assuming an identical response for palmitoyl-carnitine and [U-^{13}C]-palmitoyl-carnitine. 25 μg of fibroblast protein was added to these mixtures (in a final volume of 250 μl). Subsequently, 800 μl acetonitrile was added and the samples were processed as described above. To determine the recovery of the procedure, a known quantity of palmitoyl-carnitine was added to five reaction mixtures immediately after incubation (before the addition of acetonitrile) and to five reaction mixtures just before propylation.

In order to establish K_m values for palmitoyl-CoA and carnitine, the concentration of one compound was varied while the concentration of the other was kept constant.

Results

Development of the CPTI assay

The CPTI activity assays described to date are all rather laborious and usually involve the use of radio labeled substrate [1, 11, 16–18]. Because the product of CPTI, i.e., palmitoyl-carnitine, can be easily measured using tandem–MS [23], we investigated if we could develop a non-radioactive tandem-MS-based CPTI activity assay without elaborate extraction procedures.

In our assay we used intact fibroblasts, rather than sonicated cell homogenates as used by others [11, 16], and permeabilized the plasma membrane by adding digitonin in the reaction mixture. In initial experiments, no KCN was added to the reaction mixtures and unlabelled palmitoyl-CoA was used as substrate. After incubation, significant quantities of C14-, C12-, C10-, C8-, C6-, C4-, and C2-carnitine were observed, in addition to palmitoyl-carnitine (results not shown). These acyl-carnitines either could be endogenous acyl-carnitines or could be formed during the incubation. We synthesized [U-^{13}C]-C16-CoA to obtain a non-physiological substrate, which is converted into products (i.e. [U-^{13}C]-labeled acyl-carnitines) that can be discriminated from endogenous acylcarnitines. Surprisingly, considerable quantities of [U-^{13}C]-C14-, C12-, C10-, C8-, C6-, C4- and C2-carnitine were detected after 10 min incubation with 25 μM [U-^{13}C]-C16-CoA (figure 1). The fibroblasts also contained some endogenous C2-carnitine, but very low amounts of other acyl-carnitines.

While [U-^{13}C]-C16-carnitine is the product of CPTI, the other [U-^{13}C]-labeled acyl-carnitines are products of the combined actions of CPTI, CACT, CPTII and the enzymes of the β-oxidation pathway. The observed processing of the C16-carnitine, formed by CPTI, would lead to underestimation of the CPTI activity, because some of the product is converted into other substances. Therefore, we investigated if we could inhibit enzyme activities downstream of CPTI.

We used CACT-deficient fibroblasts (thereby ensuring that acyl-carnitines could not enter the mitochondria) to investigate whether it is possible to inhibit the degradation of C16-carnitine without inhibiting CPTI activity.

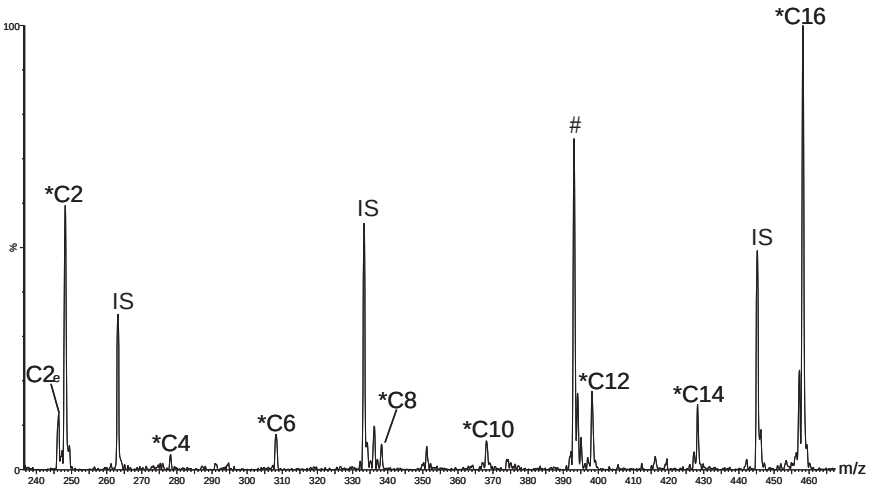

Figure 1. Acyl-carnitine spectrum of CPTI activity assay with [U-^{13}C]-palmitoyl-CoA as substrate. IS=internal standard. Acyl-carnitines denoted with * are [U-^{13}C]-labeled acyl-carnitines. The peak corresponding to endogenous acetyl-carnitine is indicated with 'C2e'. The peak indicated with # is not an acylcarnitine but derives from glutathione, which is present in the reaction mixture.

D-octanoyl-carnitine and D-decanoyl-carnitine, both claimed to be specific CACT inhibitors [24], and NEM, a non-specific inhibitor of mitochondrial carriers, all diminished CPTI activity (Table 1) and therefore were not suitable. Rotenone, antimycine A and KCN, inhibitors of the electron transport chain at the level of Complex I, III and IV, respectively, did not decrease CPTI activity, but in incubations with antimycine A or rotenone some [U-^{13}C]-C16- acyl-carnitine was converted into [U-^{13}C]-C14-acylcarnitine and [U-^{13}C]-C2-acyl-carnitine (approximately 1/5 of the amount of C16-carnitine, results not shown). Both antimycine A and rotenone were dissolved in DMSO, which may lead to permeabilization of the mitochondrial inner membrane and cause entry of the C16-acyl-carnitine into the mitochondrial matrix in the CACT-deficient fibroblasts. Indeed, when CPTI activity was measured in these fibroblasts in the presence of DMSO alone (final concentration 1%) [U-^{13}C]-C14-acyl-carnitine and [U-^{13}C]-C2-acylcarnitine were formed also (results not shown). Taken together, KCN was the only substance that did not affect CPTI activity or membrane integrity.

Table 1. CPTI activity in CACT-deficient fibroblasts with different inhibitors

	% C16-carnitine measured
No inhibitors	100
NEM (10 mM)	72
Antimycine A (0.5 mM)	100
KCN (2.5 mM)	100
Rotenone (0.5 mg/ml)	100
D-decanoyl-carnitine (1 mM)	42
D/L-octanoyl-carnitine (1mM)	84

Values are mean of two incubations. CPTI activity, measured when no inhibitors were added, was set at 100%.

Next, we used control fibroblasts to test if KCN in fact could inhibit degradation of C16-carnitine by incubating with increasing amounts of KCN. Considerable quantities of [U-^{13}C]-C14- to [U-^{13}C]-C2-acyl-carnitine could be measured when less than 1.25 mM KCN was added to the incubations (figure 2A). With 2.5 mM KCN or more, the amount of [U-^{13}C]-C14- to [U-^{13}C]-C2-acyl-carnitine formed decreased below 1% of the amount formed in the absence of KCN (figure 2A and B). For this reason, 5 mM KCN was added in subsequent experiments.

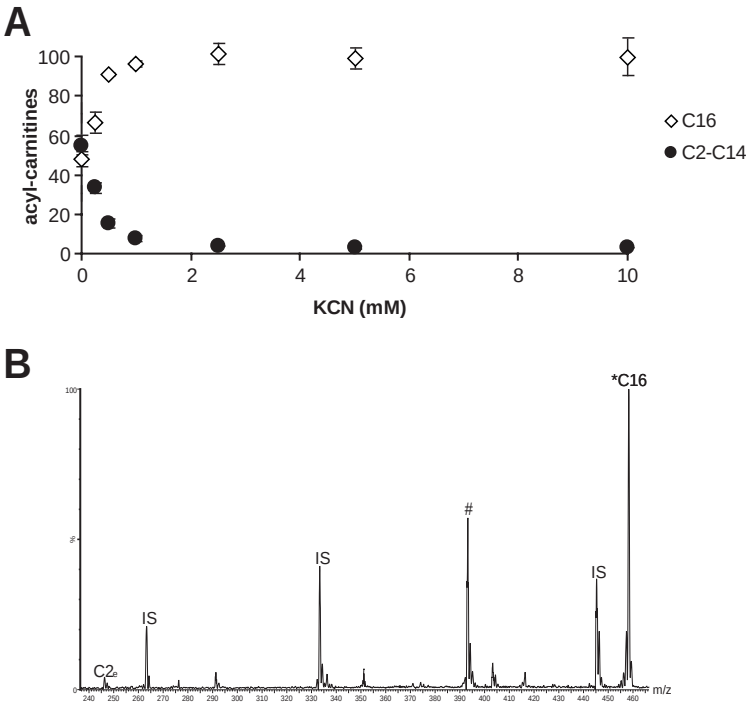

Figure 2. (A) KCN titration. Values are means ± standard deviation of two incubations. CPTI activity with 10 mM KCN was set at 100%. (B) Acyl-carnitine spectrum of CPTI activity assay with [U-^{13}C]-palmitoyl-CoA as substrate and 5 mM KCN in the reaction mixture. IS=internal standard. Acyl-carnitines denoted with * are [U-^{13}C]-labeled acyl-carnitines. The peak corresponding to endogenous acetyl-carnitine is indicated with 'C2e'. The peak indicated with # is not an acyl-carnitine but derives from glutathione, which is present in the reaction mixture.

Characterization and validation of the CPTI assay

To find optimal assay conditions, linearity with time and protein concentration was determined. CPTI activity in permeabilized fibroblasts was linear up to 20 min and proportional to the amount of protein up to 200 μg/ml (figure 3). In subsequent experiments fibroblasts were added to a final concentration of 100 μg/ml and incubated for 10 min.

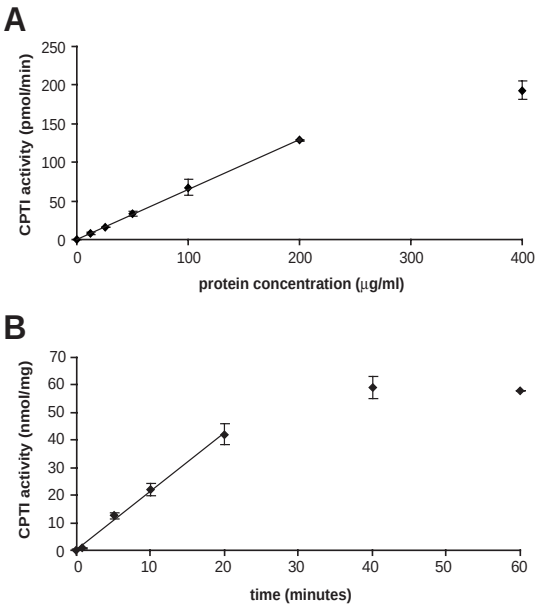

Figure 3. Protein and time dependence. Values are means ± standard deviation of two incubations. (A) Protein dependence. Incubation time was 10 min. (B) Time dependence. The final protein concentration was 100 μg/ml.

The intra-assay variation of the tandem-MS acyl-carnitine analysis was determined by injecting the same sample 10 times and was 6.7%. The intra-assay variation of the CPTI assay was determined by analyzing 10 samples on the same day, resulting in a variation of 11%. The inter-assay variation was determined by measuring the CPTI activity in the same control fibroblast cell line on 5 different days and was 15%. The detection limit (lowest signal with a signal to noise ratio of 3) of the tandem mass spectrometer was established to be 5 pmol

(which corresponds with 0.9% of control CPTI activity). The recovery of palmitoyl-carnitine was 85%.
In literature, CPTI activity is defined as the carnitine palmitoyl-CoA transferase activity that can be inhibited by malonyl-CoA. Therefore, samples are usually incubated with and without malonyl-CoA to correct for other transferase activities, such as CPTII (although in the digitonin-solubilized fibroblasts the inner mitochondrial membrane is intact [20] and CPTII should not have access to the substrate) and the peroxisomal Carnitine Octanoyl Transferase (EC 2.3.1.137).

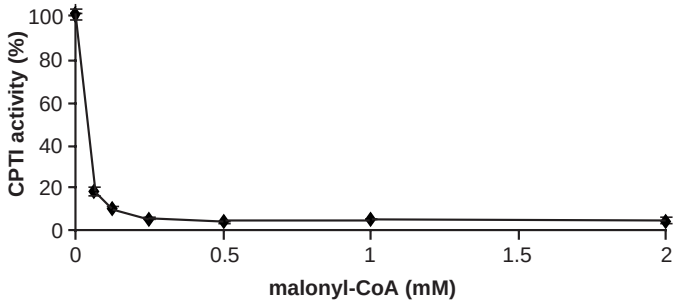

Figure 4. Malonyl-CoA titration. Values are mean ± standard deviation of two incubations. CPTI activity without malonyl-CoA was set at 100%.

When we measured CPTI activity in five control fibroblasts cell lines, 5% of the transferase activity could not be inhibited, even with 2 mM malonyl-CoA (figure 4). A CPTI activity of 2.18 ± 0.33 nmol × min^{-1} × mg^{-1} was measured in these control fibroblasts cell lines, which is considerably higher than the activity measured in two previously described CPTI activity assays in control fibroblasts (0.6 and 0.3 nmol × min^{-1} × mg^{-1} [16, 18]). K_m values for palmitoyl-CoA and carnitine were calculated using Lineweaver–Burk double-reciprocal plots and were 15 and 85 μM, respectively.
To test whether our new assay can be used to diagnose CPTI-deficient patients, we analyzed CPTI activity in fibroblast cell lines of five patients with CPTI-a deficiency [14, 18, 25]. No CPTI activity could be detected in these fibroblasts. Like in control fibroblasts, we did measure some residual transferase activity (approximately 5% of total transferase activity as measured in control fibroblasts), which also could not be inhibited by 2 mM malonyl- CoA (results not shown).

Discussion

Here we describe the development of a fast and easy tandem-MS based CPTI activity assay. When we compared our new method with a radiometric and the other mass spectrometric CPTI activity assay [16, 18] we found a 4-fold higher CPTI activity with our new method. The lower activity measured in the other methods is possibly due to enzymatic degradation of the palmitoyl-carnitine produced during incubation. When this degradation is not inhibited, the CPTI activity is underestimated considerably. Firstly, when β-oxidation is not inhibited, only half of the observed acyl-carnitines are palmitoyl-carnitine, the other acyl-carnitines are C14- to C2-carnitine, which originate from the palmitoyl-carnitine formed by CPTI. C2- and other short-chain acyl-carnitines are lost during butanol extraction, which is used in the CPTI assays described in literature for the extraction of palmitoyl-carnitine, and therefore do not contribute to the calculated CPTI activity. Secondly, even when the short-chain acyl-carnitines would be included in the calculation of the CPTI activity, underestimation can occur because not all acetyl-units generated by the β-oxidation of palmitoyl-carnitine are necessarily converted into acetyl-carnitine, but might enter the Krebs cycle. Degradation of the produced palmitoyl-carnitine, and thereby underestimation of CPTI activity, can be inhibited with KCN, a potent inhibitor of Complex IV of the respiratory chain. This inhibition

is essential for correct calculation of CPTI activity. We did not anticipate this to be so important, since the permeabilized fibroblasts constitute only a minor part in terms of volume of the 250 μl incubation volume. In fact, we had expected that the palmitoyl-carnitine produced by CPTI would diffuse into the incubation mixture instead of immediately entering the mitochondrial matrix and be converted into other substances. This suggests that in the permeabilized fibroblasts CPTI is in close contact with CACT, CPTII and the enzymes of the mitochondrial β-oxidation, as was shown for rat liver mitochondria by Fraser and Zammit [26].
When β-oxidation is not inhibited, the acyl-carnitine spectrum shows not only the product of CPTI but also the products of different β-oxidation enzymes. Therefore, this assay might also be used to identify mitochondrial β-oxidation defects; when the activity of one of the β-oxidation enzymes is absent or decreased specific acyl-carnitines are likely to accumulate.

In summary, we have developed a rapid and reliable assay for the measurement of CPTI activity, which will help in the identification of CPTI-deficient patients. An adaptation of this assay could also be used to identify other mitochondrial β-oxidation defects. This is currently under investigation.

Acknowledgments

The authors thank our mass spectrometry section for technical assistance.

References

[1] J.D. McGarry, N.F. Brown. The mitochondrial carnitine palmitoyltransferase system. From concept to molecular analysis, Eur. J. Biochem. 1 (1997) 1–14.
[2] R.R. Ramsay, R.D. Gandour, F.R. van der Leij. Molecular enzymology of carnitine transfer and transport, Biochim. Biophys. Acta 1 (2001) 21–43.
[3] S. Eaton. Control of mitochondrial beta-oxidation flux, Prog. Lipid Res. 3 (2002) 197–239.
[4] J.D. McGarry, G.F. Leatherman, D.W. Foster. Carnitine palmitoyltransferase I. The site of inhibition of hepatic fatty acid oxidation by malonyl-CoA, J. Biol. Chem. 12 (1978) 4128–4136.
[5] V. Esser, C.H. Britton, B.C. Weis, D.W. Foster, J.D. McGarry. Cloning, sequencing, and expression of a cDNA encoding rat liver carnitine palmitoyltransferase I. Direct evidence that a single polypeptide is involved in inhibitor interaction and catalytic function, J. Biol. Chem. 8 (1993) 5817–5822.
[6] C.H. Britton, R.A. Schultz, B. Zhang, V. Esser, D.W. Foster, J.D. McGarry. Human liver mitochondrial carnitine palmitoyltransferase I: characterization of its cDNA and chromosomal localization and partial analysis of the gene, Proc. Natl. Acad. Sci. USA. 6 (1995) 1984–1988.
[7] N. Yamazaki, Y. Shinohara, A. Shima, H. Terada. High expression of a novel carnitine palmitoyltransferase I like protein in rat brown adipose tissue and heart: isolation and characterization of its cDNA clone, FEBS Lett. 1–2 (1995) 41–45.
[8] N. Yamazaki, Y. Shinohara, A. Shima, Y. Yamanaka, H. Terada. Isolation and characterization of cDNA and genomic clones encoding human muscle type carnitine palmitoyltransferase I, Biochim. Biophys. Acta 2 (1996) 157–161.
[9] N. Price, F. van der Leij, V. Jackson, C. Corstorphine, R. Thomson, A. Sorensen, V. Zammit. A novel brain-expressed protein related to carnitine palmitoyltransferase I, Genomics 4 (2002) 433–442.
[10] N.F. Brown, J.K. Hill, V. Esser, J.L. Kirkland, B.E. Corkey, D.W. Foster, J.D. McGarry. Mouse white adipocytes and 3T3-L1 cells display an anomalous pattern of carnitine palmitoyltransferase (CPT) I isoform expression during differentiation. Inter-tissue and inter-species expression of CPT I and CPT II enzymes, Biochem. J. (1997) 225–231.
[11] F. Demaugre, J.P. Bonnefont, G. Mitchell, N. Nguyen-Hoang. A. Pelet, M. Rimoldi, S. Di Donato, J.M. Saudubray, Hepatic and muscular presentations of carnitine palmitoyl transferase deficiency: two distinct entities, Pediatr. Res. 3 (1988) 308–311.
[12] V. Esser, N.F. Brown, A.T. Cowan, D.W. Foster, J.D. McGarry. Expression of a cDNA isolated from rat brown adipose tissue and heart identifies the product as the muscle isoform of carnitine

palmitoyltransferase I (M-CPT I). M-CPT I is the predominant CPT I isoform expressed in both white (epididymal) and brown adipocytes, J.Biol. Chem. 12 (1996) 6972–6977.
[13] J.P. Bonnefont, F. Djouadi, C. Prip-Buus, S. Gobin, A. Munnich, J. Bastin. Carnitine palmitoyltransferases 1 and 2: biochemical, molecular and medical aspects, Mol. Aspects Med. 5–6 (2004) 495–520.
[14] R. Fingerhut, W. Roschinger, A.C. Muntau, T. Dame, J. Kreischer, R. Arnecke, A. Superti-Furga, H. Troxler, B. Liebl, B. Olgemoller, A.A. Roscher. Hepatic carnitine palmitoyltransferase I deficiency: acylcarnitine profiles in blood spots are highly specific, Clin. Chem. 10 (2001) 1763–1768.
[15] K.G. Sim, V. Wiley, K. Carpenter, B. Wilcken. Carnitine palmitoyltransferase I deficiency in neonate identified by dried blood spot free carnitine and acylcarnitine profile, J. Inherit. Metab. Dis. 1 (2001) 51–59.
[16] L. Nolte, F.H. van der Westhuizen, P.J. Pretorius, E. Erasmus. Carnitine palmitoyltransferase I activity monitoring in fibroblasts and leukocytes using electrospray ionization mass spectrometry, Anal. Biochem. 2 (1998) 178–184.
[17] J. Bremer. Carnitine In Intermediary Metabolism. The Biosynthesis Of Palmitylcarnitine By Cell Subfractions, J. Biol. Chem. (1963) 2774–2779.
[18] L. IJlst, H. Mandel, W. Oostheim, J.P. Ruiter, A. Gutman, R.J. Wanders. Molecular basis of hepatic carnitine palmitoyltransferase I deficiency, J. Clin. Invest. 3 (1998) 527–531.
[19] J.T. Rasmussen, T. Borchers, J. Knudsen. Comparison of the binding affinities of acyl-CoA-binding protein and fatty-acidbinding protein for long-chain acyl-CoA esters, Biochem. J. 3 (1990) 849–855.
[20] R.J. Wanders, J.P. Ruiter, F.A. Wijburg. Studies on mitochondrial oxidative phosphorylation in permeabilized human skin fibroblasts: application to mitochondrial encephalomyopathies, Biochim. Biophys. Acta 3 (1993) 219–222.
[21] P.K. Smith, R.I. Krohn, G.T. Hermanson, A.K. Mallia, F.H. Gartner, M.D. Provenzano, E.K. Fujimoto, N.M. Goeke, B.J. Olson, D.C. Klenk. Measurement of protein using bicinchoninic acid, Anal. Biochem. 1 (1985) 76–85.
[22] N. van Vlies, L. Tian, H. Overmars, A.H. Bootsma, W. Kulik, R.J. Wanders, P.A. Wood, F.M. Vaz. Characterization of carnitine and fatty acid metabolism in the long-chain acyl-CoA dehydrogenasedeWficient mouse, Biochem. J. (2005) 185–193.
[23] P. Vreken, A.E.M. van Lint, A. Bootsma, H. Overmars, R.J. Wanders, A.H. Gennip. Quantitative plasma acylcarnitine analysis using electrospray tandem mass spectrometry for the diagnosis of organic acidaemias and fatty acid oxidation defects, J. Inherit. Metab. Dis. (1999) 302–306.
[24] L. Baillet, R.S. Mullur, V. Esser, J.D. McGarry. Elucidation of the mechanism by which (+)-acylcarnitines inhibit mitochondrial fatty acid transport, J. Biol. Chem. 47 (2000) 36766–36768.
[25] S.H. Korman, H.R. Waterham, A. Gutman, C. Jakobs, R.J. Wanders. Novel metabolic and molecular findings in hepatic carnitine palmitoyltransferase I deficiency, Mol. Genet. Metab. 3 (2005) 337–343.
[26] F. Fraser, V.A. Zammit. Enrichment of carnitine palmitoyltransferases I and II in the contact sites of rat liver mitochondria, Biochem. J. (1998) 225–229.

Chapter 4

Characterization of carnitine and fatty acid metabolism in the long-chain acyl-CoA dehydrogenase-deficient mouse

N. van Vlies, L. Tian, H. Overmars, A.H. Bootsma, W. Kulik, R.J.A. Wanders, P.A. Wood, F.M. Vaz

Biochem. J. 387 (2005) 185-193

Abstract

In the present paper, we describe a novel method which enables the analysis of tissue acyl-carnitines and carnitine biosynthesis intermediates in the same sample. This method was used to investigate the carnitine and fatty acid metabolism in wild-type and long-chain acyl-CoA dehydrogenase-deficient (LCAD-/-) mice. In agreement with previous results in plasma and bile, we found accumulation of the characteristic C14:1-acyl-carnitine in all investigated tissues from LCAD-/- mice. Surprisingly, quantitatively relevant levels of 3-hydroxy-acyl-carnitines were found to be present in heart, muscle and brain in wild-type mice, suggesting that, in these tissues, long-chain 3-hydroxy-acyl-CoA dehydrogenase is rate-limiting for mitochondrial β-oxidation. The 3-hydroxy-acyl-carnitines were absent in LCAD-/- tissues, indicating that, in this situation, the β-oxidation flux is limited by the LCAD deficiency. A profound deficiency of acetyl-carnitine was observed in LCAD-/- hearts, which most likely corresponds with low cardiac levels of acetyl-CoA. Since there was no carnitine deficiency and only a marginal elevation of potentially cardiotoxic acyl-carnitines, we conclude from these data that the cardiomyopathy in the LCAD-/- mouse is caused primarily by a severe energy deficiency in the heart, stressing the important role of LCAD in cardiac fatty acid metabolism in the mouse.

Introduction

Carnitine (3-hydroxy-4-N,N,N-trimethylaminobutyrate) is a vital compound that plays an indispensable role in fatty acid metabolism. Before activated fatty acids, i.e. acyl-CoAs, can be broken down, they must first be transported into the mitochondrial matrix, where β-oxidation takes place. Because cytosolic acyl-CoAs cannot cross the inner mitochondrial membrane, acyl-units are transferred from CoASH (reduced CoA) to carnitine and transported as acyl-carnitine esters into the matrix by a dedicated carrier protein [1, 2]. In the matrix, the acyl-groups of the acyl-carnitines are transferred back from carnitine to CoASH, and the resulting acyl-CoAs can then undergo β-oxidation. Free carnitine can be transported back to the cytosol for another round of import, but can also be used to transport acyl-units out of the mitochondria [1, 3, 4]. This reversible acylation of carnitine allows replenishment of the free CoA pool when acyl-CoAs accumulate, for example in the case of mitochondrial β-oxidation disorders. Additionally, production of acyl-carnitines can be used to export toxic acyl-groups as acyl-carnitines, first out of mitochondria and cell, followed by excretion from the body via urine or bile [5, 6].

Omnivorous humans obtain carnitine both via the diet (meat and dairy products) and through endogenous synthesis. The first step in the carnitine biosynthesis in the hydroxylation of 6-*N*-trimethyl-lysine (TML) to 3-hydroxy-6-*N*-trimethyllysine (HTML), which is subsequently cleaved to yield 4-trimethylaminobutyraldehyde (TMABA). TMABA is converted into 4-trimethylaminobutyric acid (γ-butyrobetaine), which then is hydroxylated to carnitine [4]. The role of the carnitine biosynthetic pathway in overall carnitine homeostasis, especially in case of disturbed fatty acid metabolism, such as in mitochondrial β-oxidation disorders, remains poorly understood.

In recent years, several mouse models for mitochondrial β-oxidation defects have been generated [7] including the long-chain acyl-CoA dehydrogenase-deficient (LCAD-/-) mouse. LCAD is one of five enzymes that catalyse the α,β-dehydrogenation of acyl-CoAs, the initial step of mitochondrial β-oxidation. LCAD has been shown to be involved in the degradation of branched-chain fatty acids originating from peroxisomal catabolism of phytanic acid, but LCAD is also able to handle straight-chain and certain monounsaturated acyl-CoAs [8–10]. The phenotype of the LCAD-/- mouse is most similar to human very-long-chain acyl-CoA

dehydrogenase (VLCAD) deficiency, and is characterized by unprovoked sudden death, fasting and cold intolerance, hypoketotic hypoglycaemia, and marked fatty changes in liver and heart [7, 11]. No human deficiency of LCAD has been described so far. LCAD-/- mice have been shown to accumulate C12- and C14-acyl-carnitines in bile and serum [7, 12]. Although plasma and bile acyl-carnitine levels were determined in LCAD-/- mice, it is not known how LCAD deficiency affects carnitine metabolism in tissues, since no method is available to determine the tissue levels of carnitine metabolites, i.e. acyl-carnitines and carnitine biosynthesis intermediates.

To investigate carnitine metabolism and its regulation in normal and pathological conditions, quantification of the metabolites involved in carnitine metabolism in body fluids and tissues is of great importance. Several methods have been described for the measurement of acyl-carnitines in plasma, urine, bile and tissues [13–18]. Tissue acyl-carnitine analysis, however, has been restricted to the measurement of large subsets, e.g. free carnitine and short-, medium- and long-chain acyl-carnitines [13, 14]. Until now, no method has been described to determine the whole tissue acyl-carnitine spectrum. We devised a novel sample work-up procedure, and slightly modified the established tandem-MS detection method, which now enables the determination of discrete acyl-carnitines in tissues by tandem-MS. We also adapted this procedure to measure the levels of the carnitine biosynthesis intermediates in the same tissue sample, using a modification of our recently developed method for the analysis of carnitine biosynthesis intermediates in urine [19].

This new method was used to determine the effects of LCAD deficiency on carnitine metabolites in tissues and plasma. Our results show considerable differences in tissue carnitine content and acylation between the wild-type and LCAD-/- mice. In addition to the expected C14:1-acyl-carnitine accumulation, the acyl-carnitine pattern in wild-type and LCAD-/- mice in the different tissues unveils some of the specific metabolic conditions that exist in different tissues.

Materials and methods

Chemicals

The [$^2H_3$]-carnitine and [$^2H_3$]-C3-, C8- and C16-acyl-carnitine internal standards were obtained from Dr Herman J. ten Brink (VU Medical Hospital, Amsterdam, The Netherlands). The [$^2H_9$]-TML and γ-[$^2H_3$]-butyrobetaine internal standards were synthesized as described previously [19]. [$^2H_9$]-HTML was prepared enzymatically by incubating [$^2H_9$]-TML with *Neurospora crassa* TML dioxygenase, which was heterologously expressed in *Saccharomyces cerevisiae* as described by Swiegers *et al*. [20]. The resulting mixture of [$^2H_9$]-HTML and [$^2H_9$]-TML was applied to Microcon YM30 filters, and the deproteinized filtrate was used as an internal standard for TML and HTML. All other reagents were of analytical grade.

Animals

B6,129-*Acadl*-/- (LCAD-/-) and B6,129 *Acadl*+/+ (wild-type) mice were produced in a breeding colony at the University of Alabama at Birmingham. All experiments were approved by the local ethical committee. They were genotyped as described previously [12]. All experimental mice were male and 7–9 weeks of age at the time of sample collection. All mice were fed with a standard rodent diet (LM-485; Harlan Teklad). Mice were fasted for 7 h during the dark cycle and humanely killed for tissue collection. Tissues were immediately flash-frozen in liquid nitrogen.

Sample preparation for acyl-carnitine and carnitine biosynthesis intermediate determination in tissues

Approx. 20 mg of cardiac left ventricle and 60 mg of the other tissues (liver, kidney, brain, muscle and testis) were placed in 1.5 ml Eppendorf vials, and the exact mass of the sample was determined using a microbalance. The internal standards for both the acyl-carnitines and the carnitine biosynthesis intermediates were added (see table 1). [$^2H_3$]-carnitine was used as internal standard for free carnitine, [$^2H_3$]-C3-acyl-carnitine for C2- to C5-acyl-carnitines, [$^2H_3$]-C8-acyl-carnitine for C6- to C10-acyl-carnitines and [$^2H_3$]-C16-acyl-carnitine for C12- to C22-OH-acyl-carnitine. Because of the lack of a commercially available labelled very-long-chain acyl-carnitine internal standard, the [$^2H_3$]-C16-acyl-carnitine internal standard was used to approximate the levels of the C20- to C22-OH-acyl-carnitines. [$^2H_9$]-TML, [$^2H_9$]-HTML and γ-[$^2H_3$]-butyrobetaine were used as internal standards for TML, HTML and γ-butyrobetaine, respectively. The samples were freeze-dried overnight. The freeze-dried tissues were kept on ice and grounded to powder using an Eppendorf micropestle. A 1 ml volume of an 8:2 (v/v) acetonitrile/water solution (80% acetonitrile) was added to the tissue powder, and this suspension was sonicated twice for 20 s at 2.5 W with a probe-tip vibra-cell sonicater (Sonics & Materials, Danburry, CT, U.S.A.). Subsequently, the samples were centrifuged at 16000 × *g* for 5 min at 4°C, and the supernatant was collected. Half of this 80% acetonitrile supernatant was used for the acyl-carnitine analysis, and the other half was used for the analysis of carnitine biosynthesis intermediates (see below).

Table 1. Internal standards added to the different tissues

	Liver/Heart/Testis	Kidney/ Muscle	Brain	Plasma
[$^2H_3$]-Carnitine	16.25	6.25	6.25	1.175
[$^2H_3$]-C_3	0.25	0.125	0.125	0.25
[$^2H_3$]-C_8	0.1	0.05	0.05	0.1
[$^2H_3$]-C_{16}	0.05	0.25	0.1	0.1
[$^2H_9$]-TML	0.375	0.11	0.11	0.18
[$^2H_9$]-HTML	0.18	0.18	0.18	0.075
[$^2H_3$]-γ-BB	0.075	0.075	0.075	0.11

Values are in nmol.

Acyl-carnitine analysis in tissues, plasma and urine

Half of the 80% acetonitrile supernatant was evaporated under a stream of nitrogen at 40 °C. A 100 µl volume of propylation reagent, a 4:1 (v/v) mixture of 2-propanol and acetylchloride, was added to the residue, vortex-mixed and incubated at 65°C for 15 min. The propylation reagent was evaporated under a stream of nitrogen at 40°C, and the residue was taken up in 300 µl of acetonitrile, which was stored at -20°C until analysis. Plasma and urine samples were prepared as described previously [15], except that propylation reagent was used instead of butylation reagent, and samples were stored in acetonitrile at -20°C until analysis. On the day of analysis, 70 µl of the acetonitrile solution was mixed with 30 µl of distilled water. A Quattro II triple-quadrupole mass spectrometer (Micromass, Manchester, U.K.), using a Gilson 231XL autosampler and a Hewlett-Packard HP-1100 HPLC pump was used for detection of the acyl-carnitines. Collision energies, cone voltages and other mass spectrometric details are described by Rashed *et al*. [21]. To detect all the propylated acyl-carnitines, the scan range for parent ions of *m*/*z* 85 was enlarged to *m*/*z* 180–600. For the quantification of the acyl-carnitine levels, the area under each acyl-carnitine peak (A_{AC}) and that under the added internal standard (A_{IS}), used for that particular acyl-carnitine, was quantified using MassLynx 3.3 (Micromass). If appropriate, the peak areas were corrected for the contribution of naturally occurring isotopes. Assuming identical response to the

appropriate internal standard, semi-quantitative analysis of acyl-carnitines and hydroxyacyl-carnitines was carried out by determining the ratio (A_{AC}/A_{IS}) and multiplying this by the amount of added internal standard. To compare individual samples, the result was normalized for creatinine concentration in the case of urine, and for wet tissue mass in the case of tissues.

Carnitine biosynthesis intermediate analysis in tissues, plasma and urine

To extract the carnitine biosynthesis intermediates efficiently, the remaining tissue powder pellet (after the 80% acetonitrile extraction) was extracted for a second time with 500 μl of an 2:8 (v/v) acetonitrile/water solution (20% acetonitrile) as described in the previous section. Half of the 20% acetonitrile supernatant was pooled with the remaining half of the 80% acetonitrile supernatant, and this solution was evaporated under a stream of nitrogen at 40°C. The residue was resuspended in 100 μl of distilled water, and carnitine biosynthesis intermediates were analysed with ion-pair HPLC tandem MS and quantified as described previously [19].

To determine the concentration of the carnitine biosynthesis intermediates in plasma, internal standards (see table 1) were added to 100 μl of plasma, and this mixture was partly deproteinized by loading it onto a Microcon 30 kDa filter, which was centrifuged at 14000 × *g* for 20 min at 4°C. An 80 μl volume of filtrate was derivatized and analysed with tandem MS as described previously [19]. This method, without the filtration step, was also used for the analysis of the carnitine biosynthesis intermediates in urine.

Validation

For the determination of the recovery of the internal standards, six pieces of each tissue were prepared, and both acyl-carnitine and carnitine biosynthesis intermediate internal standards were added to three of these, after which the extraction procedure was performed as described above for all six samples. Before the first evaporation step, internal standards for acyl-carnitines and carnitine biosynthesis intermediates were added to the three samples where addition of internal standard had been omitted. The recovery of the internal standards was used as a measure for the recovery of the endogenous compounds.

The variation within one mouse was determined by analysing the acyl-carnitine and carnitine biosynthesis intermediate levels in six different pieces of each tissue of a single mouse. The variation between mice was determined by analysing each tissue (in duplicate) in six different mice.

Enzyme assays

Carnitine Palmitoyl Transferase II (CPTII) activity was measured as described by Slama *et al*. [22]. Carnitine Acetyl Transferase (CAT) activity was measured as described by Barth *et al*. [23]. TML dioxygenase was measured as described by Vaz *et al*. [24] and the γ-butyrobetaine dioxygenase assay was reported previously by Vaz *et al*. [25].

Comparison of wild-type and LCAD-/- mice

Carnitine metabolites (acyl-carnitines and carnitine biosynthesis intermediates) were analysed in duplicate in tissues of six LCAD-/- mice, and results were compared with the wild-type data obtained in the validation experiments. In a separate experiment, three wild-type and three LCAD-/- mice were fasted as described above, and urine and plasma were collected for carnitine metabolite analysis.

Immunoblot analysis

A Multiphor II Nova Blot electrophoretic transfer unit (Amersham Biosciences) was used to transfer proteins on to a nitrocellulose sheet (Schleicher & Shuell, Dassel, Germany) as

described by the manufacturer of the transfer unit. After blocking of non-specific binding sites with 50 g/l Protifar and 10 g/l BSA in PBS with Tween 20 (1 g/l) for 1 h, the blot was incubated for 2 h with a 1:5000 dilution of rabbit polyclonal antibody against VLCAD in the same buffer without Protifar. The anti-VLCAD antibody [26] was a gift from Dr T. Hashimoto (Shinshu University, Mastumoto, Japan). Goat anti-rabbit IgG antibodies conjugated to alkaline phosphatase were used for detection, according to the manufacturer's instructions (Bio-Rad, Hercules, CA, U.S.A.).

Statistical analysis

The Mann–Whitney test was used to evaluate whether significant differences exist between the LCAD-/- and wild-type carnitine metabolite levels.

Results and Discussion

Method development

To develop a new method for the extraction and efficient measurement of acyl-carnitines from tissues, several issues had to be addressed. In initial experiments, aqueous homogenates were prepared followed by simultaneous deproteinization and extraction with acetonitrile. Besides the fact that preparing aqueous homogenates of tissues such as muscle and heart is difficult and not practical for large-scale sample work-up, the extraction efficiency of long-chain acyl-carnitines was poor. Freeze-drying of the sample turned out to solve both problems. This procedure results in a brittle sample, which can be ground easily to powder and used for immediate solid–fluid extraction with a high percentage acetonitrile solution. This method resulted in an efficient extraction of all acyl-carnitines.

Another problem was the interference of glutamic acid with the quantification of acetyl-carnitine, a quantitatively important acyl-carnitine. When samples are butylated, as in the commonly used plasma method [15], both acetyl-carnitine and glutamic acid produce a parent ion of *m*/*z* 260, with a daughter fragment of 85 Da upon collision. Using the parent-scan for *m*/*z* 85, the abundance of *m*/*z* 260 can result from both compounds. Since tissues (especially brain) contain considerable amounts of glutamic acid, reliable quantitative analysis of acetyl-carnitine is impossible using butylation. When samples are propylated instead, acetyl-carnitine and glutamic acid produce parent ions which differ by 14 Da in mass: glutamic acid is a dicarboxylic acid and is propylated at two carboxylic groups, which results in a molecule with an $[M+H]^+$ ion of 232 Da. Acetyl-carnitine, however, only contains one carboxylic group, and its propylation yields an $[M+H]^+$ ion of 246 Da. Both compounds can now be detected separately in the parent-scan of *m*/*z* of 85.

Beside acyl-carnitines, we also wanted to analyse the carnitine biosynthesis intermediates in different tissues. Preliminary experiments showed that extraction of carnitine biosynthesis intermediates was most efficient with low concentrations of acetonitrile, whereas extraction with high concentrations of acetonitrile was best for acyl-carnitines. Initial extraction of the tissue powder with high concentrations of acetonitrile, however, did not affect the subsequent low-acetonitrile extraction of the carnitine biosynthesis intermediates. This enabled analysis of both acyl-carnitines and carnitine biosynthesis intermediates in the same tissue sample.

Validation

As an estimation of the recovery of the endogenous acyl-carnitines and carnitine biosynthesis intermediates, we investigated the recovery of the internal standards. By adding the internal standards, either at the beginning or at the end of the work-up procedure, and analysing the difference between the internal standard levels in these samples, the recovery of the internal standards was determined for each tissue. The amount of internal standard, added at the end

of the procedure, was set at 100%. For [$^2H_9$]-TML, [$^2H_9$]-HTML and γ-[$^2H_3$]-butyrobetaine internal standards, the recovery was more than 75% in all tissues. The recovery of [$^2H_3$]-carnitine and [$^2H_3$]-C3-, [$^2H_3$]-C8- and [$^2H_3$]-C16-acyl-carnitines was more than 70% in all tissues except testis, where 40–70% of all acyl-carnitine internal standards were recovered.
The inter-assay variation for the different tissue acyl-carnitines and carnitine biosynthesis intermediates was determined to be 30% or less for most compounds. The intra-assay variation was within acceptable limits (<30%). No intra-assay variation could be determined for plasma due to the small quantity of plasma available; however, previous studies have shown that the variation of acyl-carnitine analysis in plasma is small [15].
After validation, this new method was used to investigate the differences in carnitine metabolism between wild-type and LCAD-/- mice. First, the results of the acyl-carnitine and carnitine biosynthesis intermediates analysis from the wild-type mice will be discussed, after which these will be compared with the results obtained for the LCAD-/- mice.

Tissue distribution of carnitine metabolites in wild-type mice
In the wild-type mouse, considerable differences exist between tissues with respect to the carnitine content and acylation pattern, as can be seen in figures 1 and 2 (grey bars). Normalized per gram of wet mass, most carnitine (both free and acylated) is found in heart, followed by kidney, muscle, testis, liver and brain. In heart, approx. 25% of total carnitine is present as acyl-carnitines, primarily as acetyl-carnitine. In muscle, more than 50% of total carnitine is present as acyl-carnitines, of which half is acetyl-carnitine. A striking difference in both the percentage of acylation and the spectrum of long-chain acyl-carnitines exists between heart and muscle. The latter tissue contains primarily C16- and C18:1-acyl-carnitines, which are present in high amounts (28.7 ± 7.8 and 19.2 ± 9.7 nmol/g respectively). Heart, however, contains less acyl-carnitine (individual acyl-carnitines are in the range 1–3 nmol/g), but these encompass the whole spectrum of medium-/long-chain acyl-carnitines, varying from C12- to even C20- and C22-acyl-carnitines (figure 2, grey bars). The accumulation of long-chain acyl-carnitines in muscle could perhaps reflect the discontinuous activity of muscle as opposed to the continuous work of the heart and the corresponding energy demand. The muscle acyl-carnitines could represent stored energy units which can be readily used upon muscle activity.

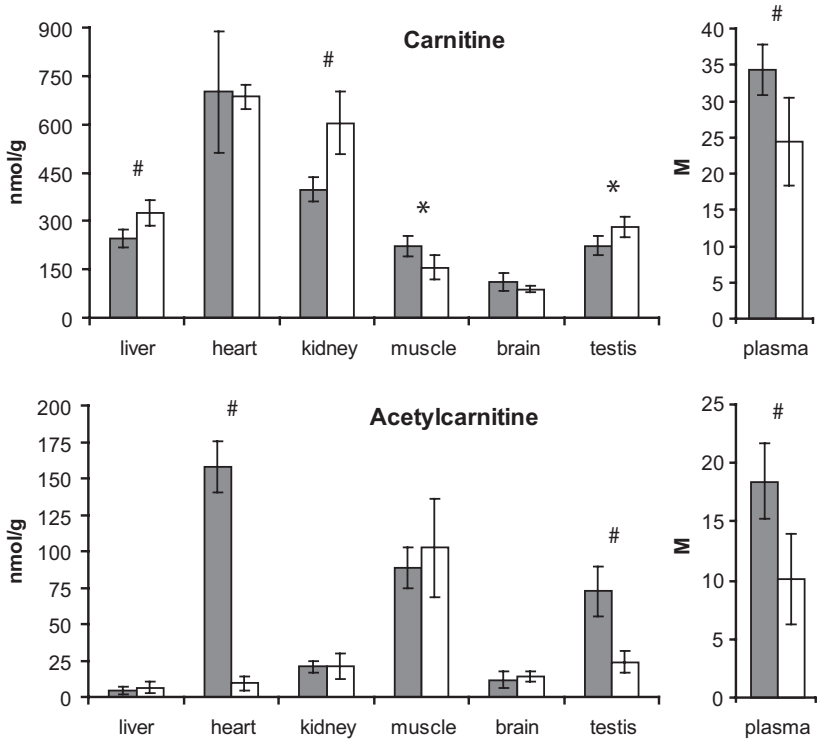

Figure 1: Tissue and plasma levels of free carnitine and acetyl-carnitine in wild-type and LCAD-/- mice. Grey bars and white bars represent wild-type and LCAD-/- mice, respectively. Values are average ± standard deviation of six mice, where each tissue was analyzed in duplicate. Only one plasma analysis per mouse was performed due to the small amount of sample available.
* indicates $p<0.05$ and # indicates $p<0.01$.

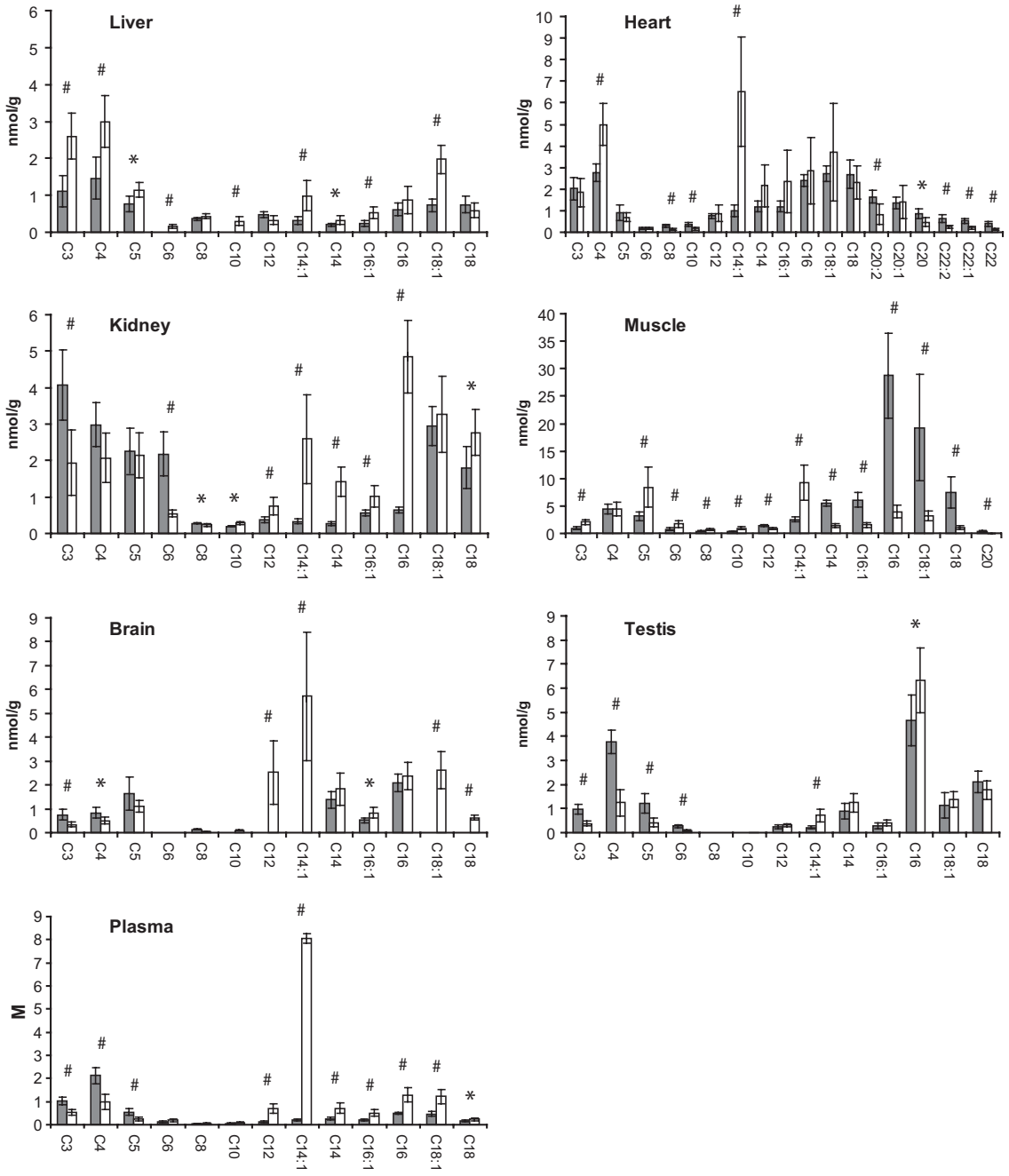

Figure 2: Tissue and plasma acyl-carnitine levels in wild-type and LCAD-/- mice. Grey bars and white bars represent wild-type and LCAD-/- mice, respectively. Values are average ± standard deviation of six mice, where each tissue was analyzed in duplicate. Only one plasma analysis per mouse was performed due to the small amount of sample available. * indicates $p<0.05$ and # indicates $p<0.01$.

An interesting finding was the presence of relatively high amounts of long-chain hydroxyl-acyl-carnitines in heart (figure 3, grey bars), which, in most cases, were even more abundant than the corresponding acyl-carnitines. Hydroxy-acyl-carnitines were also found in muscle and brain (figure 3, grey bars). Surprisingly, in brain, C12-OH-, C14:1-OH- and C18-OH-to C22-OH-acyl-carnitines were present, whereas their corresponding acyl-carnitines were not detectable. The observed hydroxyl-acyl-carnitines most likely represent 3-hydroxy β-oxidation intermediates, but mass spectrometric detection does not allow identification of the position of the hydroxyl-group.

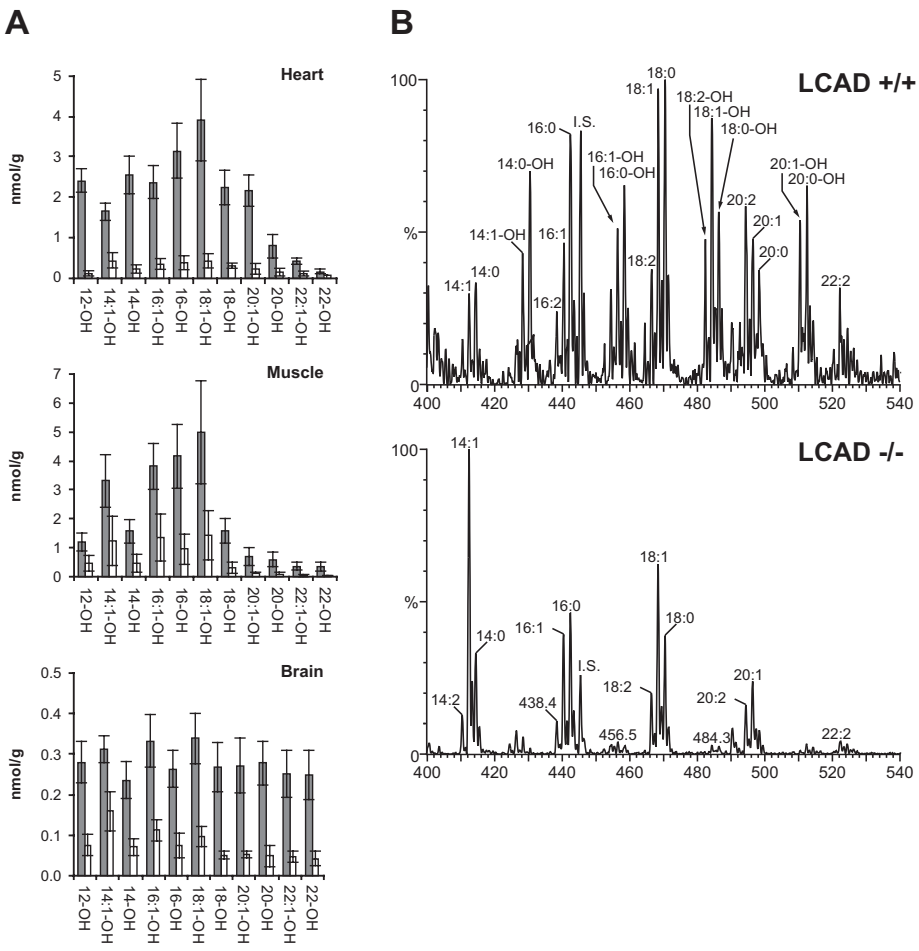

Figure 3: Hydroxy-acyl-carnitine levels in heart, muscle and brain in wild-type and LCAD-/- mice. A; Grey bars and white bars represent wild-type and LCAD-/- mice, respectively. Values are average ± standard deviation of six mice, where each tissue was analyzed in duplicate. All the differences between wild-type and LCAD-/- mice were determined to be significant ($p<0.01$). B; Parent scan of m/z 85, showing the acylcarnitine spectrum of wild-type and LCAD-/- mice in heart. Note the presence of high levels of hydroxyl-acylcarnitines in the wild-type heart and their dramatic reduction in LCAD-/- mice. The peak at m/z 445 corresponds to the internal standard [$^2H_3$]-C16.

As in previous studies, plasma acyl-carnitines represent approx. 40% of total plasma carnitine and consist mostly of acetyl-carnitine and C16-acyl-carnitine. Liver has the smallest fraction of acyl-carnitines, followed by kidney and brain.

The levels of the carnitine biosynthesis intermediates are shown in figure 4 (grey bars). The TML content is similar in all tissues except for kidney, where this compound is more abundant. In mice, TML is readily reabsorbed from the urine [27], which could explain the higher levels of this compound in kidney. No HTML was found in any of the tissues studied, which is probably caused by rapid conversion of HTML into TMABA and γ-butyrobetaine. γ-butyrobetaine levels do not differ much between the studied tissues, but are the lowest in liver. This might be explained by the presence of γ-butyrobetaine dioxygenase in this organ, which rapidly converts γ-butyrobetaine into carnitine.

Comparison of wild-type and LCAD-/- mice

Although free carnitine levels are somewhat decreased in muscle and brain (see figure 1), the LCAD-/- mice do not display carnitine deficiency, which has been reported in several human β-oxidation disorders, supposedly as a result of the excretion of non-metabolizable acyl units as acyl-carnitines [28]. Liver, testis and, especially, kidney even show an increase in free carnitine content. Possibly hepatic carnitine biosynthesis is increased and the renal reabsorption of carnitine is enhanced in LCAD-/- mice, which would counteract the loss of carnitine due to elimination of accumulating acyl-carnitines. This is supported by the observation that the kidney has a significantly higher carnitine content, suggesting that carnitine is efficiently reabsorbed. Also, tissue TML levels are generally lower in the LCAD-/- tissues (figure 4), indicating that this compound is used for carnitine synthesis. The TML

levels in kidney are dramatically reduced. This could be a result of increased TML dioxygenase activity, which is present in this tissue. We excluded this possibility by measuring TML dioxygenase activity in wild-type and LCAD-/- kidney, which did not differ between wild-type and LCAD-/- mice (12.0 ± 2.0 (n=6) and 11.6 ± 0.7 (n=6) pmol × min^{-1} × mg^{-1}, respectively). Alternatively, TML excretion could be enhanced, resulting in lower tissue and kidney TML levels. Unfortunately, urine was not available to measure carnitine and TML excretion. Therefore we repeated the experiment, collected urine and plasma, and analysed carnitine metabolites in these samples. As in the previous experiment, the same metabolic abnormalities were found in the plasma of LCAD-/- mice. Analysis of carnitine biosynthesis intermediates in urine of wild-type and LCAD-/- mice showed no enhanced excretion of TML in the LCAD-/- group (results not shown), indicating that urinary loss is not the reason for the low tissue and kidney TML levels. Based on this experiment, however, we cannot exclude the possibility that a low, but persistent, urinary loss of TML cumulatively results in TML deficiency.

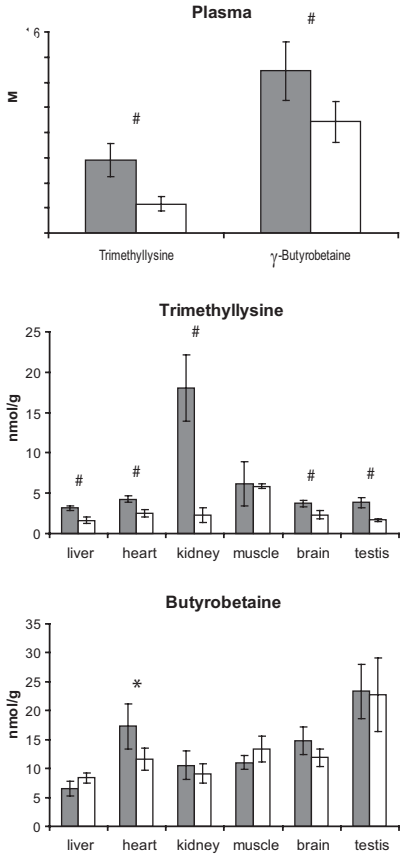

Figure 4: Carnitine biosynthesis intermediates in plasma and tissues of wild-type and LCAD-/- mice. Grey bars and white bars represent wild-type and LCAD-/- mice, respectively. Values are average ± standard deviation of six mice, where each tissue was analyzed in duplicate. Only one plasma analysis per mouse was performed due to the small amount of sample available. * indicates $p<0.05$ and # indicates $p<0.01$.

Except in plasma, no major differences can be seen in tissue γ-butyrobetaine levels between wild-type and LCAD-/- mice (figure 4). The reduction of plasma γ-butyrobetaine might result from increased hepatic γ-butyrobetaine uptake and subsequent conversion into carnitine.
Figure 1 shows that there is a profound deficiency of acetyl-carnitine in LCAD-/- heart. To a lesser extent, this is also observed in testis, but not in the other investigated tissues, where acetyl-carnitine levels are comparable with wild-type values. Normally, the heart's energy need is met primarily by fatty acid β-oxidation. LCAD is highly expressed in heart [29], and the fact that LCAD-/- mice suffer from cardiomyopathy [11, 12] indicates that LCAD plays an important role in cardiac fatty acid metabolism. There are several possible explanations for the shortage of acetyl-carnitine in the LCAD-/- heart: (1) carnitine deficiency, (2) shortage of acetyl-CoA or (3) decreased activity of CAT, which transfers acetyl groups from CoA to

carnitine. Since there is no carnitine deficiency in LCAD-/- hearts (figure 1), we measured CAT activity in homogenates of three wild-type and three LCAD-/- hearts to discriminate between the two latter possibilities. CAT activity did not differ between wild-type (242 ± 45 nmol × min^{-1} × mg^{-1}) and LCAD-/- heart (259 ± 11 nmol × min^{-1} × mg^{-1}), eliminating the possibility that lower CAT activity caused the observed acetyl-carnitine deficiency. This strongly suggests that there is a profound deficiency of acetyl-CoA in LCAD-/- hearts, implying a severe energy shortage which could result in the observed cardiomyopathy in LCAD-/- mice [12]. Previously, it was speculated that the accumulation of heart acyl-carnitines may be an important factor in the development of cardiomyopathy or cardiac arrhythmia in the LCAD-/- mice; however, the total acyl-carnitine levels in heart are only marginally elevated. This raises the important point that the deficiency of acetyl-CoA in the LCAD-/- heart is primarily responsible for the occurrence of the cardiomyopathy.

The deficiency of acetyl-CoA could be caused by low levels of mitochondrial free CoA, which in turn could result from the accumulation of non-metabolizable acyl-CoAs. A lack of free CoA would inhibit pyruvate dehydrogenase and thereby the formation of acetyl-CoA. Alternatively, if the mitochondrial free CoA levels are sufficient to sustain oxidation of pyruvate, the acetyl-CoA formed by pyruvate dehydrogenase would immediately enter the citric acid cycle (because of the energy shortage in the LCAD-/- heart caused by impaired β-oxidation), resulting in low levels of acetyl-CoA.

The most prominent difference between the wild-type and the LCAD-/- tissue and plasma acyl-carnitines (figure 2) is the increase of the characteristic C14:1-acyl-carnitine in the LCAD-/- samples. In plasma, C12- and C14- to C18:1-acyl-carnitines are also elevated, but to a lesser extent than C14:1-acyl-carnitine, which is in agreement with previous observations [11, 12]. Although the levels of C14:1-acyl-carnitine in tissues are considerably higher than in wild-type mice, this accumulation is not as dramatic as observed in plasma, suggesting that excess C14:1-acyl-carnitines are transported out of the tissues into the circulation.

In LCAD-/- muscle, a highly significant accumulation (approx. 5-fold higher than wild-type levels; $P<0.01$) of C9-, C9:1- and C11-acyl-carnitines was observed (results not shown). Although we cannot distinguish between straight-chain and branched-chain acyl-carnitines using our tandem-MS method, it is likely that these acyl-carnitines represent 2,6-dimethylheptanoyl-carnitine, 2,6-dimethylheptenoyl-carnitine and 4,8-dimethylnonanoyl-carnitine respectively, which could originate from peroxisomal catabolism of phytanic acid, since LCAD has been shown previously to be involved in the complete degradation of these compounds [8, 11]. Further studies with a diet enriched in branched-chain fatty acids could confirm that these acyl-carnitines indeed accumulate due to LCAD deficiency. These studies are currently under way.

In addition to the elevated tissue levels of C14:1-acyl-carnitine, C14- to C18-acyl-carnitines were also elevated to variable extents in all LCAD-/- tissues, except for heart and muscle, which show similar or even decreased levels respectively (figure 2). Heart does show a decrease of the very-long-chain acyl-carnitine levels, e.g. C20- to C22, in the LCAD-/- mouse. There are several mechanisms which could account for the decreased levels of (very-) long-chain acyl-carnitines in muscle and heart, including: (1) carnitine deficiency, (2) reduced activity of CPT2, which transfers acyl groups from CoA to carnitine, (3) increased VLCAD activity, (4) increased triacylglycerol synthesis or (5) excretion of acyl-carnitines from tissues into the circulation.

Since both LCAD-/- muscle and heart are not carnitine deficient (figure 1), CPT2 activity was measured in muscle and heart homogenates of three wild-type and three LCAD-/- mice. CPT2 activity in wild-type muscle (18.0 ± 3.3 nmol × min^{-1} × mg^{-1}) was similar to that in LCAD-/- muscle (18.5 ± 6.5 nmol × min^{-1} × mg^{-1}). CPT2 activity even was slightly elevated ($P<0.05$) in LCAD-/- heart (218 ± 20 nmol × min^{-1} × mg^{-1}) when compared with wild-type heart (157 ±

8 nmol × min^{-1} × mg^{-1}), excluding this as a cause of the decreased levels of (very-) long-chain acyl-carnitines in LCAD-/- heart and muscle.
The observed changes in the acyl-carnitine pattern in muscle and heart could also result from increased VLCAD activity, which has a broad substrate specificity ranging from C14- to C24-CoA [26]. Therefore the amount of VLCAD protein in heart, muscle, kidney and liver was analysed by Western blot using an anti-VLCAD antibody (figure 5). The last two tissues were included to compare the heart and muscle VLCAD levels with tissues where long-chain acyl-carnitines did accumulate. As expected, there was no difference in the VLCAD protein levels in kidney and liver between the two genotypes. In LCAD-/- heart, however, there is a small increase in VLCAD protein levels, which could contribute to the decreased levels of very-long-chain acyl-carnitines. The expression of VLCAD in muscle is very low, and, in contrast to heart, does not differ between wild-type and LCAD-/- mice, suggesting that other mechanisms are responsible for the decreased long-chain acyl-carnitine levels in muscle.

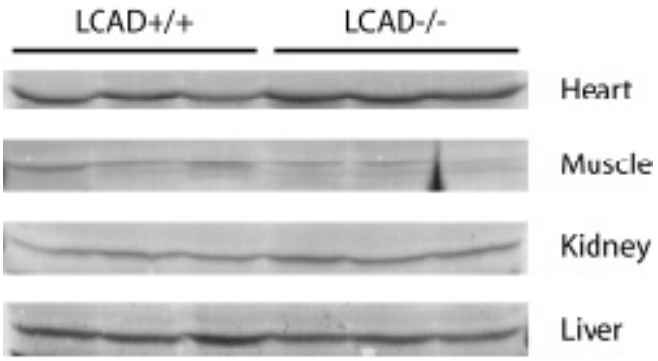

Figure 5: Western blot analysis of VLCAD in heart, muscle, kidney and liver of three wild-type and LCAD-/- mice. Each lane represents 100 μg of tissue homogenate.

Another possible mechanism to dispose of accumulating acyl-CoA esters is the production of triacylglycerols. Indeed, this is supported by the observations that triacylglycerol droplets accumulate in heart and liver of fasted LCAD-/- mice [12]. Although it is likely that, in the fasted LCAD-/- heart, triacylglycerols are synthesized to reduce the build-up of non-metabolizable acyl units, no accumulation of triacylglycerols is seen in muscle of fasted LCAD-/- mice (P.A Wood, unpublished work), which is in agreement with the fact that muscle has a very low capacity to synthesize triacylglycerols [30]. Since we have excluded the other mechanisms that could account for the decrease in LCAD-/- muscle long-chain acyl-carnitine levels, the only remaining possibility is that these acyl-carnitines are secreted into the circulation. Although there is no experimental evidence to support this, the fact that the acyl-carnitines which are lacking in LCAD-/- muscle are found in plasma (figure 2) agrees with this hypothesis.
Closer examination of the acyl-carnitine profiles revealed that the hydroxyl-acyl-carnitines observed in wild-type heart, muscle and brain were nearly absent in LCAD-/- mice (figure 3). The absence of these hydroxyl-acyl-carnitines in the LCAD-/- mice indicates that they most likely represent 3-hydroxy-acyl-carnitines and are indeed derived from 3-hydroxy-fatty acyl-CoAs. CPT2 is very likely to be responsible for the formation of these 3-hydroxy-acyl-carnitines, since it has been shown previously that this enzyme is capable of handling 3-hydroxy-fatty acyl-CoAs as substrates [31]. The production of hydroxyl-acyl-carnitines from exogenous hexadecanoate or its corresponding carnitine/CoA-ester was shown previously in rat muscle [32] and heart [33]. In the present study, we show the presence of endogenous hydroxyl-acyl-carnitines in these two mouse tissues and brain. The fact that these hydroxyl-acyl-carnitines are present in the wild-type situation suggests that, in these three tissues, the dehydrogenation of 3-hydroxy-acyl-CoA, catalysed by long-chain hydroxyl-acyl-CoA dehydrogenase, is rate-limiting. In an LCAD-/- situation, however, where only VLCAD is able to catalyse the first step of the β-oxidation, the formation of the enoyl-CoA determines

the flux through the β-oxidation pathway, which results in reduction of the hydroxyl-acyl-carnitine levels.
In conclusion, we developed and validated a novel method which enables the analysis of tissue acyl-carnitines and carnitine biosynthesis intermediates in the same sample. This method was used to investigate the carnitine and fatty acid metabolism in wild-type and LCAD-/- mice. As was reported previously for plasma and bile [11, 12], we found accumulation of the characteristic C14:1-acyl-carnitine in all investigated tissues. The most striking finding of the present study was the severe deficiency of acetyl-carnitine in heart, which most likely results from an acetyl-CoA deficiency. Since there was no carnitine deficiency and only a marginal elevation of potentially cardiotoxic acyl-carnitines, we conclude that cardiomyopathy in the LCAD-/- mouse is caused primarily by a severe energy deficiency in the heart, stressing the important role of LCAD in cardiac fatty acid metabolism in the mouse. LCAD-/- muscle showed accumulation of odd-number acyl-carnitines (C9 and C11). These acyl-carnitines could represent peroxisomal oxidation products of phytanic acid, which are confirmed LCAD substrates. This is in agreement with previous data, which show that LCAD is involved in branched-chain fatty acid metabolism [8, 11].

Acknowledgements

We thank J. Ruiter, M. van Werkhoven and A. van Cruchten for technical assistance, and Dr T. Hashimoto for the anti-VLCAD antibody. This work was supported by NIH (National Institutes of Health) grant RO1-RR02599.

References

[1] J.D. McGarry, N.F. Brown. The mitochondrial carnitine palmitoyltransferase system: from concept to molecular analysis, Eur. J. Biochem. 244 (1997) 1–14.
[2] S. Eaton, K. Bartlett, M. Pourfarzam. Mammalian mitochondrial β-oxidation, Biochem. J. 320 (1996) 345–357
[3] R.R. Ramsay, R.D. Gandour, F.R. van der Leij. Molecular enzymology of carnitine transfer and transport, Biochim. Biophys. Acta 1546 (2001) 21–43.
[4] F.M. Vaz, R.J. Wanders. Carnitine biosynthesis in mammals, Biochem. J. 361 (2002) 417–429.
[5] P. Rinaldo. Fatty acid transport and mitochondrial oxidation disorders, Semin. Liver Dis. 21 (2001) 489–500.
[6] M.J. Bennett, P. Rinaldo, A.W. Strauss. Inborn errors of mitochondrial fatty acid oxidation, Crit. Rev. Clin. Lab. Sci. 37 (2000) 1–44.
[7] A.M. Schuler, P.A. Wood. Mouse models for disorders of mitochondrial fatty acid b-oxidation, ILAR J. 43 (2002) 57–65.
[8] R.J. Wanders, S. Denis, J. Ruiter, L. IJlst, G. Dacremont. 2,6-Dimethylheptanoyl-CoA is a specific substrate for long-chain acyl-CoA dehydrogenase (LCAD): evidence for a major role of LCAD in branched-chain fatty acid oxidation, Biochim. Biophys. Acta 1393 (1998) 35–40.
[9] W. Le, A.S. Abbas, H. Sprecher, J. Vockley, H. Schulz. Long-chain acyl-CoA dehydrogenase is a key enzyme in the mitochondrial beta- oxidation of unsaturated fatty acids, Biochim. Biophys. Acta 1485 (2000) 121–128.
[10] K.P. Battaile, M. McBurney, P.P. Van Veldhoven, J. Vockley. Human long chain, very long chain and medium chain acyl-CoA dehydrogenases are specific for the S-enantiomer of 2-methylpentadecanoyl-CoA, Biochim. Biophys. Acta 1390 (1998) 333–338.
[11] K.B. Cox, D.A. Hamm, D.S. Millington, D. Matern, J. Vockley, P. Rinaldo, C.A. Pinkert, W.J. Rhead, J.R. Lindsey, P.A. Wood. Gestational, pathologic and biochemical differences between very long-chain acyl-CoA dehydrogenase deficiency and long-chain acyl-CoA dehydrogenase deficiency in the mouse, Hum. Mol. Genet. 10 (2001) 2069–2077.
[12] D. Kurtz, P. Rinaldo, W.J. Rhead, L. Tian, D. Millington, J. Vockley, D. Hamm, A. Brix, J.R. Lindsey, C.A. Pinkert. Targeted disruption of mouse long-chain acyl-CoA dehydrogenase gene reveals crucial roles for fatty acid oxidation, Proc. Natl. Acad. Sci. U.S.A. 95 (1998) 15592–15597.

[13] C Nakano,. S. Takashima, K. Takeshita, Carnitine concentration during the development of human tissues, Early Hum. Dev. 19 (1989) 21–27.
[14] C. de Sousa, N.R. English, T.E. Stacey, R.A. Chalmers. Measurement of L-carnitine and acyl-carnitines in body fluids and tissues in children and in adults, Clin. Chim. Acta 187 (1990) 317–328.
[15] P. Vreken, A.E. van Lint, A. Bootsma, H. Overmars, R.J. Wanders, A. Gennip. Quantitative plasma acyl-carnitine analysis using electrospray tandem mass spectrometry for the diagnosis of organic acidaemias and fatty acid oxidation defects, J. Inherit. Metab. Dis. 22 (1999) 302–306.
[16] Y. Shigematsu, S. Hirano, I. Hata, Y. Tanaka, M. Sudo, N. Sakura, T. Tajima, S. Yamaguchi. Newborn mass screening and selective screening using electrospray tandem mass spectrometry in Japan, J. Chromatogr. 776 (2002) 39–48.
[17] M.S. Rashed, P.T. Ozand, M.J Bennett,. J.J. Barnard,. D.R. Govindaraju, P. Rinaldo. Inborn errors of metabolism diagnosed in sudden death cases by acyl-carnitine analysis of postmortem bile, Clin. Chem. 41 (1995) 1109–1114.
[18] D.H. Chace, S.L. Hillman,. J.L. Van Hove, E.W. Naylor. Rapid diagnosis of MCAD deficiency: quantitatively analysis of octanoyl-carnitine and other acyl-carnitines in newborn blood spots by tandem mass spectrometry, Clin. Chem. 43 (1997) 2106–2113.
[19] F.M. Vaz, B. Melegh, J. Bene, D. Cuebas, D.A. Gage, A. Bootsma, P. Vreken, A.H. van Gennip, L.L. Bieber, R.J. Wanders. Analysis of carnitine biosynthesis metabolites in urine by HPLC–electrospray tandem mass spectrometry, Clin. Chem. 48 (2002) 826–834.
[20] J.H. Swiegers, F.M. Vaz, I.S. Pretorius, R.J. Wanders, F.F. Bauer. Carnitine biosynthesis in Neurospora crassa: identification of a cDNA coding for ε-N-trimethyllysine hydroxylase and its functional expression in Saccharomyces cerevisiae, FEMS Microbiol. Lett. 210 (2002) 19–23.
[21] M.S. Rashed, M.P. Bucknall, D. Little, A. Awad, M. Jacob, M. Alamoudi, M. Alwattar, P.T. Ozand. Screening blood spots for inborn errors of metabolism by electrospray tandem mass spectrometry with a microplate batch process and a computer algorithm for automated flagging of abnormal profiles, Clin. Chem. 43 (1997) 1129–1141.
[22] A. Slama, M. Brivet, A. Boutron, A. Legrand, J.M. Saudubray, F. Demaugre. Complementation analysis of carnitine palmitoyltransferase I and II defects, Pediatr. Res. 40 (1996) 542–546.
[23] P.G. Barth, H.R. Scholte, J.A. Berden, J.M. Van der Klei-Van Moorsel, I.E. Luyt-Houwen, E.T. Van't Veer-Korthof, J.J. Van der Harten, M.A. Sobotka-Plojhar. An X-linked mitochondrial disease affecting cardiac muscle, skeletal muscle, and neutrophil leucocytes, J. Neurol. Sci. 62 (1983) 327–355.
[24] F.M. Vaz, R. Ofman, K. Westinga, R.J. Wanders. Molecular and biochemical characterization of rat ε-N-trimethyllysine hydroxylase, the first enzyme of carnitine biosynthesis, J. Biol. Chem. 276 (2001) 33512–33517.
[25] F.M. Vaz, S. van Gool, R. Ofman, L. Ijlst, R.J. Wanders. Carnitine biosynthesis: identification of the cDNA encoding human γ-butyrobetaine hydroxylase, Biochem. Biophys. Res. Commun. 250 (1998) 506–510.
[26] K. Izai, Y. Uchida, T. Orii, S. Yamamoto, T. Hashimoto. Novel fatty acid β-oxidation enzymes in rat liver mitochondria. I. Purification and properties of very-long-chain acyl-coenzyme A dehydrogenase, J. Biol. Chem. 267 (1992) 1027–1033.
[27] C.L. Hoppel, A.T. Davis. Inter-tissue relationships in the synthesis and distribution of carnitine, Biochem. Soc. Trans. 14(1986) 673–674.
[28] M. Duran, N.E. Loof, D. Ketting, L. Dorland. Secondary carnitine deficiency, J. Clin. Chem. Clin. Biochem. 28 (1990) 359–363.
[29] M.E. Hinsdale, S.C. Farmer, K.R. Johnson, M.T. Davisson, D. Hamm, R.J. Tolwani, P.A. Wood. RNA expression and chromosomal location of the mouse long-chain acyl-CoA dehydrogenase gene, Genomics 28 (1995) 163–170.
[30] M. Watford. Functional glycerol kinase activity and the possibility of a major role for glyceroneogenesis in mammalian skeletal muscle, Nutr. Rev. 58 (2000) 145–148.
[31] F.V. Ventura, L. IJlst, J. Ruiter, R. Ofman, C.G. Costa, C. Jakobs, M. Duran, I. Tavares de Almeida, L.L. Bieber, R.J. Wanders. Carnitine palmitoyltransferase II specificity towards β-oxidation intermediates – evidence for a reverse carnitine cycle in mitochondria, Eur. J. Biochem. 253 (1998) 614–618.
[32] S. Eaton, A.K. Bhuiyan, R.S. Kler, D.M. Turnbull, K. Bartlett. Intramitochondrial control of the oxidation of hexadecanoate in skeletal muscle: a study of the acyl-CoA esters which accumulate during rat skeletal-muscle mitochondrial β-oxidation of [U-^{14}C]-hexadecanoate and [U-^{14}C-]hexadecanoyl-carnitine, Biochem. J. 289 (1993) 161–168.
[33] S. Eaton, M. Pourfarzam, K. Bartlett. The effect of respiratory chain impairment of β-oxidation in rat heart mitochondria, Biochem. J. 319 (1996), 633–640.

Chapter 5

Identification of SLC6A13 as a γ-butyrobetaine transporter

N. van Vlies, R.J.A. Wanders, F.M. Vaz

Abstract

Carnitine plays an essential role in fatty acid metabolism. While most mouse tissues can synthesize its direct precursor γ-butyrobetaine, this compound can only be converted into carnitine by the liver. Extra-hepatic γ-butyrobetaine must therefore be transported into the liver for complete carnitine biosynthesis and previous experiments indeed have demonstrated that hepatic γ-butyrobetaine transport systems exist. In order to identify this transport system, we expressed two candidate transporters. The studies reported in this paper show that γ-butyrobetaine is transported very efficiently by SLC6A13, which was originally described as a γ-aminobutyric acid transporter. γ-Aminobutyric acid inhibited γ-butyrobetaine transport, however, plasma γ-aminobutyric acid concentrations are most likely too low to inhibit SLC6A13-mediated hepatic γ-butyrobetaine transport significantly. We also report that both carnitine biosynthesis enzyme activities as well as the hepatic expression of SLC6A13 is elevated in mice with primary carnitine deficiency (JVS mice). This indicates that carnitine biosynthesis is enhanced in these mice and supports the role of SLC6A13 as a hepatic γ-butyrobetaine transporter.

Introduction

Carnitine (3-hydroxy-4-N,N,N-trimethylaminobutyrate) is an essential compound in fatty acid metabolism. Mammals acquire carnitine both from the diet (meat, fish and dairy products) and through endogenous synthesis [1]. The first metabolite of the carnitine biosynthesis pathway is 6-N-trimethyllysine (TML) and is generated by lysosomal degradation of proteins containing trimethylated lysine residues. TML is hydroxylated by TML-dioxygenase (EC 1.14.11.8, TMLD) to 3-hydroxy-6-N-trimethyllysine (HTML), which is converted to 4-trimethylaminobutyraldehyde (TMABA) by HTML-aldolase. TMABA-dehydrogenase (EC 1.2.1.47, TMABA-DH) oxidizes TMABA to 4-trimethylaminobutyric acid (EC 1.14.11.1, γ-butyrobetaine, γ-BB), which is hydroxylated to carnitine by γ-BB dioxygenase (γ-BBD). γ-BB is synthesized in all tissues [2], but in the mouse γ-BBD is only expressed in liver, which readily takes up circulatory γ-BB, converts it into carnitine and releases this into the circulation [2-4]. Extra-hepatic tissues take up carnitine via the plasma membrane carnitine transporter OCTN2, which apart from carnitine, can also transport γ-BB [1]. OCTN2 also mediates the dietary carnitine uptake and renal reabsorption [1]. A deficiency of OCTN2 leads to primary systemic carnitine deficiency. Patients typically present in infancy with episodic hypoketotic hypoglycemic encephalopathy, progressive cardiomyopathy and failure to thrive [5]. In 1988, Koizumi and colleagues [6] described a C3H.OH strain of mice in which microvesicular fatty infiltration of viscera was inherited in an autosomal recessive manner. These mice, named Juvenile Visceral Steatosis (JVS) mice, displayed symptoms similar to those of OCTN2-/- patients, had very low plasma and tissue carnitine levels and were shown to have a missense mutation in the OCTN2 gene [7, 8]. Although the hepatic γ-BBD activity is increased in OCTN2-/- mice, the carnitine biosynthesis pathway apparently does not produce enough carnitine to compensate for the defect in renal carnitine reabsorption [9]. Although frequent high-dose carnitine administration ameliorates the symptoms of OCTN2-deficiency in both mice and human patients, plasma and tissue carnitine levels are not restored to normal levels [5, 6]. Higashi *et al*. showed, however, that γ-BB administration resulted in higher brain, liver and kidney carnitine concentrations and lower liver free fatty acid levels as compared to carnitine administration [10]. This indicates that in the OCTN2-/- mouse, γ-BB is used more efficiently than carnitine and that γ-BB is imported into the liver via a transport system that is different from OCTN2.

Little is known about hepatic γ-BB transport. However, two distinct hepatic transport systems for γ-BB have been characterized biochemically. Christiansen and Bremer reported a low-affinity γ-BB transporter (K_m value of approximately 500 μM) using primary rat hepatocytes. This transport system had a 10-fold higher K_m value for carnitine (5.6 mM) than for γ-BB and could be inhibited by carnitine [11]. A high-affinity γ-BB transporter (K_m value of approximately 5 μM) was described by Berardi *et al*. [12]. Using rat liver basolateral plasma membrane vesicles, they demonstrated that γ-BB transport was stimulated by sodium and chloride ions and transport could be inhibited by propionyl-carnitine, but surprisingly not by carnitine or acetyl-carnitine.
In contrast to the low expression of OCTN2 in liver [13], renal γ-BB reabsorption is most likely mediated via OCTN2. This transporter is highly expressed in mouse kidney, handles γ-BB very efficiently [13] and OCTN2-/- mice have diminished γ-BB reabsorption [9].
In order to identify the liver γ-BB transporter we selected known transporters that (1) are expressed in liver and kidney, tissues that are known to contain γ-BB transport activity [3] and (2). transport compounds that have structural resemblance to γ-BB, such as γ-aminobutyric acid (GABA) and betaine. GABA contains a primary amino group at the position where γ-BB (4-trimethylaminobutyric acid) has a quaternary amino group but has the same carbon-chain length and carboxylic acid function. Betaine (2-trimethylamino-ethanoic acid) is two carbon atoms shorter but contains both a quaternary amino group and a carboxylic acid function.
Two transporters were found that best matched these criteria: SLC6A12 and SLC6A13. Both transporters are expressed in liver and kidney and transport GABA. SLC6A12 also transports betaine [14-16]. SLC6A12 and SLC6A13 were originally cloned and described as GABA transporters and named GABA transporter (GAT) 2 and 3. Four distinct GATs exist; SLC6A1, SLC6A11, SLC6A12 and SLC6A13 and the nomenclature of these transporters is somewhat complicated. While SLC6A1 is designated GAT1 in both mice, rats and humans, SLC6A11 is called GAT3 in rats and humans but GAT4 in mice. Mouse SLC6A12 is termed GAT2 and is the homolog of the human betaine/GABA transporter 1 (BGT1). SLC6A13, labeled GAT2 in man and rat, is mouse GAT3. SLC6A12 and SLC6A13 differ considerably from the other two GATs. SLC6A1 and SLC6A11 are present only in the central nervous system and the retina, and display different substrate/inhibitor specificities when compared to SLC6A12 and SLC6A13 [14-16].
In this paper we report the identification and characterization of SLC6A13 as a γ-BB transporter and showed that this transporter is upregulated in livers of OCTN2-/- mice which probably contributes to the enhanced carnitine biosynthesis in these mice.

Materials and Methods

Chemicals
Carnitine was obtained from Sigma-Aldrich. DMEM and DMEM:F12 medium were obtained from BioWhittaker, the 'Human Dermal Fibroblast transfection kit' from Amaxa. CHO cells, Trizol reagent and the pcDNA3, pcDNA5/FRT, pog44 and peGFP vertors were purchased from Invitrogen. Microcon 30kD filters were from Amicon. The [$^2H_9$]-carnitine internal standard was obtained from Dr. Herman J. ten Brink, VU Medical Center Amsterdam, the Netherlands. The [$^2H_3$]-γ-BB was synthesized as described earlier [17]. All other reagents were of analytical grade.

Animals.
Until the age of 7 weeks C3H.OH JVS (OCTN2-/-) mice [6] were supplemented with carnitine either via their drinking water (300 mg carnitine/L) or were injected intraperitonially

with 5 μmol of carnitine-HCL, dissolved in physiological saline and neutralized with sodium hydroxide, every 2 days from the age of 5 days. At 8 weeks of age wild type and OCTN2-/- mice were anesthetized with isoflurane and blood was collected by cardiac puncture. Tissues were collected and a small piece was immediately submerged in Trizol reagent and placed on ice for RNA isolation, the rest was immediately frozen in liquid nitrogen and stored at -80°C until further use. All animal experiments were approved by the local ethical committee.

Cloning of candidate γ-BB transporters

The complete open reading frame (ORF) of both mouse SLC6A12 and SLC6A13 were amplified by the polymerase chain reaction from mouse liver cDNA using *Taq* DNA polymerase, HindIII-tagged forward primers and an EcoRV-tagged reverse primers containing a histidine-tag (5'-aagcttATGTCATCAAGAGCTTGGGA-3' and 5'-gatatcCTAatggtgatggtgatgatg CAAATGAGTCTCCTTCTCCC-3' for SLC6A12 and 5'-aagcttATGGAGAACAGGGCCTCGG-3' and 5'-gatatcCTAatggtgatggtgatgatgGCAGTTAGACTCCAGTTCTGT-3' for SLC6A13). The PCR products were cloned downstream of the P_{CMV} promoter into the HindIII and EcoRV sites of the mammalian expression vector pcDNA3. Both ORFs were sequenced to exclude sequence errors introduced by *Taq* DNA polymerase during the PCR.

The SLC6A13 ORF was subsequently subcloned downstream of the P_{CMV} promoter into the HindIII and EcoRV sites of the mammalian expression vector pcDNA5/FRT for stable expression in CHO/FlipIn cells.

Transfection of fibroblasts and CHO cells

Human skin fibroblasts were cultured as described before [18]. Cells were harvested by trypsinisation and washed twice with phosphate buffered saline (PBS). The fibroblasts were transfected using the Human Dermal Fibroblast Nucleofector kit as described in the manufacturer's manual (Amaxa) with pcDNA3, pcDNA3+OCTN2 [19], pcDNA3+SLC6A12, pcDNA3+SLC6A13, or pEGFP-C3 and cells were seeded in 6-wells plates. Transfection efficiencies were determined using the pEGFP-C3 vector, which leads to expression of the green fluorescent protein. Transfection efficiencies were usually ≥ 50%. After 24 hours, expression of the recombinant proteins was checked by immunoblot analysis using a polyclonal anti-histag antibody (Santa Cruz Biotechnology)

CHO/FlipIn cells were cultured and transfected with pcDNA5/FRT and pOG44 vector, pcDNA5/FRT+SLC6A13 and pOG44 or with pcDNA5/FTR+SLC6A13 or pOG44 alone, as described in the manufacturer's manual (Invitrogen). To obtain a monoclonal cell line, cells were harvested two weeks after transfection and seeded in 96-wells plate with one cell per well. After 6 days the wells containing only one colony per well were selected. These cell lines were analyzed for γ-BB transport activity and those with high γ-BB transport activity were used for subsequent experiments

γ-BB transport in fibroblasts and CHO cells

γ-BB transport in fibroblasts was measured one day after transfection. Cells were washed twice with PBS, followed by the addition of 1 ml DMEM medium containing 50 μM [$^2H_3$]-γ-BB per well. After 4 hours of incubation at 37°C or 4°C cells were washed twice with 2 ml ice-cold PBS and taken up in 200 μl PBS containing 0.2% Triton-X-100. The [$^2H_9$]-carnitine internal standard (100 pmol) was added to 100 μl of the cell solution and the mixture was loaded on a Microcon 30 kDa filter and centrifuged at 14,000 × *g* for 20 minutes at 4°C, which removes most of the proteins. One hundred microliters of the filtrate was derivatized with methylchloroformate and the amount of transported [$^2H_3$]-γ-BB was quantified using ion-pair HPLC-Tandem mass spectrometry as described previously [17]. The protein

concentration of the cell solution was determined using bicinchoninic acid [20] with bovine serum albumin as standard.
For the γ-BB transport activity measurements in CHO cells, cells were harvested and seeded in 6-wells plates (approximately 100 μg protein per well, unless indicated otherwise). The following day the cells were washed twice with PBS and 1 ml of Krebs-Henseleit medium (1.2 mM potassium phosphate buffer, containing 118 mM NaCl, 5 mM KCl, 1.2 mM $MgSO_4$, 25 mM $NaHCO_3$, 2.5 mM $CaCl_2$, 20 mM Hepes and 10 mM glucose, pH 7.4) supplemented with 400 μM [$^2H_3$]-γ-BB, was added to each well. Instead of using 50 μM γ-BB as done previously, we used 400 μM γ-BB in order to measure optimal rates of γ-BB transport, since the K_m value of SLC6A13 for γ-BB was found to be 50 μM. The cells were incubated at 37°C or 4°C for 3 minutes (unless indicated otherwise). Subsequently, the cells were washed twice with 2 ml ice-cold PBS and taken up in 200 μl PBS containing 0.2% Triton-X-100. The [$^2H_9$]-carnitine internal standard (100 pmol) was added to 100 μl of the cell solution and samples were processed as described for the fibroblasts samples.

Characterization of γ-BB transport by SLC6A13
In order to establish the K_m values of SLC6A13 for γ-BB, pcDNA5/FRT+SLC6A13 transfected cells and cells transfected with pcDNA5/FRT were incubated with varying concentrations of [$^2H_3$]-γ-BB. The latter cell line was included to correct for diffusion at high [$^2H_3$]-γ-BB concentrations. Import activity of this cell line was subtracted from the import activity of the pcDNA5/FRT+SLC6A13 transfected cell line. A Lineweaver-Burk double-reciprocal plot was made from the resulting transport activities.
To investigate the ionic dependency of the γ-BB transport, sodium was replaced by potassium in the transport medium and vice versa, to test for sodium or potassium dependence and chloride was replaced by acetate to test for chloride dependence.

Carnitine metabolites and biosynthesis enzymes
Levels of carnitine biosynthesis intermediates/acylcarnitines in tissues and activities of carnitine biosynthesis enzymes were determined as described previously [21, 22].

Quantitative real-time RT-PCR analysis
Total RNA was isolated from mouse tissues using Trizol extraction, after which cDNA was prepared using a first-strand cDNA synthesis kit for RT-PCR (Roche). Quantitative real-time PCR analysis of SLC6A13 and β-actin was performed in these tissues using the LightCycler FastStart DNA Master SYBR Green I kit (Roche). The following primers were used: 5'-GGAACTGGTCCTGTGCCTC-3' and 5'-GGCGATGCAGTCCCTGTAG-3' for SLC6A13 and 5'-GTGGGCCGCTCTAGGCACCAA-3' and 5'-CTCTTTGATGTCACGCACGATTTC-3' for β-actin, as described previously [23]. To confirm the generation of a single product both melting curve analysis and agarose gel electrophoresis was carried out. All samples were analyzed in duplicate. Data were analyzed using linear regression calculations as described by Ramakers *et al*. [24]. To compare the SLC6A13 expression between different samples, values were normalized against the values for the housekeeping gene β–actin.

Statistical analyses
Data are expressed as means ± standard deviation. Statistical significance was evaluated using an unpaired Student's *t*-test. The results were considered significant at $P \leq 0.05$.

Results

γ-BB transport by SLC6A12 and SLC6A13

We first tested whether control fibroblasts, which express OCTN2, are able to import γ-BB. These studies revealed a low rate of γ-BB transport (250 ± 77 pmol × mg^{-1} × $hour^{-1}$). For this reason OCTN2-deficient fibroblasts were transfected with either pcDNA3+SLC6A12 or pcDNA3+SLC6A13 to test whether SLC6A12 and SLC6A13 are able to transport γ-BB. Expression of SLC6A12 and SLC6A13 was verified by SDS-PAGE and subsequent immunoblot analysis using an anti-his antibody (Santa Cruz Biotechnology) (figure 1A) which confirmed the expression of both recombinant proteins.

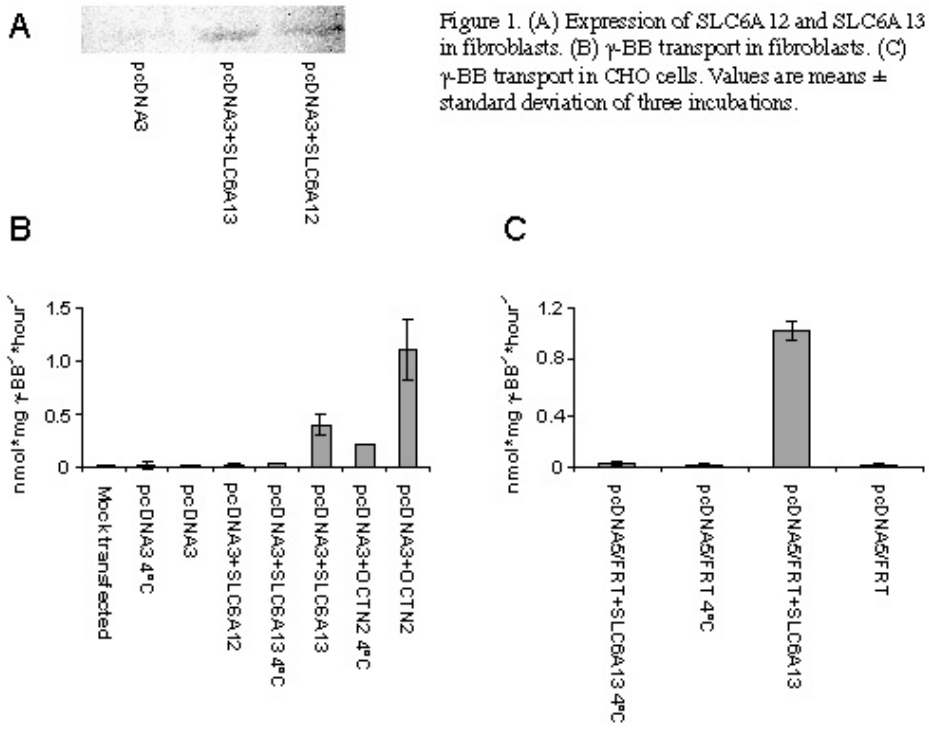

Figure 1. (A) Expression of SLC6A12 and SLC6A13 in fibroblasts. (B) γ-BB transport in fibroblasts. (C) γ-BB transport in CHO cells. Values are means ± standard deviation of three incubations.

Very little γ-BB import was observed in fibroblasts which were transfected with either pcDNA3 or pcDNA3+SLC6A12, in mock transfected cells or when cells were incubated at 4°C (figure 1B). The fibroblasts transfected with pcDNA3+SLC6A13, however, did show considerable γ-BB import (400 ± 94 pmol × mg^{-1} × $hour^{-1}$, figure 1B). The fibroblasts transfected with pcDNA3+OCTN2 were used as positive control and, as expected, transported γ-BB very well. These results show that SLC6A13 transports γ-BB, whereas SLC6A12 does not.

Table 1. Ionic-dependency of γ-BB transport.

	% γ-BB transport
Complete transport medium	100 ± 5
- Na^+	4 ± 2
- K^+	100 ± 8
- Cl^-	40 ± 3
- Na^+ and Cl^-	2 ± 4

Values are means ± standard deviation of three incubations. Transport activity in the complete transport medium was set at 100%.

Table 2. Inhibitors of γ-BB transport.

	% γ-BB transport
No inhibitors	100 ± 4
Carnitine (1 mM)	100 ± 6
Acetyl-carnitine (1 mM)	100 ± 6
Propionyl-carnitine (1 mM)	100 ± 5
Dinitrophenol (1 mM)	100 ± 10
Betaine (30 μM)	100 ± 7
Betaine (240 μM)	78 ± 7
GABA (30 μM)	50 ± 2
GABA (240 μM)	20 ± 3

Values are means ± standard deviation of three incubations. Transport activity with no inhibitors was set at 100%.

Characterization of γ-BB transport by SLC6A13

To further characterize the γ-BB transport by SLC6A13, we produced stable transfectants of SLC6A13 in CHO cells. Only cells transfected with pcDNA5/FRT+SLC6A13 incubated at 37°C transported γ-BB (figure 1C), confirming the results of the fibroblast transfection experiment. Next, we analyzed the time- and protein dependence of the γ-BB transport. γ-BB transport was linear with time up to 3 minutes (figure 2A) and linear with protein up to 100 μg per well (figure 2B). With our optimized assay, we determined the K_m, the ionic dependency of SLC6A13-dependent γ-BB transport and whether selected compounds inhibit γ-BB transport. The K_m value of γ-BB transport, as determined in CHO cells transfected with SLC6A13, was 50 μM (results not shown). Table 1 shows the results of the ionic dependency experiments, which indicate that γ-BB transport by SLC6A13 is Na^+- and Cl^--dependent, which is in agreement with the results of Berardi *et al*. for γ-BB transport into rat liver plasma membrane vesicles [12]. The γ-BB transport in our CHO cell expression system, however, displayed a 10-fold higher K_m value for γ-BB (50 μM) than the K_m value that was determined using the vesicle system (5 μM [12]). Table 2 shows that the addition of carnitine (1 mM), acetyl-carnitine (1 mM), propionyl-carnitine (1 mM) or dinitrophenol (1 mM) to the transport medium had no effect on γ-BB transport activity. Because the addition of dinitrophenol did not influence γ-BB transport, it appears that γ-BB transport is not dependent on the proton gradient. γ-BB transport as determined previously by Berardi *et al*. [12] could be inhibited by propionyl-carnitine, whereas this compound had no effect on γ-BB transport into the CHO cells expressing SLC6A13. Betaine did inhibit γ-BB transport by approximately 20% at concentrations of 240 μM. GABA, however, already decreased the γ-BB transport activity at low GABA concentrations (table 2).

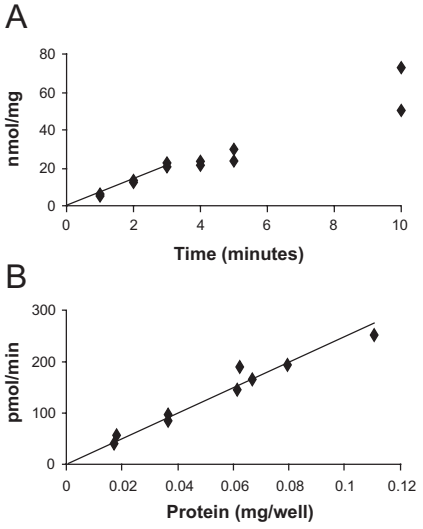

Figure 2. (A) time-dependence of γ-BB transport in CHO cell stably expressing SLC6A13. Values are means ± standard deviation of three incubations. 100 μg protein per well. (B) protein-dependence of γ-BB transport. Values are means ± standard deviation of three incubations, incubation time was 3 minutes.

Carnitine and γ-BB in the OCTN2-/- mouse

As was shown by Higashi *et al*. [10], γ-BB is used very efficiently by OCTN2-/- mice which indicates that OCTN2 deficient liver cells import γ-BB efficiently. To investigate if SLC6A13 is indeed involved in this process, we measured SLC6A13 mRNA levels in liver, carnitine metabolites levels in tissues, urine and plasma and carnitine biosynthesis enzyme activities in tissues of wild type and OCTN2-/- mice.

OCTN2-/- mice had very low plasma and tissue carnitine levels compared to wild type mice (table 3). The relative excretion of carnitine in OCTN2-/- mice, however, was considerably higher than in wild type mice, even though their urinary carnitine content was only half that of wild type mice (figure 3). Considerable quantities of γ-BB were also excreted by OCTN2-/- mice. 17-fold more γ-BB was excreted by OCTN2-/- mice, compared to wild type mice (figure 3), which suggests that renal γ-BB reabsorption is mediated primarily by OCTN2. Also, the high urinary γ-BB excretion in JVS mice suggests that total body γ-BB synthesis is increased.

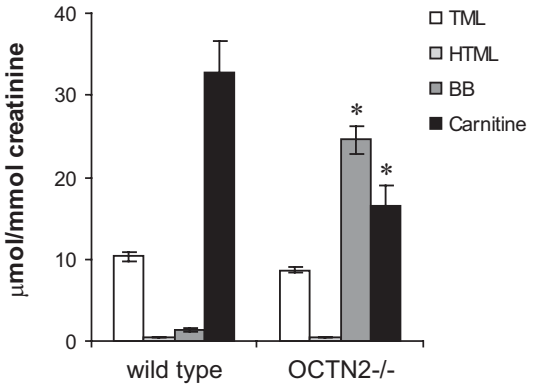

Figure 3. Concentrations of carnitine and biosynthesis intermediates in urine of wild type (n=4) and OCTN2-/- mice (n=4). Values are means ± standard deviation. * indicates a significant difference ($p < 0.05$) between wild type and OCTN2-/- mice.

Table 3. Carnitine levels in tissues and plasma of wild type and OCTN2-/- mice.

	Wild type mice	OCTN2-/- mice
	nmol/g	
Liver	441 ± 104	19.4 ± 3.6 *
Kidney	500 ± 30	21.8 ± 2.7*
Heart	1363 ± 71	21.0 ± 5.1 *
Muscle	344 ± 88	4.0 ± 1.2 *
	μM	
Plasma	40.9 ± 4.9	2.8 ± 0.7 *

Values are means ± standard deviation. * indicates a significant difference ($p < 0.05$) between wild type and OCTN2-/- mice.

In the OCTN2-/- liver, γ-BB levels were decreased when compared to the levels in livers of wild type animals (figure 4). This could be caused by (1) decreased γ-BB biosynthesis, (2) increased γ-BB conversion into carnitine or by (3) decreased hepatic γ-BB uptake. Several observations indicate that hepatic γ-BB synthesis is not decreased in the OCTN2-/- mice. In fact, it is more likely that γ-BB synthesis is actually increased. Liver TMLD activity in these mice was more than twice the activity found in wild type mice (table 4), resulting in somewhat lower hepatic TML levels (1.1 ± 0.2 nmol/g wet weight) compared to wild type animals (1.7 ± 0.3 nmol/g wet weight). TMABA-DH activity did not differ between groups (table 4). The lower hepatic γ-BB levels in the OCTN2-/- mice could result from an increased conversion of γ-BB into carnitine. Indeed, the γ-BBD activity in OCTN2-/- liver indeed was 2-fold higher than the activity found in wild type mice (table 4) which agrees with previous

results [9]. If there is enhanced γ-BB transport into the liver of OCTN2-/- mice and SLC6A13 is involved in this process, one would expect that expression of SLC6A13 is increased. We therefore measured SLC6A13 mRNA levels in livers of wild type and OCTN2-/- mice. Liver SLC6A13 expression was 3.6-fold higher in the OCTN2-/- livers when compared to wild type (2.5 ± 0.6 vs. 0.7 ±0.2, figure 5). These data suggest that, most likely, γ-BB uptake in OCTN2-/- livers is higher due to the increased SLC6A13 expression and, in combination with the elevated γ-BBD activity, leads to enhanced hepatic carnitine biosynthesis.

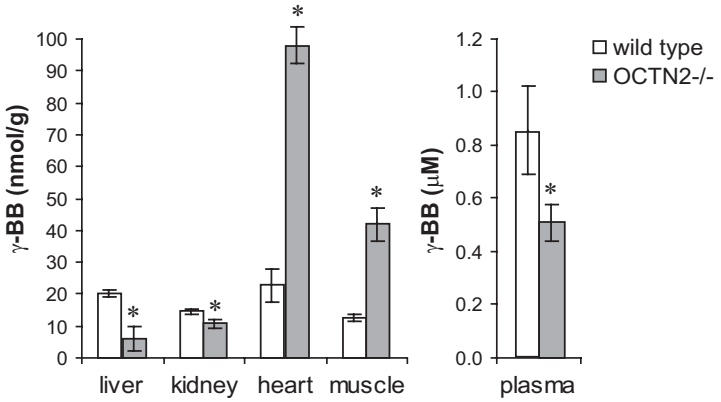

Figure 4. γ-BB levels in tissues and plasma of wild type (open bars, n=4) and OCTN2-/- mice (closed bars, n=4). Values are means ± standard deviation.
* indicates a significant difference ($p<0.05$) between wild type and OCTN2-/- mice.

In contrast to the hepatic γ-BB concentration, γ-BB levels are elevated in heart and skeletal muscle of OCTN2-/- mice (figure 4). While in skeletal muscle this might be caused by increased activity of biosynthetic enzymes (table 4), no differences in cardiac TMLD and TMABA-DH activity was found between wild type and OCTN2-/- mice (table 4). It is possible that the export of γ-BB is impaired in these tissues, as proposed by Horiuchi *et al*. [9], which could contribute to the elevated heart and skeletal muscle γ-BB levels. Another possibility is that γ-BB uptake is increased in hearts and skeletal muscle of OCTN2-/- mice. The profound carnitine deficiency in these mice may lead to upregulation of transporters that handle carnitine-like compounds and upregulation of these transporters could result in enhanced γ-BB uptake. This putative process, however, is unlikely to be mediated by SLC6A13, since we could not detect SLC6A13 expression in heart or skeletal muscle of both wild type and OCTN2-/- mice (results not shown).

Table 4. Carnitine biosynthesis enzyme activities in tissues of wild type and OCTN2-/- mice.

		Wild type mice	OCTN2-/- mice
		pmol × min^{-1} × mg^{-1}	
Liver	TMLD	17.6 ± 2.2	39.0 ± 2.1 *
	TMABA-DH	3843 ± 490	4455 ± 497
	γ-BBD	126.7 ± 8.3	256.9 ± 27.2 *
Kidney	TMLD	23.7 ± 2.6	28.9 ± 1.8 *
	TMABA-DH	2914 ± 644	4065 ± 1087
Heart	TMLD	42.6 ± 2.8	34.8 ± 5.1
	TMABA-DH	324 ± 34	167 ± 41 *
Muscle	TMLD	1.9 ± 0.4	6.3 ± 0.4 *
	TMABA-DH	10.8 ± 5.8	50.1 ± 1.0 *

Values are means ± standard deviation. * indicates a significant difference ($p <0.05$) between wild type and OCTN2-/- mice.

Discussion

By analyzing the γ-BB transport activity in CHO cells transfected with candidate γ-BB transporters, we have demonstrated that SLC6A13 transports γ-BB very effectively. The ionic dependence of γ-BB transport in CHO cells transfected with SLC6A13 was similar to that observed for γ-BB transport into rat liver plasma membrane vesicles. The apparent K_m value and inhibitor specificity of the γ-BB transport in CHO cells transfected with SLC6A13 were different as compared to the results previously reported by Berardi *et al*. [12]. The plasma membrane vesicles used by Berardi *et al*., however, likely contain more than one transporter that contributes to the observed γ-BB transport. It is probable that liver plasma membrane vesicles contain OCTN2 since this transporter is expressed in liver and transports γ-BB. In fact, γ-BB is one of the best inhibitors of OCTN2-mediated carnitine transport [13, 25]. Our expression system solely measures SLC6A13 transport activity since any background γ-BB transport activity (which in fact was very low) was corrected for using the cell line transformed with the vehicle only. This could explain the discrepant K_m values and inhibitory studies.

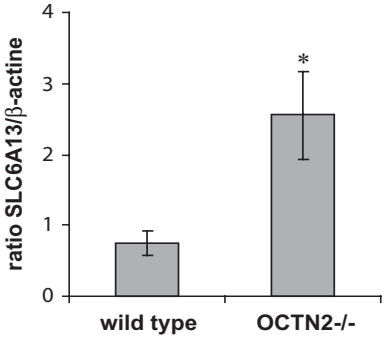

Figure 5. SLC6A13 mRNA levels in livers of wild type (n=4) and OCTN2-/- mice (n=4). Values are means ± standard deviation. * indicates a significant difference ($p < 0.05$) between wild type and OCTN2-/- mice.

Although γ-BB transport could be inhibited by GABA and betaine, it is unlikely that these substances influence hepatic γ-BB transport by SLC6A13 *in vivo*. The plasma concentration of betaine is only 35 μM [26], which is very likely too low to inhibit SLC6A13 mediated γ-BB transport. In humans, the γ-BB concentration in plasma ranges between 1.8 μM and 4.8 μM [1], which is at least 10-fold higher than the plasma GABA concentration (approximately 0.19 μM [27]). Although SLC6A13 has a higher affinity for GABA (K_m value of 18 μM, [14]) than for γ-BB, when considering the very low plasma GABA concentrations it is likely that liver SLC6A13 primarily transports γ-BB and not GABA. Also, the fact that hepatic SLC6A13 expression is increased in OCTN2-/- mice compared to wild type mice strongly suggests that SLC6A13 functions as a liver γ-BB transporter and contributes to the enhanced carnitine biosynthesis in these mice.

Besides SLC6A13, other transporters may also contribute to hepatic γ-BB import. Even though OCTN2 expression in liver is low in the fed state (chapter 6), OCTN2 surely contributes to γ-BB import into the liver. When mice are fasted, hepatic OCTN2 expression increases approximately 4-fold (chapter 6) which very likely enhances hepatic γ-BB uptake. In the absence of OCTN2, SLC6A13 expression is enhanced to provide the carnitine-deficient liver with carnitine equivalents. Also, other unknown transporters could mediate γ-BB import, for instance the low-affinity γ-BB transporter activity described by Christiansen and Bremer [11], however, this low affinity transporter is not likely to contribute to γ-BB transport *in vivo* since the K_m is very high when compared to the plasma γ-BB concentration. The interplay of different transporters is likely to influence carnitine homeostasis during different physiological situations

In summary, we have shown that SLC6A13 transports γ-BB. Although this transporter was originally described as a GABA transporter, it is likely that in the liver SLC6A13 acts primarily as a γ-BB transporter. The plasma GABA concentration is probably too low to inhibit hepatic γ-BB transport and the function of GABA in the liver remains unclear.
Importantly, hepatic expression of SLC6A13 is increased in OCTN2-/- mice which may well contribute to the enhanced carnitine biosynthesis in these mice and thus supports the role of SLC6A13 as a hepatic γ-BB transporter.

Acknowledgements

The authors thank J. de Vos, H. Overmars, A. Bootsma and A. van Cruchten for technical assistance.

References

[1] F.M. Vaz, R.J. Wanders. Carnitine biosynthesis in mammals, Biochem J 361 (2002) 417-429
[2] C.J. Rebouche, Sites and regulation of carnitine biosynthesis in mammals, Federation Proceedings 41 (1982) 2848-2852
[3] B.J. Zaspel, K.J. Sheridan, L.M. Henderson. Transport and metabolism of carnitine precursors in various organs of the rat, Biochimica et Biophysica Acta 631 (1980) 192-202
[4] A.L. Carter, R. Frenkel. The role of the kidney in the biosynthesis of carnitine in the rat, J Biol Chem 254 (1979) 10670-10674
[5] I. Tein., Carnitine transport: pathophysiology and metabolism of known molecular defects, J Inherit Metab Dis 26 (2003) 147-169
[6] T. Koizumi, H. Nikaido, J. Hayakawa, A. Nonomura, T. Yoneda., infantile disease with microvesicular fatty infiltration of viscera spontaneously occurring in the C3H-H-2(0) strain of mouse with similarities to Reye's syndrome, Lab Anim. 22 (1988) 83-87
[7] M. Horiuchi, K. Kobayashi, S. Yamaguchi, N. Shimizu, T. Koizumi, Nikaido, H, J. Hayakawa, M. Kuwajima, T. Saheki. Primary defect of juvenile visceral steatosis (jvs) mouse with systemic carnitine deficiency is probably in renal carnitine transport system, Biochimica et Biophysica Acta 1226 (1994) 25-30
[8] K. Lu, H. Nishimori, Y. Nakamura, K. Shima, M. Kuwajima. A missense mutation of mouse OCTN2, a sodium-dependent carnitine cotransporter, in the juvenile visceral steatosis mouse, Biochem Biophys Res Commun 252 (1998) 590-594
[9] M. Horiuchi, K. Kobayashi, N. Asaka, T. Saheki. Secondary abnormality of carnitine biosynthesis results from carnitine reabsorptional system defect in juvenile visceral steatosis mice, Biochimica et Biophysica Acta 1362 (1997) 263-268
[10] Y. Higashi, K. Yokogawa, N. Takeuchi, I. Tamai, M. Nomura, N. Hashimoto, J.I. Hayakawa, K.I. Miyamoto, A. Tsuji. Effect of gamma-butyrobetaine on fatty liver in juvenile visceral steatosis mice, J Pharm Pharmacol 53 (2001) 527-533.
[11] R.Z. Christiansen, J. Bremer. Active transport of butyrobetaine and carnitine into isolated liver cells, Biochim Biophys Acta 448 (1976) 562-577.
[12] S. Berardi, B. Stieger, S. Wachter, B. O'Neill, S. Krahenbuhl. Characterization of a sodium-dependent transport system for butyrobetaine into rat liver plasma membrane vesicles, Hepatology 28 (1998) 521-525.
[13] I. Tamai, R. Ohashi, J. Nezu, H. Yabuuchi, A. Oku, M. Shimane, Y. Sai, A. Tsuji. Molecular and functional identification of sodium ion-dependent, high affinity human carnitine transporter OCTN2, J Biol Chem 273 (1998) 20378-20382.
[14] Q.R. Liu, B. Lopez-Corcuera, S. Mandiyan, H. Nelson, N. Nelson. Molecular characterization of four pharmacologically distinct gamma-aminobutyric acid transporters in mouse brain [corrected], J Biol Chem 268 (1993) 2106-2112
[15] A. Gadea, A.M. Lopez-Colome. Glial transporters for glutamate, glycine, and GABA: II. GABA transporters, J Neurosci Res 63 (2001) 461-468

[16] L.A. Borden, K.E. Smith, P.R. Hartig, T.A. Branchek, R.L. Weinshank. Molecular heterogeneity of the gamma-aminobutyric acid (GABA) transport system. Cloning of two novel high affinity GABA transporters from rat brain, J Biol Chem 267 (1992) 21098-21104

[17] F.M. Vaz, B. Melegh, J. Bene, D. Cuebas, D.A. Gage, A. Bootsma, P. Vreken, A.H. van Gennip, L.L. Bieber, R.J. Wanders. Analysis of carnitine biosynthesis metabolites in urine by HPLC- electrospray tandem mass spectrometry, Clin Chem 48 (2002) 826-834.

[18] R.J. Wanders, J.P. Ruiter, F.A. Wijburg. Studies on mitochondrial oxidative phosphorylation in permeabilized human skin fibroblasts: application to mitochondrial encephalomyopathies, Biochim Biophys Acta 1181 (1993) 219-222

[19] F.M. Vaz, H.R. Scholte, J. Ruiter, L.M. Hussaarts-Odijk, R.R. Pereira, S. Schweitzer, J.B. de Klerk, H.R. Waterham, R.J. Wanders. Identification of two novel mutations in OCTN2 of three patients with systemic carnitine deficiency, Hum Genet 105 (1999) 157-161

[20] P.K. Smith, R.I. Krohn, G.T. Hermanson, A.K. Mallia, F.H. Gartner, M.D. Provenzano, E.K. Fujimoto, N.M. Goeke, B.J. Olson, D.C. Klenk. Measurement of protein using bicinchoninic acid, Anal Biochem 150 (1985) 76-85.

[21] N. van Vlies, L. Tian, H. Overmars, A.H. Bootsma, W. Kulik, R.J. Wanders, P.A. Wood, F.M. Vaz. Characterization of carnitine and fatty acid metabolism in the long-chain acyl-CoA dehydrogenase-deficient mouse., Biochem. J. 387 (2005) 185-193

[22] N. van Vlies, R.J. Wanders, F.M. Vaz. Measurement of carnitine biosynthesis enzyme activities by tandem mass spectrometry: differences between the mouse and the rat, Anal Biochem 354 (2006) 132-139

[23] M.M. Sousa, S. Du Yan, R. Fernandes, A. Guimaraes, D. Stern, M.J. Saraiva. Familial amyloid polyneuropathy: receptor for advanced glycation end products-dependent triggering of neuronal inflammatory and apoptotic pathways, J Neurosci 21 (2001) 7576-7586

[24 C. Ramakers, J.M. Ruijter, R.H. Deprez, A.F. Moorman. Assumption-free analysis of quantitative real-time polymerase chain reaction (PCR) data, Neurosci Lett 339 (2003) 62-66

[25] I. Tamai, R. Ohashi, J.I. Nezu, Y. Sai, D. Kobayashi, A. Oku, M. Shimane, A. Tsuji. Molecular and functional characterization of organic cation/carnitine transporter family in mice, J Biol Chem 275 (2000) 40064-40072

[26] A. Melse-Boonstra, P.I. Holm, P.M. Ueland, M. Olthof, R. Clarke, P. Verhoef. Betaine concentration as a determinant of fasting total homocysteine concentrations and the effect of folic acid supplementation on betaine concentrations, Am J Clin Nutr 81 (2005) 1378-1382

[27] H.J. Bremer, M. Duran, J.P. Kamerling, H. Przyrembel, S.K. Wadman. Disturbances of amino acid metabolism: clinical chemistry and diagnosis. Baltimore, MD: Urban & Schwarzenberg; 1981.

Chapter 6

PPARα-activation results in enhanced carnitine biosynthesis and OCTN2-mediated hepatic carnitine accumulation

N. van Vlies, S. Ferdinandusse, R.J.A. Wanders, F.M. Vaz

Abstract

In fasted rodents hepatic carnitine concentration increases considerably which is not observed in PPARα-/- mice, indicating that PPARα is involved in carnitine homeostasis. To investigate the mechanisms underlying the PPARα-dependent hepatic carnitine accumulation we measured carnitine biosynthesis enzyme activities, levels of carnitine biosynthesis intermediates, acyl-carnitines and OCTN2 mRNA levels in tissues of untreated, fasted or Wy14643-treated wild type and PPARα-/- mice. Here we show that both enhancement of carnitine biosynthesis (due to increased γ-butyrobetaine dioxygenase activity), extra-hepatic γ-butyrobetaine synthesis and increased hepatic carnitine import (OCTN2 expression) contributes to the increased hepatic carnitine levels after fasting and that these processes are PPARα-dependent.

Introduction

Peroxisome Proliferator Activated Receptor α (PPARα) is a ligand-dependent transcription factor. Upon ligand binding, PPARα heterodimerizes with the Retinoid X Receptor and binds to specific response elements (PPARα response elements, PPREs) to stimulate expression of target genes. PPARα is expressed in tissues with a high rate of fatty acid oxidation (such as liver, heart, skeletal muscle, kidney and brown adipose tissue) [1] and several aspects of fatty acid metabolism are regulated by PPARα, including the cellular uptake of fatty acids, the activation of fatty acids, peroxisomal and mitochondrial β-oxidation, ketogenesis, ω-oxidation and lipoprotein metabolism [1-6].

Several observations suggest that PPARα is involved in carnitine homeostasis. Carnitine is an essential compound in fatty acid metabolism due to its role in the transfer of long-chain fatty acids into the mitochondrial matrix, where β-oxidation takes place [7, 8]. Carnitine is also used to transport peroxisomal β-oxidation products to the mitochondria, to export accumulating acyl-groups and to modulate the level of free CoA in different subcellular compartments [9, 10].

Carnitine can be absorbed from the diet and synthesized endogenously [10]. OCTN2 is the sodium-dependent carnitine transporter responsible for the dietary absorption of carnitine. This transporter also mediates cellular uptake and renal reabsorption of both carnitine and its precursor, 4-trimethylaminobutyric acid (γ-butyrobetaine, γ-BB) (figure 1) [10, 11]. The first metabolite of the carnitine biosynthesis pathway (figure 1) is 6-N-trimethyllysine (TML), which is generated by lysosomal degradation of proteins containing trimethylated lysine residues (such as calmodulin, histones, actin and myosin). Free TML is hydroxylated by the enzyme TML-dioxygenase (EC 1.14.11.8, TMLD) to 3-hydroxy-6-N-trimethyllysine (HTML). HTML is subsequently converted to 4-trimethylaminobutyraldehyde (TMABA), which is oxidized by TMABA-dehydrogenase (EC 1.2.1.47, TMABA-DH) to γ-BB. Finally, γ-BB is hydroxylated to carnitine by γ-BB dioxygenase (EC 1.14.11.1, γ-BBD), which in mice is only present in liver [12], (figure 1) [10, 13, 14].

In both rat and mouse, treatment with PPARα agonists has been shown to influence liver carnitine metabolism [5, 15]. Upon treatment, hepatic carnitine concentration increased considerably in two independent studies [5, 15]. Based on experiments with clofibrate-fed rats (a synthetic PPARα ligand) Paul *et al*. proposed that the increase was due to an increase in the rate of hepatic carnitine synthesis [15]. More recently, however, we could not demonstrate increased activity of carnitine biosynthesis enzymes in phytol-treated mice (phytanic acid and its precursor phytol, are natural PPARα ligands [16, 17]), despite an obvious increase in hepatic carnitine concentration [5]. When mice or rats are fasted, which also results in PPARα

activation, liver carnitine levels also rise considerably [6, 18]. This is not observed in fasted or PPARα agonist-fed PPARα-/- mice, indicating that this effect is mediated via PPARα [5, 6]. To investigate the role of PPARα in carnitine metabolism and determine what mechanism underlies the hepatic increase of carnitine concentration we used wild type and PPARα-/-mice which were either fed normal chow, chow containing the potent PPARα agonist Wy14643 [1] or were fasted for 48 hours. Our results show that both enhanced carnitine biosynthesis and differential OCTN2 expression contribute to the PPARα-dependent changes in carnitine metabolism.

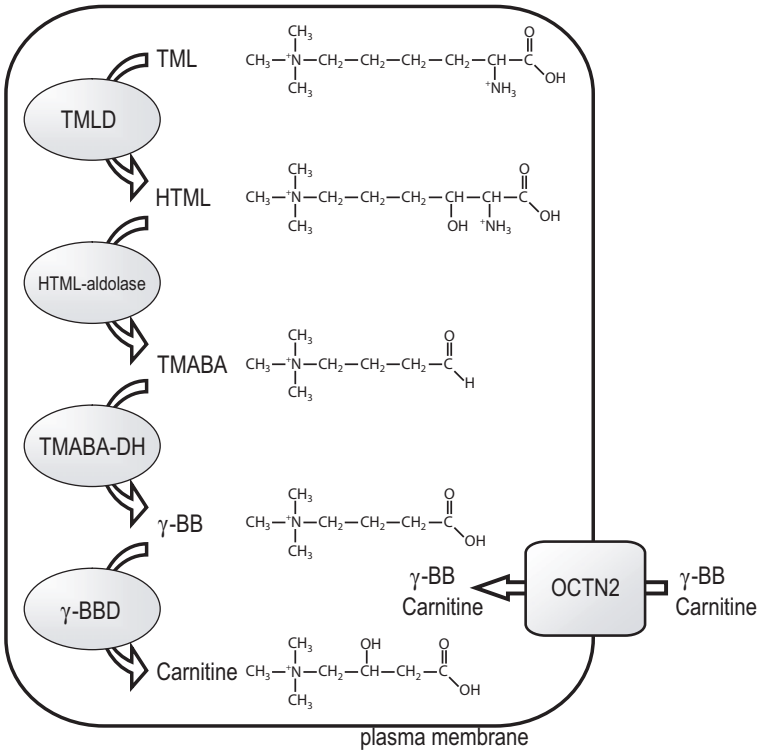

Figure 1. Cellular import and biosynthesis of carnitine: TML (6-N-trimethyllysine) is hydroxylated by TMLD (TML-dioxygenase) to HTML (3-hydroxy-6-N-trimethyllysine), which is converted to TMABA (4-trimethylaminobutyraldehyde) by HTML-aldolase. TMABA-DH (TMABA-dehydrogenase) oxidizes TMABA to γ-BB (4-trimethylaminobutyric acid), which is hydroxylated to carnitine by γ-BBD (γ-BB dioxygenase). OCTN2 imports carnitine and and its precursor, γ-BB [10].

Materials and Methods

Chemicals

RNA*later* reagent was obtained from Qiagen, the Trizol reagent from Invitrogen, The first-strand cDNA synthesis kit and the LightCycler FastStart DNA Master SYBR Green I kit from Roche and Wy14643 was purchased from Tocris Bioscience.

Animals

Control diet was produced by soaking pelleted mouse chow (CRM(pl), Technilab SDS) in ethanol (33 ml ethanol per 100 g pellets) and the pellets were left to dry. For the 0.1% (w/w) Wy14643-diet, 100 g pellets were soaked in 33 ml ethanol containing 3 mg/ml (e.g. 100 mg) Wy14643. Subsequently, the pellets were left to dry.

All mice were obtained from the Jackson Laboratory. Male 129 wild type and PPARα-/- mice were fed normal mouse chow until 9 weeks of age. Next, mice were divided into three groups. The first group (wild type n=5 and PPARα-/- n=5) was fed control food for two weeks. The second group (wild type n=5 and PPARα-/- n=5) received chow supplemented with 0.1% Wy14643 for two weeks. The last group (wild type n=5 and PPARα-/- n=4) was fed control diet for two weeks and subsequently fasted for 48 hours. All mice had free access to water

and were killed at the same time of day. At the end of the experiment, mice were anesthetized with isoflurane and blood was collected by cardiac puncture. Tissues were collected and a small piece was treated with RNA*later* reagent according to the manufacturer's instructions and stored at -80°C until RNA isolation, the rest was immediately frozen in liquid nitrogen and stored at -80°C until further use. All experiments were approved by the local ethical committee.

Carnitine metabolites and biosynthesis enzymes
Levels of carnitine biosynthesis intermediates, acylcarnitines and activities of carnitine biosynthesis enzymes were determined as described previously [12, 19].

Immunoblot analysis
Immunoblot analysis of peroxisomal straight-chain acyl-CoA oxidase was performed as described previously [5].

Quantitative real-time RT-PCR analysis
Total RNA was isolated from RNA*later*-treated tissues using Trizol extraction. cDNA was produced using a first-strand cDNA synthesis kit. For the quantitative real-time PCR the LightCycler FastStart DNA Master SYBR Green I kit was used and the following primers: 5'GTGGGCCGCTCTAGGCACCAA3' and 5'CTCTTTGATGTCACGCACGATTTC3' for β-actin [20] and 5'ACCCCACTGTGGTCAGAAAC3' and 5'CACCAAAGCTCTCAGGGAAG3' for OCTN2. All samples were analyzed in duplicate. To confirm that a single product was formed during PCR, melting curve analysis and agarose gel electroforesis were performed. The data were analyzed using linear regression calculations as described previously [21] and values for OCTN2 were normalized against the values for the housekeeping gene β-actin to adjust for variations in the amount of input RNA.

Statistical analyses
Data are expressed as means ± standard deviation. Statistical significance was evaluated using an unpaired Student's *t*-test. The results were considered significant at $P \leq 0.05$.

Results

The involvement of PPARα in carnitine metabolism has been shown both in experiments with rats [15] and mice [5, 6]. PPARα activation alters tissue carnitine concentration but the underlying mechanism is still unknown. Carnitine homeostasis can be altered either by changes in: 1. biosynthetic activity, 2. transport of carnitine or its precursors (between tissues, intestinal absorption or renal reabsorption) or 3. degree of acylation. To investigate which of these mechanisms are involved in the observed changes in carnitine homeostasis, we used wild type and PPARα-/-mice, which were either fed normal chow, Wy14643-supplemented chow or were fasted for 48 hours. We measured carnitine biosynthesis enzyme activities, levels of carnitine biosynthesis intermediates, acylcarnitines and OCTN2 mRNA levels in selected tissues and compared the data from the different treatment groups.

Activation of PPARα
First, we used immunoblot analysis of peroxisomal straight-chain acyl-CoA oxidase, a known PPARα target, to confirm activation of PPARα and enhanced expression of its target genes by the 0.1% Wy14643 diet and the 48 hour fasting period. Compared to wild type mice on the control diet, straight-chain acyl-CoA oxidase was much more abundant in livers of fasted wild type mice and wild type mice on the Wy14643-diet (figure 2), demonstrating that both

treatment protocols activate PPARα and induce expression of this target gene. As expected, the Wy14643-diet had no effect in PPARα-/- mice. Fasting does appear to increase the quantity of straight-chain acyl-CoA oxidase in PPARα-/- mice, indicating that the abundance of this protein is also regulated in a PPARα-independent manner. This effect has been observed previously [5].

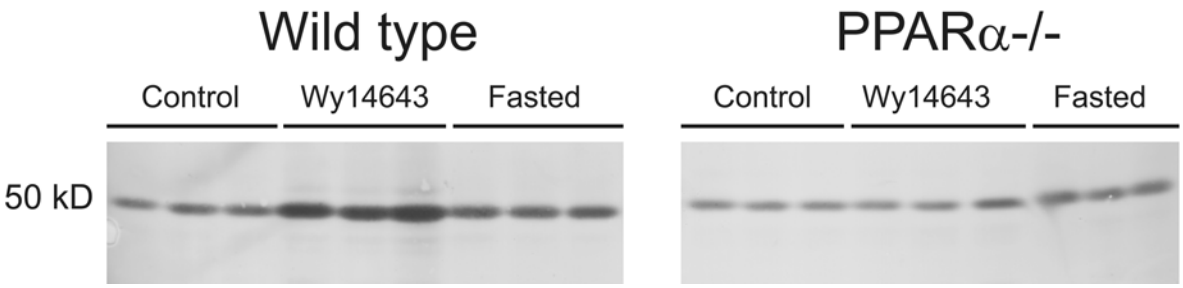

Figure 2. Western blot analysis of peroxisomal straight-chain acyl-CoA oxidase in livers of wild type and PPARα-/- mice on control diet, on Wy14643-diet or fasted for 48 hours.

Wild type mice versus PPARα-/- mice on control diet

Measurement of carnitine levels showed that they differ profoundly between wild type and PPARα-/- mice on the control diet (figure 3). Because the differences in free carnitine levels between the groups were very similar when compared to the differences observed in total carnitine levels, we only show results for free carnitine. This also implies that the degree of acylation is not different, which was confirmed by analysis of the acylcarnitine spectra (results not shown). Compared to wild type mice, PPARα-/- mice had lower plasma carnitine concentration (16 ± 4 μM vs. 30 ± 4 μM) and lower carnitine levels in all investigated tissues (figure 3). Since the carnitine biosynthesis enzyme activities (table 1) and the levels of carnitine biosynthesis intermediates (figure 4) are similar for both groups, the lower carnitine levels in the PPARα-/- group were probably not due to diminished carnitine biosynthesis. The activity of the different enzymes involved in carnitine biosynthesis only was lower in skeletal muscle and kidney of the PPARα-/- mice (table 1). In skeletal muscle, however, the γ-BB production probably is minimal even in wild type mice, given the very low TMLD and TMABA-DH activity in this tissue. TMABA-DH activity is always much higher than the TMLD activity, which suggests that the lower TMABA-DH activity observed in PPARα-/- kidney probably has no effect on γ-BB production in this tissue. This conclusion is supported by the fact that the γ-BB levels in muscle and kidney do not differ significantly between wild type and PPARα-/- mice (figure 4). As shown previously [12], HTML is not detectable in any of the investigated mouse tissues and plasma. Because no differences in carnitine biosynthetic capacity (enzyme activity and metabolite levels) or degree of carnitine acylation were observed, we investigated whether differences in OCTN2 mRNA levels could explain the differences in tissue carnitine levels. In liver and heart, PPARα-/- mice had considerably lower levels of OCTN2 mRNA (5-fold and 3.5-fold, respectively) compared to the wild type mice (figure 5). This could contribute to the lower carnitine levels in these tissues in the PPARα-/- mice. Surprisingly, no significant difference in kidney or skeletal muscle OCTN2 expression was found between wild type and PPARα-/- mice (results not shown).

Wild type mice on control diet versus wild type mice on Wy14643 supplemented diet

When wild type mice are fed Wy14643, the carnitine levels in plasma, liver, kidney, and heart rise significantly when compared to mice fed the control diet (figure 3). Concomitantly, the γ-BB levels decrease in all tissues and plasma compared to the control diet (figure 4). This is

most likely caused by enhanced conversion of γ-BB into carnitine, because there is a highly significant increase in liver γ-BBD activity after the Wy14643-diet (208 ± 19 vs. 141 ± 17 pmol × min^{-1} × mg^{-1}, table 1). The lower γ-BB levels in the Wy14643 group were probably not caused by a decrease in γ-BB synthesis, because TML levels (figure 4) and TMLD activity (table 1) were similar to those of the control group in all tissues except heart, which showed a lower TMLD activity. Tissue TMABA-DH activity was similar in both groups except in kidney, where a higher TMABA-DH was measured after the Wy14643-diet. In our previous experiments, no increase in γ-BBD activity was found upon phytol treatment of wild type mice, despite a clear phytol-dependent increase in hepatic carnitine levels [5]. This difference is most likely due to the fact that phytol-derived metabolites (including phytanic acid) are less potent PPARα ligands than Wy14643 [1].

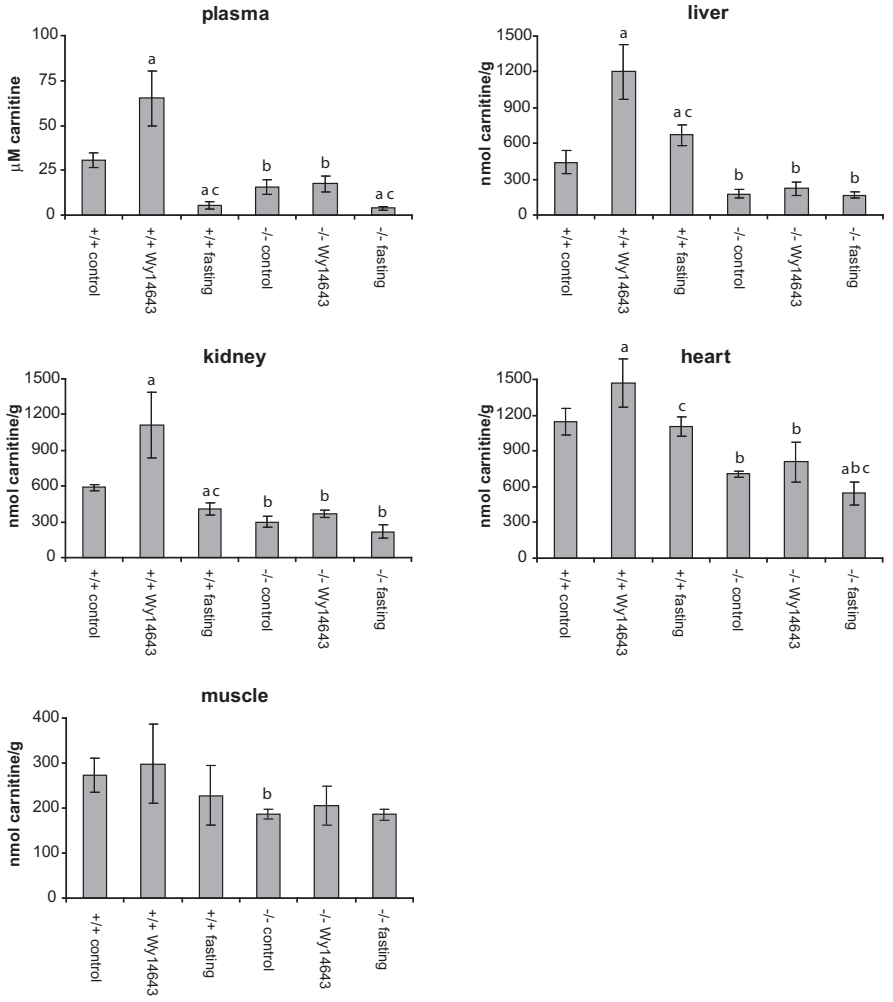

Figure 3. Carnitine levels in plasma and different tissues of wild type (+/+) and PPARα-/- mice (-/-) on control diet, on Wy14643-diet or fasted for 48 hours. Values are means ± standard deviation. [a] indicates a significant difference ($p < 0.05$) between mice with the same genotype on the control diet and another treatment. [b] indicates a significant difference ($p < 0.05$) between mice with a different genotype but the same treatment. [c] indicates a significant difference ($p < 0.05$) between Wy14643-treated mice and fasted mice with the same genotype.

In addition to the increase in hepatic γ-BBD activity, OCTN2 mRNA analysis showed a 6-fold higher expression in liver after Wy14643 treatment (figure 5A). This most likely contributes directly to the increased hepatic carnitine level, but also indirectly given that OCTN2 also transports γ-BB, which (via γ-BBD) also yields carnitine. Surprisingly, OCTN2 expression was unchanged in kidney, heart and skeletal muscle by Wy14643 (results not shown). Unfortunately, neither urine nor intestine was collected, so we can not exclude the possibility that renal carnitine reabsorption or increased intestinal carnitine uptake also contributes to the increased carnitine levels. However, because the kidney OCTN2 mRNA levels (the main transport system for carnitine reabsorption) were unchanged after Wy14643 treatment, it is

unlikely that there is enhanced renal reabsorption of carnitine contributing to the higher tissue carnitine levels.
As expected, none of these effects were observed in PPARα-/- mice on the Wy14643 diet, indicating that the enhanced hepatic γ-BBD activity and increase in OCTN2 mRNA are PPARα-dependent processes.

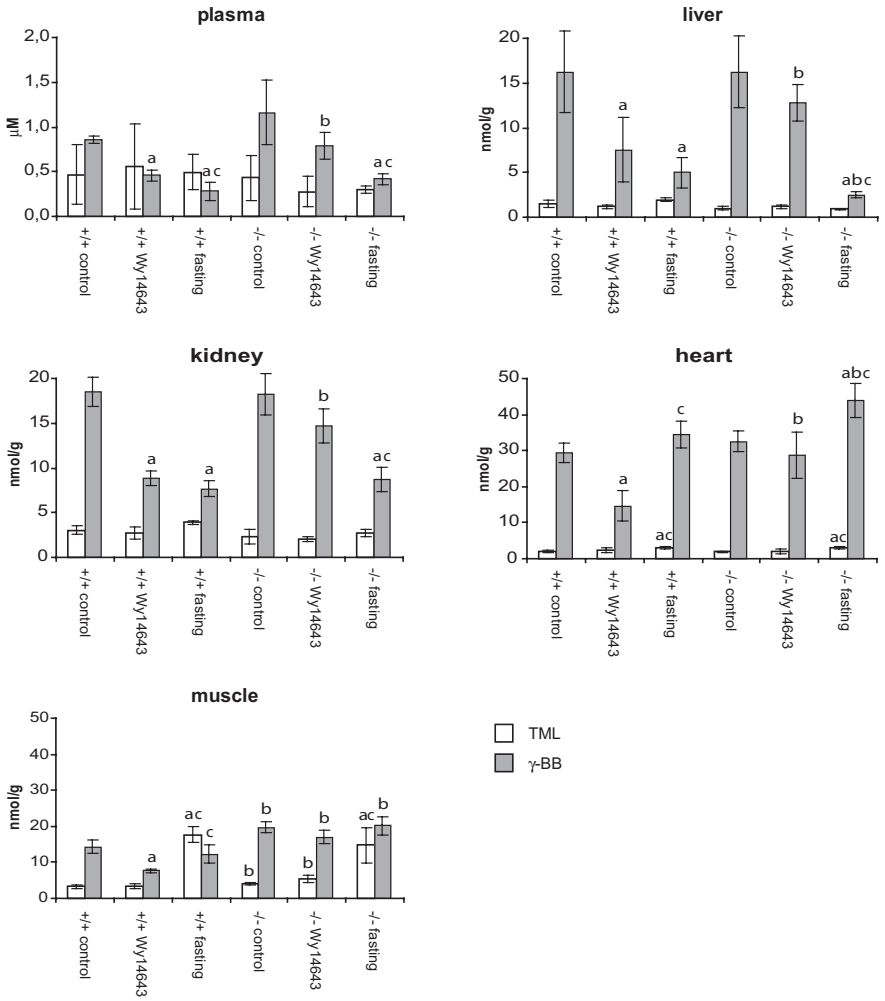

Figure 4. TML (open bars) and γ-BB (filled bars) levels in plasma and different tissues of wild type (+/+) and PPARα-/- (-/-) mice on control diet, on Wy14643-diet or fasted for 48 hours. Values are means ± standard deviation. [a] indicates a significant difference ($p < 0.05$) between mice with the same genotype on the control diet and another treatment. [b] indicates a significant difference ($p < 0.05$) between mice with a different genotype but the same treatment. [c] indicates a significant difference ($p < 0.05$) between Wy14643-treated mice and fasted mice with the same genotype.

Fed versus fasted wild type and PPARα-/- mice

Although Wy14643 supplemented chow strongly activates PPARα, this treatment does not reflect the physiological situation since PPARα normally is activated in the fasted, and not in the fed state. Therefore, we also investigated the effects of fasting on carnitine homeostasis in both wild type and PPARα-/- mice.
In fasted wild type mice, liver carnitine levels were elevated 1.5-fold compared to fed mice (figure 3). This is most likely caused by the increase in liver γ-BBD activity (table 1) and OCTN2 expression (figure 5A). This is supported by the fact that γ-BB levels were decreased in plasma, liver and kidney of fasted mice (figure 4), whereas γ-BB synthesis does not appear to be reduced given the normal plasma, kidney and liver TML levels (figure 4) and TMLD and TMABA-DH activity (table 1)). In brief; γ-BB appears to be taken up by the liver via OCTN2 and converted into carnitine by γ-BBD.
In agreement with previous results [6], fasted PPARα-/- mice did not show an increase in liver carnitine concentration (figure 3). Also, hepatic γ-BBD activity in these mice was similar to that of fed PPARα-/- mice (table 1). Hepatic OCTN2 mRNA levels, however, did increase

upon fasting, when compared to fed PPARα-/- mice (figure 5A). Nevertheless, expression of OCTN2 in the liver of fasting PPARα-/- mice was still lower (~2-fold) than in wild type mice on control diet and therefore probably too low to increase the liver carnitine concentration.
An interesting observation is that the TML levels in heart and skeletal muscle of fasted wild type and PPARα-/- mice were considerably elevated (1.5-fold in heart and 4-fold in skeletal muscle) compared to fed mice (figure 4). TML originates from protein breakdown [13, 22], and for this reason this increase most likely reflects fasting-induced proteolysis. The elevated levels of TML indirectly, via extrahepatic conversion to γ-BB, provide the liver with additional carnitine precursors. In heart, the higher TML levels are accompanied by an increase in γ-BB, but this is not observed in skeletal muscle (figure 4). This could be explained by the very low muscle TMLD activity and the almost complete absence of TMABA-DH activity (table 1).

Table 1. Activity of carnitine biosynthesis enzymes in tissues of wild type and PPARα-/-mice.

		Wild type mice			**PPARα-/- mice**		
		Control diet	Wy14643 diet	fasted	Control diet	Wy14643 diet	fasted
Liver	TMLD	21.7 ± 6.9	19.4 ± 5.3	19.0 ± 3.4	37.4 ± 8.7 [b]	37.7 ± 4.2 [b]	40.0 ± 7.2 [b]
	TMABA-DH	4654 ± 712	5137 ± 981	4015 ± 587	4218 ± 368	4340 ± 608	3259 ± 271 [ac]
	γ-BBD	140.8 ± 17.2	207.7 ± 19.4 [a]	269.1 ± 34.4 [ac]	151.4 ± 21.1	176.8 ± 13.6 [b]	147.6 ± 19.2 [b]
Kidney	TMLD	45.1 ± 6.0	52.2 ± 8.0	43.5 ± 7.2	44.0 ± 6.0	51.2 ± 15.8	52.0 ± 17.7
	TMABA-DH	2241 ± 314	3753 ± 93 [a]	2838 ± 120 [ac]	1632 ± 167 [b]	1732 ± 189 [b]	2109 ± 315 [ab]
Heart	TMLD	30.5 ± 5.5	18.1 ± 6.0 [a]	21.2 ± 4.4 [a]	33.9 ± 3.3	34.9 ± 5.5 [b]	33.0 ± 4.6 [b]
	TMABA-DH	189 ± 87	225 ± 86	166 ± 20	250 ± 70	207 ± 48	156 ± 31 [a]
Muscle	TMLD	3.6 ± 2.1	3.6 ± 1.1	1.8 ± 0.3 [c]	0.6 ± 0.4 [b]	0.9 ± 0.7 [b]	1.4 ± 1.2
	TMABA-DH	102 ± 61	64 ± 13	36 ± 18	ND	ND	ND

All activities are given in pmol × min^{-1} × mg $protein^{-1}$. Values are means ± standard deviation. [a] indicates a significant difference ($p < 0.05$) between mice with the same genotype on the control diet and another treatment. [b] indicates a significant difference ($p < 0.05$) between mice with a different genotype but the same treatment. [c] indicates a significant difference ($p < 0.05$) between Wy14643-treated mice and fasted mice with the same genotype. ND = not detectable.

Wy14643-treated versus fasted wild type and PPARα-/- mice

Although Wy14643-supplemented chow and fasting both stimulate PPARα, these treatments have different effects on carnitine homeostasis. As described above, stimulation of PPARα in fed mice does not reflect the physiological situation and during fasting carnitine metabolism is also influenced by other factors than PPARα. This is apparent in figure 4, which shows considerable differences between Wy14643-treated and fasted mice. For instance, heart and skeletal muscle TML and γ-BB levels are elevated in fasted animals compared to Wy14643 treated mice (figure 4). These differences are PPARα-independent because they are also observed in PPARα-/- mice and likely reflect fasting-induced proteolysis as mentioned above.
In Wy14643-treated wild type mice, plasma, liver, kidney and heart carnitine levels were higher when compared to fasted wild type mice (figure 3). Since there was no significant difference in carnitine acylation (results not shown) or carnitine biosynthesis enzyme activities between these two groups, the difference in free carnitine level is probably due to the difference in length of the treatment. Mice were treated with Wy14643 for 2 weeks but fasted for "only" 48 hours. In both situations carnitine synthesis was enhanced, γ-BBD

activity after fasting was even more increased than after Wy14643-treatment (table 1), but Wy14643-treated mice had more time to accumulate carnitine than fasted mice. We cannot exclude, however, that differences in urinary carnitine excretion contribute to the observed carnitine levels.

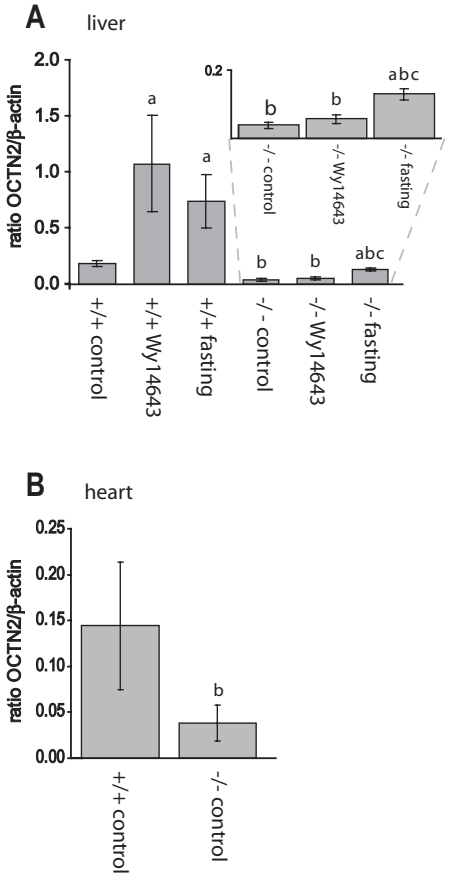

Figure 5. (A) OCTN2 mRNA levels in livers of wild type (+/+) and PPARα-/- (-/-) mice on control diet, on Wy14643-diet or fasted for 48 hours. (B) OCTN2 mRNA levels in hearts of wildtype (+/+) and PPARa-/- (-/-) mice on control diet. Values are means ± standard deviation. [a] indicates a significant difference ($p < 0.05$) between mice with the same genotype on the control diet and another treatment. [b] indicates a significant difference ($p < 0.05$) between mice with a different genotype but the same treatment. [c] indicates a significant difference ($p < 0.05$) between Wy14643-treated mice and fasted mice with the same genotype.

PPARα-dependent changes in TMLD activity

In contrast to liver γ-BBD, which appears to be upregulated in a PPARα-dependent manner, TMLD activity was not altered by Wy14643-treatment, except in heart (table 1). In this tissue TMLD activity was decreased in both fasted and Wy14643-fed wild type mice when compared to the control diet (table1). This was not observed in the PPARα-/- mice, indicating that the reduction in heart TMLD activity is PPARα-dependent. In contrast, liver TMLD activity is not altered by Wy14643-treatment or fasting in both wild type and PPARα-/- mice (table 1). PPARα-/- mice, however, have an almost 2-fold higher basal TMLD activity as compared to wild type mice, indicating that like in heart, TMLD activity is negatively influenced by PPARα. Oddly, the opposite was observed in skeletal muscle, where the TMLD activity in PPARα-/- mice on control or on Wy14643-diet was lower than in wild type mice. Given these discrepancies, it seems that TMLD is not only regulated by PPARα, but also by other factors.

Discussion

Fasting or treatment with PPARα agonists increases the carnitine concentration in liver. The reason for this increase in hepatic carnitine content is still a matter of speculation however, it seems logical to increase the liver carnitine levels during fasting when β-oxidation is

enhanced, since carnitine is an important buffer of acyl-groups and thereby ensures that there is enough free CoA to sustain the high metabolic flux.
We have shown that in fasted and Wy14643-fed wild type mice the elevation of the liver carnitine level is caused by an enhancement of both biosynthesis (primarily by increasing γ-BBD activity) and hepatic carnitine uptake (OCTN2 expression). In PPARα-/- mice, neither the Wy14643-treatment nor fasting induced liver γ-BBD activity. This indicates that γ-BBD activity is regulated by PPARα.
Previously, we did not observe higher γ-BBD activity in phytol treated mice [5], despite a clear elevation of the liver carnitine content. Although we did not measure OCTN2 mRNA levels in these mice, it is very likely that enhanced hepatic carnitine uptake was the cause of the increased liver carnitine concentration after the phytol diet. Because phytol metabolites are much weaker PPARα agonists than Wy14643, a difference in PPARα sensitivity between OCTN2 and γ-BBD might explain the fact that we did not find increased γ-BBD activity in our phytol-treated mice.
In contrast to γ-BBD activity, fasting (but not Wy14643-treatment) did lead to a relatively large increase (3-fold) in liver OCTN2 expression in PPARα-/- mice, although OCTN2 mRNA levels only increased to half of wild type levels on control diet. This indicates that OCTN2 expression is regulated both by a PPARα-dependent and independent mechanism. In fed rats (where levels of endogenous PPARα agonists are low) treatment with glucagon or anti-insulin serum (which mimics the levels of these hormones during fasting) led to an increase in liver carnitine [18]. Although this experiment does not differentiate between elevation of the carnitine concentration by biosynthesis or by hepatic carnitine uptake, these results together with the observed increase in OCTN2 expression in the fasted PPARα-/- mice suggest that liver OCTN2 levels could be influenced by high glucagon or low insulin levels. More studies are needed to investigate whether this relation indeed exists.

During preparation of this manuscript Luci *et al.* reported that OCTN2 expression is increased in the liver of clofibrate-fed rats [23]. The authors did not find an increase in mRNA levels coding for carnitine biosynthesis enzymes after PPARα agonist treatment. Based on this observation and the fact that TML levels in medium of rat hepatoma cells did not decrease upon Wy14643 treatment they concluded that the increase in liver carnitine levels was solely mediated by enhanced OCTN2 expression and not by enhanced carnitine biosynthesis. This is in contrast to our results with Wy14643-fed wild type mice, where an increase in both γ-BBD activity and OCTN2 expression was found, which both contribute to elevated carnitine levels. The fact that we did find an increase in γ-BBD activity could be the result of the difference in treatment periods (2 weeks of Wy14643 treatment vs. 4 days of clofibrate treatment [23]), the difference in species (mice vs. rats) or because clofibrate is a weaker PPARα ligand when compared to Wy14643. Although the studies of Luci *et al.* are well designed, the authors forgot to take into account several aspects of carnitine homeostasis. Firstly, γ-BB is an excellent substrate for OCTN2 [11]. For this reason, upregulation of this transporter also enhances the delivery of carnitine equivalents to the liver and given the very large capacity of the liver to convert γ-BB into carnitine [24], the upregulation of OCTN2 enhances the flux through the carnitine biosynthesis pathway. Secondly, TML is poorly absorbed by the liver [25]. The kidney converts most of the circulatory TML into γ-BB, which is subsequently imported into the liver and converted into carnitine [26]. The fact that TML levels in medium of rat hepatoma cells remain the same after Wy14643 treatment [23] does not disprove that the increase of the carnitine concentration in livers of rodents treated with PPARα agonists is caused by an increased hepatic carnitine synthesis. In general, experiments in cell culture systems are not suited to draw conclusions concerning whole organism metabolism. As

mentioned above, treatment with PPARα agonists in fed animals does not represent the physiological situation of PPARα activation. For instance, muscle TML concentrations are greatly increased after fasting and are likely to contribute to enhanced carnitine biosynthesis. This is in contrast to muscle TML levels in Wy14643 treated animals, which are similar to untreated mice. Additionally, γ-BBD activity is significantly higher in fasted animals when compared to the Wy14643-treated group. These observations stress the importance of investigating PPARα stimulation in its physiological context.

In conclusion, we show that the observed increase in liver carnitine levels upon fasting or PPARα agonist treatment is mediated by a PPARα-dependent increase in hepatic transport of both carnitine and its precursor γ-butyrobetaine, as well as enhanced systemic carnitine biosynthesis.

Acknowledgements

The authors thank J. de Vos and the mass spectrometry section for technical assistance.

References

[1] J. Berger, D.E. Moller. The mechanisms of action of PPARs, Annu. Rev. Med. 53 (2002) 409-435.
[2] T. Aoyama, J.M. Peters, N. Iritani, T. Nakajima, K. Furihata, T. Hashimoto, F.J. Gonzalez. Altered constitutive expression of fatty acid-metabolizing enzymes in mice lacking the peroxisome proliferator-activated receptor alpha (PPARalpha), J. Biol. Chem.273 (1998) 5678-5684.
[3] S. Kersten, J. Seydoux, J.M. Peters, F.J. Gonzalez, B. Desvergne, W. Wahli. Peroxisome proliferator-activated receptor alpha mediates the adaptive response to fasting, J. Clin. Invest. 103 (1999) 1489-1498.
[4] P. Lefebvre, G. Chinetti, J.C. Fruchart, B. Staels. Sorting out the roles of PPAR alpha in energy metabolism and vascular homeostasis, J. Clin. Invest. 116 (2006) 571-580.
[5] J. Gloerich, N. van Vlies, G.A. Jansen, S. Denis, J.P. Ruiter, M.A. van Werkhoven, M. Duran, F.M. Vaz, R.J. Wanders, S. Ferdinandusse. A phytol-enriched diet induces changes in fatty acid metabolism in mice both via PPARalpha-dependent and -independent pathways, J. Lipid Res. 46 (2005) 716-726.
[6] T. Hashimoto, W.S. Cook, C. Qi, A.V. Yeldandi, J.K. Reddy, M.S. Rao. Defect in peroxisome proliferator-activated receptor alpha-inducible fatty acid oxidation determines the severity of hepatic steatosis in response to fasting, J. Biol.Chem .275 (2000) 28918-28928.
[7] J.D. McGarry, N.F. Brown. The mitochondrial carnitine palmitoyltransferase system. From concept to molecular analysis, Eur. J. Biochem. 244 (1997) 1-14.
[8] R.R. Ramsay, R.D. Gandour, F.R. van der Leij. Molecular enzymology of carnitine transfer and transport, Biochim. Biophys. Acta. 1546 (2001) 21-43.
[9] P. Rinaldo. Fatty acid transport and mitochondrial oxidation disorders, Semin. Liver Dis. 21 (2001) 489-500.
[10] F.M. Vaz, R.J. Wanders. Carnitine biosynthesis in mammals, Biochem. J. 361 (2002) 417-429.
[11] I. Tamai, R. Ohashi, J. Nezu, H. Yabuuchi, A. Oku, M. Shimane, Y. Sai, A. Tsuji. Molecular and functional identification of sodium ion-dependent, high affinity human carnitine transporter OCTN2, J. Biol. Chem. 273 (1998) 20378-20382.
[12] N. van Vlies, R.J. Wanders, F.M. Vaz. Measurement of carnitine biosynthesis enzyme activities by tandem mass spectrometry: differences between the mouse and the rat, Anal. Biochem. 354 (2006) 132-139.
[13] J. LaBadie, W.A. Dunn, N.N. Aronson, Jr. Hepatic synthesis of carnitine from protein-bound trimethyl-lysine. Lysosomal digestion of methyl-lysine-labelled asialo-fetuin, Biochem. J. 160 (1976) 85-95.
[14] R.A. Cox, C.L. Hoppel. Biosynthesis of carnitine and 4-N-trimethylaminobutyrate from 6- N-trimethyl-lysine, Biochem. J. 136 (1973) 1083-1090.
[15] H.S. Paul, C.E. Gleditsch, S.A. Adibi. Mechanism of increased hepatic concentration of carnitine by clofibrate, Am. J. Physiol. 251 (1986) E311-315.

[16] P. Ellinghaus, C. Wolfrum, G. Assmann, F. Spener, U. Seedorf. Phytanic acid activates the peroxisome proliferator-activated receptor alpha (PPARalpha) in sterol carrier protein 2-/ sterol carrier protein x-deficient mice, J. Biol. Chem. 274 (1999) 2766-2772.
[17] A.W. Zomer, B. van Der Burg, G.A. Jansen, R.J. Wanders, B.T. Poll-The, P.T. van Der Saag. Pristanic acid and phytanic acid: naturally occurring ligands for the nuclear receptor peroxisome proliferator-activated receptor alpha, J. Lipid Res. 41 (2000) 1801-1807.
[18] J.D. McGarry, C. Robles-Valdes, D.W. Foster. Role of carnitine in hepatic ketogenesis, Proc. Natl. Acad. Sci. U. S. A.72 (1975) 4385-4388.
[19] N. van Vlies, L. Tian, H. Overmars, A.H. Bootsma, W. Kulik, R.J. Wanders, P.A. Wood, F.M. Vaz. Characterization of carnitine and fatty acid metabolism in the long-chain acyl-CoA dehydrogenase-deficient mouse., Biochem. J. 387 (2005) 185-193.
[20] M.M. Sousa, S. Du Yan, R. Fernandes, A. Guimaraes, D. Stern, M.J. Saraiva. Familial amyloid polyneuropathy: receptor for advanced glycation end products-dependent triggering of neuronal inflammatory and apoptotic pathways, J. Neurosci. 21 (2001) 7576-7586.
[21] C. Ramakers, J.M. Ruijter, R.H. Deprez, A.F. Moorman. Assumption-free analysis of quantitative real-time polymerase chain reaction (PCR) data, Neurosci. Lett. 339 (2003) 62-66.
[22] W.A. Dunn, G. Rettura, E. Seifter, S. Englard. Carnitine biosynthesis from gamma-butyrobetaine and from exogenous protein-bound 6-N-trimethyl-L-lysine by the perfused guinea pig liver. Effect of ascorbate deficiency on the in situ activity of gamma-butyrobetaine hydroxylase, J. Biol. Chem. 259 (1984) 10764-10770.
[23] S. Luci, S. Geissler, B. Konig, A. Koch, G.I. Stangl, F. Hirche, K. Eder. PPARalpha agonists up-regulate organic cation transporters in rat liver cells, Biochem. Biophys. Res. Commun. 350 (2006) 704-708.
[24] C.J. Rebouche. Effect of dietary carnitine isomers and gamma-butyrobetaine on L- carnitine biosynthesis and metabolism in the rat, J. Nutr. 113 (1983) 1906-1913..
[25] B.J. Zaspel, K.J. Sheridan, L.M. Henderson. Transport and metabolism of carnitine precursors in various organs of the rat, Biochim. Biophys. Acta 631 (1980) 192-202.
[26] A.L. Carter, R. Frenkel. The role of the kidney in the biosynthesis of carnitine in the rat, J. Biol. Chem. 254 (1979) 10670-10674.

Chapter 7

Submitochondrial localization of 6-N-trimethyllysine dioxygenase; implications for carnitine biosynthesis

N. van Vlies, R. Ofman, R.J.A. Wanders, F.M. Vaz

Abstract

The first enzyme of carnitine biosynthesis is the mitochondrial 6-N-trimethyllysine dioxygenase, which converts 6-N-trimethyllysine into 3-hydroxy-6-N-trimethyllysine. Using progressive membrane solubilization with digitonin and protease protection experiments we show that this enzyme is localized in the mitochondrial matrix. Latency experiments showed that 3-hydroxy-6-N-trimethyllysine formation is limited by 6-N-trimethyllysine transport over the mitochondrial inner membrane. The transport of 6-N-trimethyllysine appears to be tightly coupled to hydroxylation by 6-N-trimethyllysine dioxygenase. Because the subsequent carnitine biosynthesis enzymes are cytosolic, a mitochondrial 6-N-trimethyllysine/3-hydroxy-6-N-trimethyllysine transporter system must exit. This transport system represents an additional step in the carnitine biosynthesis, which could have considerable implication for the regulation of carnitine biosynthesis.

Introduction

Carnitine (3-hydroxy-4-N,N,N-trimethylaminobutyrate) is a vital compound in fatty acid metabolism since it enables the transport of activated long-chain fatty acids and peroxisomal β-oxidation products into the mitochondrial matrix, where β-oxidation takes place [1, 2].
Mammals acquire carnitine both from their diet and through endogenous synthesis [3-5]. Carnitine is ultimately synthesized from the amino acids lysine and methionine. In some proteins (e.g. calmodulin, histones, myosin and actin) lysine residues are trimethylated on the ε-amino group by specific methyltransferases, which use S-adenosyl methionine as methyl donor [6]. After lysosomal degradation of these proteins free 6-N-trimethyllysine (TML) can be used for carnitine biosynthesis: The first step is the hydroxylation of TML to 3-hydroxy-6-N-trimethyllysine (HTML) by the enzyme 6-N-trimethyllysine dioxygenase (EC 1.14.11.8, TMLD). HTML is subsequently converted to 4-trimethylaminobutyraldehyde, which is oxidized to yield 4-trimethylaminobutyric acid (γ-butyrobetaine). Finally 4-trimethylaminobutyric acid is converted to carnitine [3-5].
Hulse *et al*. were the first to show that rat liver mitochondria are able to convert TML into HTML [7]. Further studies revealed that TMLD is a 2-oxoglutarate-depended non-heme ferrous-iron dioxygenase, which requires the presence of ascorbate for activity [7, 8]. Because the other three carnitine biosynthesis enzymes are cytosolic [4], the exact location of TMLD in the mitochondrion could have considerable implications for the biosynthesis of carnitine. If TMLD resides in the inter membrane space or on the outer mitochondrial membrane, which is permeable for small molecules, diffusion would suffice to deliver cytosolic TML to TMLD and return the HTML produced to the cytosol. If TMLD is localized in the mitochondrial matrix, however, a transport system for TML and HTML is required, since these metabolites are not very likely to pass the inner mitochondrial membrane by diffusion. Additionally, such a transport system could be involved in the regulation of carnitine biosynthesis by controlling the concentrations of TML and HTML in the cytosol and mitochondrial matrix [9].
In this article we show that TMLD is localized in the mitochondrial matrix. Furthermore, we provide presumptive evidence in favor of a transport system for TML (and HTML).

Materials and Methods

Chemicals
Digitonin was obtained from Merck, Darmstadt, FRG. TML and proteinase K were purchased from Sigma. St. Louis, USA. All other reagents were of analytical grade. The Microcon 30 filters were obtained from Millipore, Billercia, USA. Nitrocellulose membranes were

purchased from Schleicher & Schuell, Sanford, USA. [$^2H_9$]-TML and [$^2H_6$]-TML were synthesized as described earlier [10]. [$^2H_9$]-HTML was prepared enzymatically by incubating [$^2H_9$]-TML with *Neurospora crassa* TMLD, which was heterologously expressed in *S. cerevisiae* as described by Swiegers *et al*. [11]. The resulting mixture of [$^2H_9$]-HTML and [$^2H_9$]-TML was applied to Microcon YM 30 filters to deproteinize the solution.
The goat-anti-rabbit IgG was from Biorad. The anti-TMLD polyclonal antibody was generated as described previously [9]. The anti-crotonase antibody was generated against crotonase purchased from Sigma Chemical Co. The anti-AcylCoA-synthetase antibody was a kind gift from Dr. T. Hashimoto, Shinshu University, Matsumoto, Japan [12].

Animals
Adult male Wistar rats were anesthetized and sacrificed by decapitation. The kidneys were excised and immediately suspended in ice cold 5 mM MOPS buffer containing 250 mM sucrose and 2 mM EGTA, pH 7.4 (Sucrose-EGTA-MOPS; SEM). All experiments were approved by the local ethical committee.

Preparation of mitochondria
Rat kidneys were homogenized in SEM-buffer with 3 strokes of a teflon pestle in a Potter-Elvehjem glass homogenizer at 500 rpm. The crude homogenate was centrifuged at 800 × *g* for 10 minutes at 4°C to remove nuclei and whole cells. The supernatant was centrifuged at 5,000 × *g* for 10 minutes at 4°C. The mitochondrial pellet was washed twice in SEM and finally resuspended in 5 ml SEM. The mitochondrial protein concentration was determined according to the method of Bradford, using bovine serum albumin as standard [13].

Determination of mitochondrial membrane integrity
As a measure for membrane integrity at the metabolite level, citrate synthase activity was measured in an aliquot of mitochondria using an adapted DTNB-based assay as described previously [14]. Briefly, the reaction was started by adding the mitochondria (80 µg mitochondrial protein/ml, final concentration) to the reaction mixture, which contained 0.1 mM DTNB, 0.2 mM oxaloacetic acid and 0.1 mM acetylCoA, all dissolved in SEM. Subsequently, the increase in A_{412}, due to DTNB-CoASH complex formation, was measured for 3 minutes at room temperature. Next, 0.1% (w/v) Triton-X-100 in SEM was added, to disrupt the mitochondrial membranes and the increase in A_{412} was measured again for 3 minutes. The citrate synthase activity determined after the addition of Triton–X-100 was set at 100%. Only mitochondria which showed ≤ 1% of total citrate synthase activity before the addition of Triton-X-100 were used in the experiments.

Digitonin titration/preparation of mitoplasts
One milligram of mitochondrial protein was incubated in 0.5 ml SEM for 10 minutes on ice with 0, 1, 1.25, 1.5, 1.75, 2, 2.25, 2.5, 2.75, 3, 3.5, 4, 4.5 or 5 mg/ml digitonin (final concentration) followed by centrifugation at 12,000 × *g* for 10 minutes at 4°C. The supernatants were collected and the activity of TMLD and marker enzymes was determined.
Mitochondria which showed the same release of marker enzymes as was seen with 1.25 mg/ml digitonin (65% release of adenylate kinase and only 3% release of citrate synthase (figure 1)) were used as mitoplasts. To remove the digitonin, the mitoplast-pellet was washed three additional times with 1.5 ml of ice-cold SEM. Subsequently, the mitoplasts were used for the protease protection assay, as described below.

TMLD activity and marker enzyme activity
TMLD activity was measured as described previously [15]. The activity of monoamine oxidase, an outer membrane marker, was measured as described by Youdim *et al*. [16]. Adenylate kinase, an intermembrane space marker, was measured as described by Criss *et al*. [17]. Citrate synthase, a mitochondrial matrix marker, was measured as described by Srere [14] The activity of cytochrome *c* oxidase, a marker for the mitochondrial inner membrane, was determined by incubating the samples with 65 μM reduced cytochrome *c* in a 30 mM potassium phosphate buffer, pH 7.4 at 37°C and measuring the decrease in absorbance at 550 nm for ten minutes.

Proteinase K protection assay
Prior to the proteinase protection assay, an aliquot of mitochondria or mitoplasts was incubated with 1% (w/v) Triton-X-100 in SEM on ice for three minutes. Two hundred micrograms protein equivalent of Triton-X-100-treated or untreated mitochondria or mitoplasts were incubated for 15 minutes at 37°C with 0, 0.5, 0.75, 1, 1.25, 1.5, 2 or 2.5 mg/ml (final concentration) proteinase K, dissolved in SEM (final volume of 100 μl). The reaction was stopped by adding 10 μl of a 200 mM Phenylmethyl sulfonyl fluoride (PMSF) solution (in propanol) after which the sample was placed on ice for 20 minutes. Subsequently, 100 μl of SDS-PAGE loading buffer (0.125 M Tris/HCl buffer, containing 4% (w/v) SDS, 20% (w/v) glycerol, 4% (v/v) β-mercaptoethanol, 5‰ (w/v) broomphenol blue and 8 M ureum, pH 6.8) was added. The samples were boiled for 3 minutes after which another 10 μl of PMSF solution was added. The samples were analyzed using SDS-PAGE and subsequent Western blotting with antibodies against TMLD and two marker enzymes.

TMLD activity latency
Prior to the TMLD latency test, the membrane integrity of mitochondria suspended in the reaction mixture (1 mM 2-oxoglutarate, 0.5 mM ammonium iron sulfate and 2 mM TML, all dissolved in SEM) was checked with the citrate synthase assay, as described above. Only mitochondria with at least 98% membrane integrity (i.e. mitochondria that showed ≤ 2% of total citrate synthase activity) were used.
An aliquot of mitochondria was incubated with 1% (w/v) Triton-X-100 in SEM on ice for three minutes for the determination of the maximal TMLD activity. Subsequently, 1 mg mitochondrial protein equivalent of Triton-X-100-treated or untreated mitochondria was incubated with 2 mM TML or with the complete reaction mixture (total volume 250 μl) at 25°C. For the Triton-X-100 treated mitochondria, the TMLD reaction was stopped by addition of 1 mM $ZnCl_2$ (final concentration) and internal standards (360 pmol [$^2H_9$]-TML and 150 pmol [$^2H_9$]-HTML) and samples were placed on ice. At the end of the incubation time the reaction mixtures with untreated mitochondria were centrifuged for 15 seconds at 16,000 × *g* at 4°C. The supernatant was collected, placed on ice and 1 mM $ZnCl_2$ and internal standards were added. The pellet was washed twice with ice-cold SEM, kept on ice and resuspended in 250 μl SEM to which 1 mM $ZnCl_2$ and internal standards were added. Subsequently, all samples were loaded on a Microcon 30 kDa filters and centrifuged at 14,000 × *g* for 20 minutes at 4°C. One hundred microliters of the filtrate was derivatized and the quantities of TML and HTML were analyzed by HPLC-Tandem MS as described previously [10].

Results and Discussion

Previously, TMLD has been shown to be localized in mitochondria [7], whereas the other three enzymes of the carnitine biosynthesis pathway are presumed to be cytosolic (see [4] for

review). The exact sub-mitochondrial localization of TMLD, however, has remained unknown. In order to resolve whether TMLD is localized in the outer or inner mitochondrial membrane or in the mitochondrial matrix, we first performed digitonin-titration experiments, which are based on the notion that the cholesterol content of the outer membrane is higher as compared to that of the inner mitochondrial membrane. In order to determine the sub-mitochondrial localization of TMLD, intact freshly isolated rat kidney mitochondria were incubated in an isotonic medium supplemented with increasing concentrations of digitonin to dissolve the mitochondrial membranes sequentially. After 10 minutes at 4º C, samples were centrifuged, followed by enzyme activity measurements. Figure 1 shows that monoamine oxidase and adenylate kinase, the outer membrane and inter-membrane space markers, were released into the supernatant already at low concentrations of digitonin, whereas higher concentrations of digitonin were required to release citrate synthase into the medium. Release of the inner mitochondrial membrane enzyme cytochrome *c* oxidase required even higher concentration of digitonin. The fact that the release of TMLD coincides with that of citrate synthase, a soluble matrix enzyme, indicates that TMLD is localized in the mitochondrial matrix.

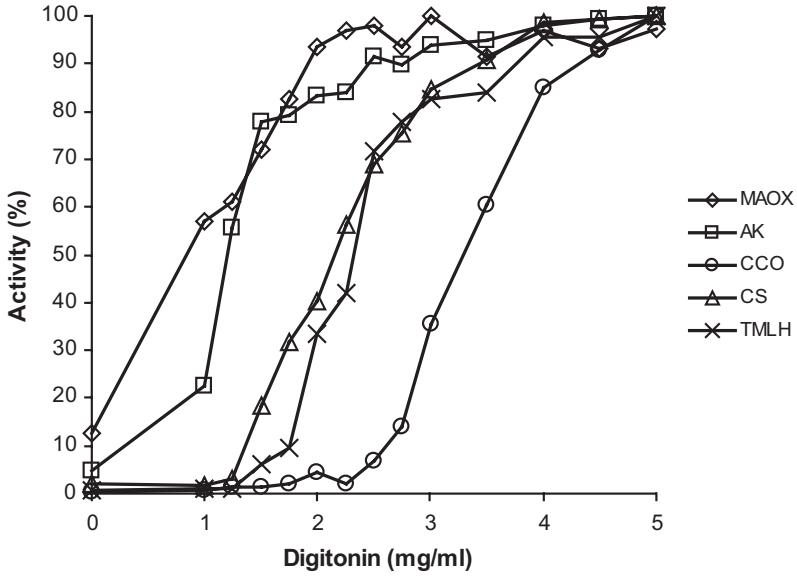

Figure 1. Digitonin titration of rat kidney mitochondria. Maximum activities found in the supernatant fractions were set at 100%. MAOX = monoamine oxidase, outer-membrane. AK = adenylate kinase, inter-membrane space. CS = citrate synthase, matrix. CCO = cytochrome *c* oxidase, inner membrane. TMLD release into the supernatant coincides with the release of the matrix marker, citrate synthase.

Proteinase K protection assay

To confirm the results of the digitonin-experiment, we performed proteinase K protection assays. Proteinase K is a protease, which cannot penetrate the outer and inner mitochondrial membranes, at least under isotonic conditions. In the experiment of figure 2 rat kidney mitochondria were incubated in the standard medium supplemented with proteinase K at increasing concentrations. After 15 minutes at 37ºC PMSF was added to block proteinase K activity, followed by SDS-PAGE and Western blot analysis. The results of figure 2 show that the mitochondrial matrix protein crotonase is resistant to proteinase K treatment unless Triton-X-100 is added which dissolves the mitochondrial membranes. On the other hand the outer mitochondrial membrane enzyme acyl-CoA synthetase was completely degraded already at the lowest concentrations of proteinase K used. Importantly, as for crotonase, TMLD was degraded only when the membranes were dissolved by Triton-X-100, indicating that TMLD is either an inter membrane space protein or a matrix protein To differentiate between these two possibilities digitonin was used to produce mitochondria without an outer membrane (mitoplasts). When proteinase K is added to the mitoplasts remaining outer-membrane and inter-membrane space proteins will be degraded, while matrix proteins will

still be protected by the inner membrane. As expected, crotonase was not degraded when mitoplasts were incubated with the protease unless Triton-X-100 was added to disrupt the inner membrane (figure 2B). Western blot analysis using an anti-TMLD antibody showed the same pattern as for crotonase. These findings support the results of the digitonin titration experiment and indicate that TMLD is located in the mitochondrial matrix.

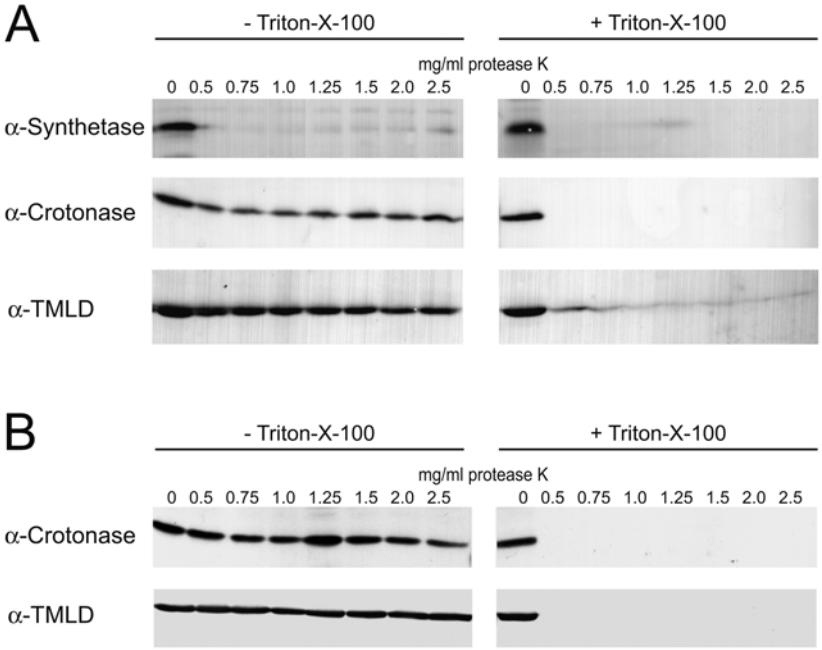

Fig.2. Western blot analysis of mitochondria (A) and mitoplasts (B) with various concentrations proteinase K, in the presence (+) and absence (-) of triton-X-100, probed with anti-TMLD, anti-acyl-CoA-synthase (Synthetase, outer membrane marker) and anti-crotonase (matrix marker) anti-bodies. TMLD shows the same pattern as crotonase, indicating that TMLD is located in the mitochondrial matrix.

Latency of TMLD activity

When enzymes are surrounded by an impermeable membrane, they usually exhibit latency; less enzyme activity is measured in the intact organelle compared to the activity measured after the membrane is disrupted. The enzyme activity is limited by the transfer of substrate/product over the membrane. If TMLD is indeed localized in the mitochondrial matrix, then the rate of HTML formation should display latency. To test this, the membrane integrity of mitochondria suspended in an iso-osmotic reaction mixture (1 mM 2-oxoglutarate, 0.5 mM ammonium iron sulfate and 2 mM TML, all dissolved in SEM) was determined first, since addition of these substances could effect membrane integrity. When mitochondria were incubated in this reaction mixture, membrane integrity was more than 98% at three minutes in the DTNB-citrate synthase assay and this time point was chosen as maximal incubation time.

When mitochondria (either intact or lysed) were incubated with only TML, no HTML formation could be detected (results not shown). The endogenous levels of 2-oxoglutarate and Fe^{2+} most likely are too low to drive HTML formation. We have shown previously that the presence of Triton-X-100 does not influence TMLD activity [15].

When 2-oxoglutarate and Fe^{2+} were added to the reaction mixture, a substantial quantity (approximately 550 pmol/mg protein) of HTML was formed in 3 minutes by lysed mitochondria (figure 3A). In contrast, in intact mitochondria the TMLD activity was only 90 pmol/mg protein which amounts to 16% of the activity of lysed mitochondria (figure 3A). This implies that TMLD activity is indeed limited by TML import and confirms the matrix localization of TMLD, although it can not be excluded that the low apparent TMLD activity in intact mitochondria is due to low intra-mitochondrial levels of $Fe2^{+}$ and/or 2-oxoglutarate.

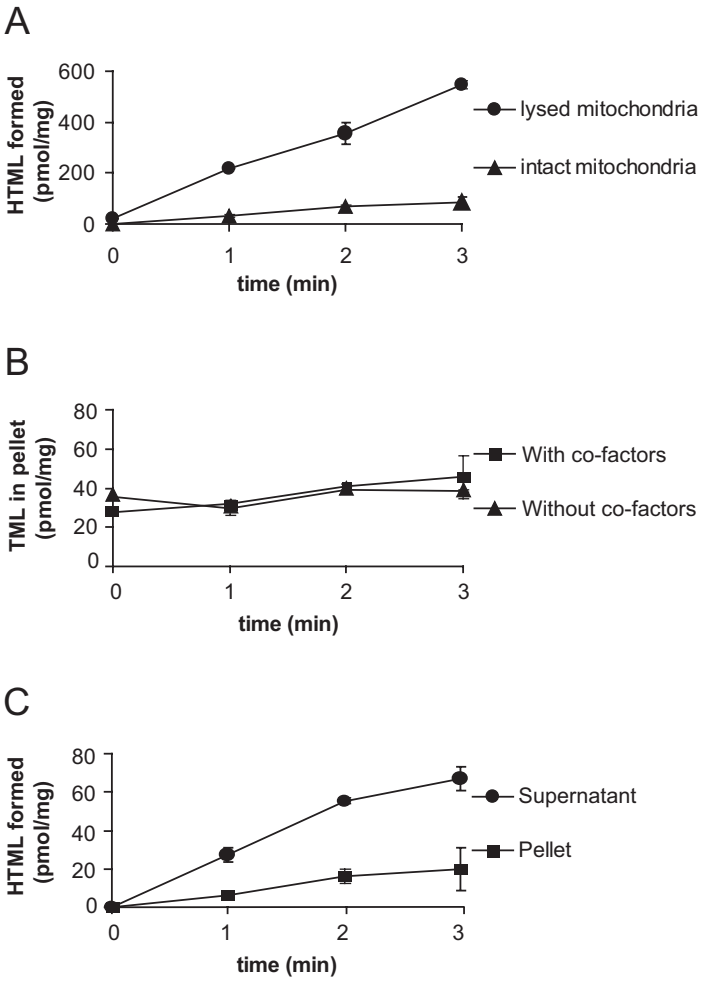

Figure 3. A: HTML formation in intact and lysed mitochondria, incubated with the complete reaction mixture. B: TML import into mitochondria incubated with the complete reaction mixture or with only TML. C: distribution of HTML between the pellet and supernatant fractions of intact mitochondria incubated with the complete reaction mixture. Each time-point is an average ± standard deviation of three incubations.

Transport of TML into mitochondria

Next, we investigated the import of TML into intact mitochondria. To this end, intact freshly isolated mitochondria were incubated in the standard medium and supplemented with increasing concentrations of TML. Subsequently, the samples were centrifuged to separate the mitochondria (pellet fraction) from the reaction mixture (supernatant fraction), the pellet was washed twice and the amount of TML in this fraction was determined. No time-dependent TML import was observed when mitochondria were incubated with only TML. At both t=0 and t=3 minutes approximately 35 pmol TML was found in the pellet fraction (figure 3B). To investigate if these 35 pmol TML represent endogenous TML or TML from the reaction mixture, we repeated the experiment using [$^2H_6$]-TML. In this experiment also approximately 35 pmol [$^2H_6$]-TML was found in the pellet fraction at both t=0 and t=3 minutes (results not shown). Therefore, this most likely represents aspecific binding to the mitochondria and not endogenous TML.

Transport of TML into mitochondria in the presence of TMLD cofactors

Mitochondria incubated with TML only did not import TML. In the presence of all TMLD cofactors, however, HTML was produced in intact mitochondria (figure 3A). Because we have shown that TMLD is a mitochondrial matrix enzyme, TML must first be imported before it can be converted to HTML. No time-dependent TML accumulation was observed in the pellet fraction (figure 3B) suggesting efficient intra-mitochondrial conversion into HTML. These results suggest that TML import is coupled to HTML formation by TMLD. HTML did accumulate in a time-dependent manner in the pellet fraction and this effect was even more

pronounced in the supernatant fraction (figure 3C). This suggests that, after TML is converted into HTML, it is efficiently exported from the mitochondria either by a distinct transporter or possibly by a dedicated TML/HTML antiporter (figure 4). Unfortunately, we could not test whether HTML was imported into mitochondria or whether HTML-loaded mitochondria exported HTML in exchange for TML since the chemical purity of (not commercially available) HTML did not allow experiments with intact mitochondria.

Concluding remarks

Because TMLD is localized in the mitochondrial matrix a transport system for TML (and HTML) must exist. This transport system represents an additional step in the carnitine biosynthesis (figure 4) and the activity of this transporter very likely influences the flux through this pathway. Several experiments have demonstrated that the capacity of the carnitine biosynthesis enzymes to generate carnitine greatly exceeds the daily carnitine production [18, 19]. Experiments where exogenous carnitine precursors (TML, γ-butyrobetaine) were administered to rats also showed that the availability of the precursors appeared to be the only rate-limiting factor for carnitine synthesis [20, 21]. Therefore, Rebouche proposed that the availability of TML, and not the activity of the carnitine biosynthesis enzymes, is rate-limiting for carnitine biosynthesis [19]. Our results have shown that the formation of HTML in intact mitochondria was limited by the transport of TML over the mitochondrial inner-membrane. This suggests that not just the availability of TML, but also the intra-mitochondrial TML availability and therefore the activity of the TML transport system is rate-limiting for the biosynthesis of carnitine. The specific properties of the TML (and HTML) transport system could be investigated using mitochondrial membrane protein-containing proteoliposomes. This is currently under investigation.

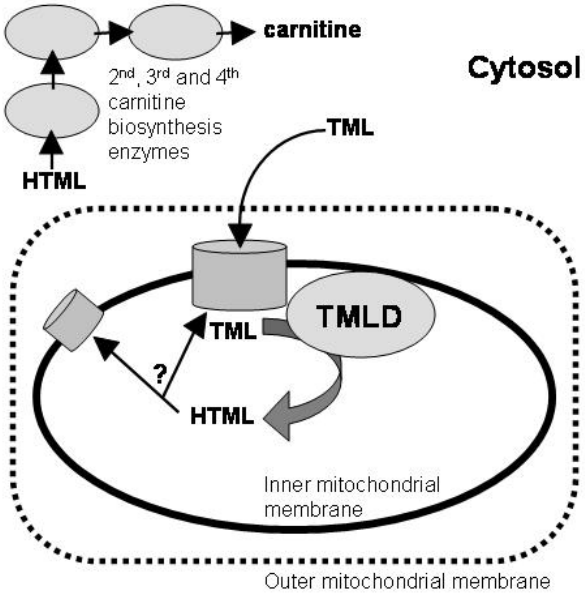

Figure 4. Carnitine biosynthesis. Free 6-N-trimethyllysine (TML), released upon lysosomal degradation of proteins containing trimethylated lysine residues, must first be transported into the mitochondrial matrix where 6-N-trimethyllysine dioxygenase (TMLD) is localized. Next, TML is hydroxylated by TMLD to 3-hydroxy-6-N-trimethyllysine (HTML). Subsequently, HTML must be transported back to the cytosol where it is converted into carnitine via three consecutive enzyme reactions. TML and HTML could be handled either by distinct transporters or possibly by an antiporter.

Acknowledgements

The authors thank J.P. Ruiter and the mass spectrometry section for technical assistance.

References

[1] J.D. McGarry, N.F. Brown. The mitochondrial carnitine palmitoyltransferase system. From concept to molecular analysis, Eur. J. Biochem, 244 (1997) 1-14.
[2] R.R. Ramsay, R.D. Gandour, F.R. van der Leij. Molecular enzymology of carnitine transfer and transport, Biochim. Biophys. Acta 1546 (2001) 21-43.
[3] J. LaBadie, W.A. Dunn, N.N. Aronson, Jr. Hepatic synthesis of carnitine from protein-bound trimethyl-lysine, Lysosomal digestion of methyl-lysine-labelled asialo-fetuin, Biochem. J. 160 (1976) 85-95.
[4] F.M. Vaz, R.J. Wanders. Carnitine biosynthesis in mammals, Biochem. J. 361 (2002) 417-429.
[5] R.A. Cox, C.L. Hoppel. Biosynthesis of carnitine and 4-N-trimethylaminobutyrate from 6- N-trimethyl-lysine, Biochem. J. 136 (1973) 1083-1090.
[6] W.K. Paik, S. Kim. Protein methylation, Science 174 (1971) 114-119.
[7] J.D. Hulse, S.R. Ellis, L.M. Henderson. Carnitine biosynthesis. beta-Hydroxylation of trimethyllysine by an alpha-ketoglutarate-dependent mitochondrial dioxygenase, J. Biol. Chem. 253 (1978) 1654-1659.
[8] D.S. Sachan, C.L. Hoppel. Carnitine biosynthesis. Hydroxylation of N6-trimethyl-lysine to 3-hydroxy-N6-trimethyl-lysine, Biochem. J.188 (1980) 529-534.
[9] F.M. Vaz, R. Ofman, K. Westinga, R.J. Wanders. Molecular and biochemical characterization of rat epsilon-N-trimethyllysine hydroxylase, the first enzyme of carnitine biosynthesis, J. Biol. Chem. 276 (2001) 33512-33517.
[10] F.M. Vaz, B. Melegh, J. Bene, D. Cuebas, D.A. Gage, A. Bootsma, P. Vreken, A.H. van Gennip, L.L. Bieber, R.J. Wanders. Analysis of carnitine biosynthesis metabolites in urine by HPLC- electrospray tandem mass spectrometry, Clin. Chem. 48 (2002) 826-834.
[11] J.H. Swiegers, F.M. Vaz, I.S. Pretorius, R.J. Wanders, F.F. Bauer. Carnitine biosynthesis in Neurospora crassa: identification of a cDNA coding for epsilon-N-trimethyllysine hydroxylase and its functional expression in Saccharomyces cerevisiae, FEMS Microbiol. Lett. 210 (2002) 19-23.
[12] S. Miyazawa, H. Ozasa, S. Furuta, T. Osumi, T. Hashimoto. Purification and properties of carnitine acetyltransferase from rat liver, J. Biochem. (Tokyo) 93 (1983) 439-451.
[13] M.M. Bradford. A rapid and sensitive method for the quantitation of microgram quantities of protein utilizing the principle of protein-dye binding, Anal. Biochem. 72 (1976) 248-254.
[14] P.A. Srere. Citrate Synthase, Methods Enzymol. 13 (1969) 3-11.
[15] N. van Vlies, R.J. Wanders, F.M. Vaz. Measurement of carnitine biosynthesis enzyme activities by tandem mass spectrometry: differences between the mouse and the rat, Anal. Biochem. 354 (2006) 132-139.
[16] M.B. Youdim, M. Tenne. Assay and purification of liver monoamine oxidase, Methods Enzymol. 142 (1987) 617-627.
[17] W.E. Criss, T.K. Pradhan. Purification and characterization of adenylate kinase from rat liver, Methods Enzymol. 51 (1978) 459-467.
[18] A.T. Davis, C.L. Hoppel. Effect of starvation on the disposition of free and peptide-l inked trimethyllysine in the rat, J. Nutr. 116 (1986) 760-767.
[19] C.J. Rebouche, L.J. Lehman, L. Olson. epsilon-N-trimethyllysine availability regulates the rate of carnitine biosynthesis in the growing rat, J. Nutr. 116 (1986) 751-759.
[20] T. Bohmer. Conversion of butyrobetaine to carnitine in the rat in vivo, Biochim. Biophys. Acta 343 (1974) 551-557.
[21] A.L. Carter, R. Frenkel. The role of the kidney in the biosynthesis of carnitine in the rat, J. Biol. Chem. 254 (1979) 10670-10674.

Chapter 8

Discussion

Discussion

In order to study carnitine metabolism, assays to measure carnitine biosynthesis enzyme activities and carnitine metabolites levels are indispensable. Therefore, we developed tandem-MS based assays to measure TMLD, TMABA-DH, γ-BBD and CPTI activity. In addition to enzyme activity assays, a method to simultaneously determine the levels of carnitine biosynthesis intermediates and acyl-carnitines in tissues was developed. These assays were used to investigate carnitine biosynthesis in mouse and rat, the regulation of carnitine homeostasis and carnitine metabolism in two mouse models for human β-oxidation disorders.

Because it was speculated that the cardiomyopathy or cardiac arrhythmia observed in VLCAD-deficient patients results from accumulation of long chain acyl-carnitines and concomitant carnitine deficiency in the heart, we investigated carnitine metabolism in the LCAD-/- mouse. After 7 hours fasting the LCAD-/- mice did not have carnitine deficiency. Also, after 16 hours fasting these mice did not display carnitine deficiency. Plasma and heart carnitine levels in LCAD-/- mice were decreased, but were still approximately 60% of the levels found in wild type mice (unpublished results). Acyl-carnitine levels in hearts of LCAD-/- mice, which were fasted for 7 hours, were only mildly elevated. The cardiac acetyl-carnitine level, however, was severely decreased, which most likely was due to an acetyl-CoA deficiency. Therefore, the cardiomyopathy in the LCAD-/- mouse is caused primarily by a severe energy deficiency in the heart and not by carnitine deficiency or accumulating long-chain acyl-carnitines.
In contrast to VLCAD deficiency, which indirectly influences carnitine metabolism, OCTN2 deficiency directly affects carnitine homeostasis and, compared to other human β-oxidation disorders, has the most drastic effect on carnitine homeostasis. OCTN2-deficient patients and mice demonstrate profound carnitine deficiency [1]. OCTN2-deficient patients and mice are treated with high-dose oral carnitine therapy, which ameliorates their symptoms but does not restore their plasma and tissue carnitine content to normal levels [1]. Experiments where OCTN2-/- mice were given γ-BB instead of carnitine have demonstrated that endogenously synthesised carnitine (from exogenously administered γ-BB) is used more efficiently than exogenously administered carnitine [2]. Also, experiments using rats [3, 4], perfused rat liver [5], hepatocytes [6] or liver plasma membrane vesicles [7], have demonstrated that γ-BB is very effectively taken up by the liver and that this transport is mediated via specific γ-BB transporters. We have identified a liver γ-BB transporter and showed that the carnitine biosynthesis and the hepatic expression of this transporter is increased in OCTN2-/- mice.
These results substantiate the results of Higashi *et al.* [2] that suggest that endogenous carnitine synthesis is enhanced. This might have implications for the treatment of OCTN2 deficiency. Indeed, orally administered γ-BB therapy might be more effective than carnitine therapy. Before changes in treatment of OCTN2 deficiency can be made, however, the differences in metabolic fate of exogenous carnitine and γ-BB have to be investigated more thoroughly.

Although the studies described here provide new insights in the homeostasis of carnitine, several important questions concerning whole body carnitine metabolism and its precise molecular components remain unanswered.
Firstly, the carnitine biosynthesis pathway is a multi-tissue pathway and both inter-cellular and intra-cellular metabolite transport is necessary for the production of carnitine. Apart from the fact that various tissues are capable of transporting different carnitine metabolites, very little is known about the transporter systems that are involved in carnitine homeostasis, such as the plasma membrane TML import system, which is present in rat and mouse kidney, the

mechanism via which carnitine and its acyl-derivatives are exported from cells and the mitochondrial TML/HTML transporter. These and other transporters could be involved in the regulation of the biosynthesis and homeostasis of carnitine. Their identification and characterization is, therefore, necessary for a complete understanding of this pathway. Furthermore, still only three of the four carnitine biosynthesis enzymes have been purified and their genes identified (for review, [8]). The gene encoding the HTML-aldolase remains to be identified.

Recent studies performed in collaboration with the group of Dr. Distel, Department of Medical Biochemistry, Academic Medical Center, have shown that the yeast *Candida albicans* expresses genes homologous to the genes encoding the human carnitine biosynthesis enzymes. This opens up the possibility to investigate the carnitine biosynthesis pathway in an organism that can be easily manipulated and may provide new ways to identify missing carnitine biosynthesis genes, such as the HTML-aldolase and the mitochondrial TML/HTML transporter.

Secondly, it is still not precisely clear how carnitine homeostasis is regulated. We have shown that the effects of hyperlipidemic drugs were mainly due to an increase in hepatic γ-BBD activity and OCTN2 expression. It is not clear, however, from our results if these effects are directly induced by PPARα or that γ-BB activity and/or OCTN2 expression are stimulated indirectly, via other factors. Also, not only PPARα-agonists, but also several hormones affect carnitine metabolism. For instance, insulin stimulates OCTN2 expression in skeletal muscle [9], but probably has the opposite effect in liver [10]. A decrease in insulin level is accompanied by an increase in hepatic carnitine content [10] and fasted PPARα-/- mice also show a relative increase in OCTN2 expression. Many more regulatory factors, besides PPARα and the insulin/glucagon system, could affect carnitine metabolism under different physiological conditions (feeding, fasting, exercise). Therefore, more studies have to be performed to completely unravel the regulation of carnitine metabolism. Especially studies into the promoter regions of the genes coding for the different enzymes involved in carnitine homeostasis should clarify this subject.

In addition, various aspects of carnitine metabolism appear to be regulated differently between species. The tissue distribution of γ-BBD, for instance, varies significantly between rats, mice, hamsters, rabbits, dogs, cats, humans and monkeys. In rats, mice and guinea pigs γ-BBD is present only in liver, while in the other animals this enzyme is also expressed in kidney [11]. Furthermore, we have demonstrated that the activity of TMLD and TMABADH in various tissues greatly varies between rat and mouse, two closely related rodent species. The inter-tissue relationship of the carnitine biosynthesis pathway probably differs greatly between humans and rodents due to the fact that rodents can reabsorb urinary TML and humans can not [8]. In man TML is probably converted into γ-BB in the tissue of origin, while it was proposed that in rat part of the produced TML is released into the circulation and taken up and metabolized by the kidney [12]. This is supported by our finding that TMLD and TMABA-DH activity in rat muscle, which is the major source TML, are very low. Although mouse kidney can also transport TML, the role of the kidney is much less clear in this animal. Mouse muscle has even less biosynthetic capacity, compared to rat, but kidney TMLD activity is also much lower. Because TML originates from protein turnover, it is very complicated to study the metabolism of endogenously synthesized TML. Studies using rats and mice fed a lysine deficient diet supplemented with labeled lysine for different periods of time may well reveal how different tissues contribute to the production of γ-BB and if there are indeed differences between mouse and rat.

The mechanisms which underlie all the observed inter-species differences in tissue distribution and carnitine biosynthesis enzyme activity are unknown. By studying and comparing the promoter regions of the genes coding for the various components of carnitine

metabolism and/or studying the expression of possible transcript-variants of these genes in different species, the observed differences in carnitine metabolism might be explained.

One of the most intriguing aspect of carnitine homeostasis is the precise role of the carnitine biosynthesis. Possibly the most important mechanism via which plasma carnitine levels are regulated is the rate of renal carnitine reabsorption [1]. Consequently, OCTN2-deficient patients and mice, which have impaired carnitine uptake and renal reabsorption but normal carnitine biosynthesis, are severely carnitine deficient [1]. Although both the extrahepatic γ-BB synthesis, possibly the hepatic γ-BB uptake, and the hepatic γ-BBD activity are increased in OCTN2-/- mice, the biosynthesis pathway can not compensate the urinary loss of carnitine and γ-BB.
There are no patients known with a defect in carnitine biosynthesis. A defect in the biosynthesis of carnitine probably does not lead to carnitine deficiency when dietary carnitine intake is high. In omnivorous humans approximately 75% of total body carnitine originates from dietary sources [8] and an increase in renal carnitine reabsorption might very well compensate for the absence of biosynthetic carnitine. In strict vegetarians, however, the dietary carnitine content is low and 90% of total body carnitine originates from biosynthesis [8]. It is possible that the combination of a defect in carnitine biosynthesis and a vegetarian diet leads to carnitine deficiency.
To test this hypothesis an animal model with a defect in the biosynthesis of carnitine, for instance a γ-BBD knock-out mouse, must be developed. Possibly, when fed enough carnitine, the γ-BBD-/- mouse may well show no distinct phenotype. On a carnitine-free diet, however, this mouse would become carnitine deficient and may well show symptoms similar to those of OCTN2-/- mice.

In conclusion, although the studies described here provide new insights in the homeostasis of carnitine, several questions concerning whole body carnitine metabolism and its precise molecular components remain unanswered. More experiments have to be performed to resolve these issues for a complete understanding of the carnitine biosynthesis pathway and its role in carnitine homeostasis.

References

[1] I. Tein, Carnitine transport: pathophysiology and metabolism of known molecular defects, J Inherit Metab Dis 26 (2003) 147-169

[2] Y. Higashi, K. Yokogawa, N. Takeuchi, I. Tamai, M. Nomura, N. Hashimoto, J.I. Hayakawa, K.I. Miyamoto, A. Tsuji, Effect of gamma-butyrobetaine on fatty liver in juvenile visceral steatosis mice, J Pharm Pharmacol 53 (2001) 527-533.

[3] A.L. Carter, R. Frenkel, The role of the kidney in the biosynthesis of carnitine in the rat, J Biol Chem 254 (1979) 10670-10674

[4] T. Bohmer, Conversion of butyrobetaine to carnitine in the rat in vivo, Biochim Biophys Acta 343 (1974) 551-557.

[5] B.J. Zaspel, K.J. Sheridan, L.M. Henderson, Transport and metabolism of carnitine precursors in various organs of the rat, Biochimica et Biophysica Acta 631 (1980) 192-202

[6] R.Z. Christiansen, J. Bremer, Active transport of butyrobetaine and carnitine into isolated liver cells, Biochim Biophys Acta 448 (1976) 562-577.

[7] S. Berardi, B. Stieger, S. Wachter, B. O'Neill, S. Krahenbuhl, Characterization of a sodium-dependent transport system for butyrobetaine into rat liver plasma membrane vesicles, Hepatology 28 (1998) 521-525.

[8] F.M. Vaz, R.J. Wanders, Carnitine biosynthesis in mammals, Biochem J 361 (2002) 417-429

[9] F.B. Stephens, D. Constantin-Teodosiu, D. Laithwaite, E.J. Simpson, P.L. Greenhaff, Insulin stimulates L-carnitine accumulation in human skeletal muscle, Faseb J 20 (2006) 377-379

[10] J.D. McGarry, C. Robles-Valdes, D.W. Foster, Role of carnitine in hepatic ketogenesis, Proc Natl Acad Sci U S A 72 (1975) 4385-4388.
[11] C.J. Rebouche, Sites and regulation of carnitine biosynthesis in mammals, Federation Proceedings 41 (1982) 2848-2852
[12] C.J. Rebouche, L.J. Lehman, L. Olson, epsilon-N-trimethyllysine availability regulates the rate of carnitine biosynthesis in the growing rat, Journal of Nutrition 116 (1986) 751-759

Chapter 9

Summary

Summary

Carnitine (3-hydroxy-4-N-trimethylaminobutyric acid) is an essential substance in fatty acid metabolism. It enables the transport of activated long-chain fatty acids from the cytosol into the mitochondrial matrix, where β-oxidation takes place, via the subsequent actions of Carnitine Palmitoyl Transferase I (CPTI), the Carnitine/Acyl-Carnitine Transporter and Carnitine Palmitoyl Transferase II (CPTII). Carnitine is also used to transport peroxisomal β-oxidation products to the mitochondria, to excrete accumulating acyl-groups and to modulate the level of free CoA.
Carnitine can be both absorbed from the diet and synthesized endogenously. Dietary carnitine is taken up via the sodium-dependent carnitine transporter OCTN2. This transporter also mediates cellular uptake and renal reabsorption of both carnitine and its precursor, 4-trimethylaminobutyric acid (γ-butyrobetaine, γ-BB). Carnitine biosynthesis starts with 6-N-trimethyllysine (TML), which is generated by lysosomal degradation of proteins containing trimethylated lysine residues. Free TML is hydroxylated by the enzyme TML-dioxygenase (TMLD) to 3-hydroxy-6-N-trimethyllysine (HTML), which is subsequently converted to 4-trimethylaminobutyraldehyde (TMABA). Next, TMABA-dehydrogenase (TMABA-DH) produces γ-BB, which is hydroxylated to carnitine by γ-BB dioxygenase (γ-BBD).

In order to study carnitine metabolism, assays to measure carnitine biosynthesis enzyme activities and carnitine metabolites levels are indispensable. We developed tandem-MS based assays to measure TMLD, TMABA-DH, γ-BBD and CPTI activity. In addition to enzyme activity assays, a method to simultaneously determine the levels of carnitine biosynthesis intermediates and acyl-carnitines in tissues was developed. These assays were used to investigate (1) carnitine biosynthesis in mouse and rat, (2) carnitine metabolism in two mouse models for human β-oxidation disorders and (3) the regulation of carnitine homeostasis.
Considerable differences were found in the activities of the various enzymes involved in carnitine biosynthesis between mouse and rat. Indeed, mouse tissues contain much less TMLD and TMABA-DH activity than rat tissues. In contrast to these enzyme activities, the levels of carnitine biosynthesis intermediates are similar in mouse and rat tissues. Differences in rat and mouse TMLD activity and affinity for TML could possibly lead to the observed tissue levels of carnitine biosynthesis intermediates.
Because it was speculated that the cardiomyopathy or cardiac arrhythmia observed in VLCAD-deficient patients results from accumulation of long chain acyl-carnitines and concomitant carnitine deficiency in the heart, we investigated carnitine metabolism in the LCAD-/- mouse, because, in contrast to the VLCAD-/- mice, LCAD-/- mice display symptoms similar to VLCAD-deficient patients. The LCAD-/- mice did not have carnitine deficiency. Acyl-carnitine levels in hearts of LCAD-/- mice were only mildly elevated. The cardiac acetyl-carnitine level, however, was severely decreased, which most likely was due to an acetyl-CoA deficiency. Therefore, the cardiomyopathy in the LCAD-/- mouse is caused primarily by a severe energy deficiency in the heart and not by carnitine deficiency or accumulating long-chain acyl-carnitines.
OCTN2-deficient patients and mice demonstrate profound carnitine deficiency. OCTN2-deficient patients and mice are treated with high-dose oral carnitine therapy, which ameliorates their symptoms but does not restore their plasma and tissue carnitine content to normal levels. Several experiments have demonstrated that γ-BB is taken up by the liver very effectively, that this transport is mediated via specific γ-BB transporters and that endogenously synthesised carnitine (from exogenously administered γ-BB) is used more efficiently than exogenously administered carnitine. To identify this hepatic γ-BB transporter and investigate its role in the carnitine biosynthesis in the OCTN2-/- mouse, we first selected

transporters, which are (1) expressed in tissues that transport γ-BB and (2) transport compounds similar to γ-BB. By determining their γ-BB transport activity, we identified and characterized SLC6A13 as a γ-BB transporter. Furthermore, we show that the carnitine biosynthesis is increased in OCTN2-/- mice and that SLC6A13 is possibly involved in the enhanced carnitine biosynthesis in these mice.
Little is known about the regulation of carnitine homeostasis. In both rats and mice hepatic carnitine levels increase upon fasting or after activation of Peroxisome Proliferator Activated Receptor α (PPARα), a transcription factor involved in the regulation of energy metabolism. This effect is not observed in PPARα -/- mice, which indicates that it is mediated via PPARα. We have demonstrated that both liver OCTN2 mRNA levels and γ-BBD activity are highly increased by fasting and PPARα-agonist treatment in wild type mice, suggesting that enhanced carnitine import and synthesis contribute to the hepatic carnitine accumulation. These effects were not observed in the PPARα-/- animals suggesting that OCTN2 and γ-BBD are regulated by PPARα.
Apart from studies concerning whole body carnitine metabolism, we have also investigated the submitochondrial localisation of TMLD. We have demonstrated that TMLD is localized in the mitochondrial matrix. Because the other three biosynthesis enzymes reside in the cytosol and TML and HTML are not very likely to pass the inner mitochondrial membrane by diffusion, this result indicates that a mitochondrial TML/HTML transport system must exist. The properties of this transport system might have considerable implications for the flux through the carnitine biosynthesis pathway which is supported by our finding that HTML formation is limited by the transfer of TML over the mitochondrial inner membrane. This transport system, therefore, represents an additional step in the carnitine biosynthesis.

Although the studies described here provide new insights in the homeostasis of carnitine, more experiments have to be performed to gain complete understanding of the carnitine biosynthesis and homeostasis.

Chapter 10

Samenvatting

Samenvatting

Carnitine is een essentieel onderdeel van het vetzuurmetabolisme. Om afgebroken te worden moeten vetzuren naar de matrix van het mitochondrion getransporteerd worden. Lang-keten vetzuren kunnen alleen als carnitine-ester, d.w.z. acyl-carnitine, getransporteerd worden. Eerst wordt een acyl-CoA omgezet tot acyl-carnitine door Carnitine Palmitoyl Transferase I (CPTI), op het mitochondriele buitenmembraan. Daarna wordt de acyl-carnitine over het mitochondriele binnenmembraan getransporteerd door de Carnitine/Acyl-Carnitine Transporter. Vervolgens wordt, in de mitochondriele matrix, de acyl-carnitine omzet in een acyl-CoA door Carnitine Palmitoyl Transferase II, waarna de acyl-CoA kan worden afgebroken in de mitochondriele β-oxidatie. Carnitine wordt ook gebruikt om de verhouding vrij CoA/geacyleerd CoA te veranderen en om stapelende vetzuren te binden zodat deze uitgeschieden kunnen worden in de urine of gal.
Carnitine wordt zowel opgenomen uit de voeding (vlees en zuivelproducten bevatten veel carnitine) als door het lichaam zelf gesynthetiseerd. Carnitine wordt uit de voeding opgenomen via OCTN2, de plasmamembraan carnitine transporter. Opname van carnitine uit de circulatie en renale reabsoptie loopt ook via OCTN2. De eerste metaboliet in de carnitine biosynthese is 6-N-trimethyllysine (TML). TML wordt omgezet in 3-hydroxy-6-N-trimethyllysine (HTML) door TML-dioxygenase (TMLD). HTML wordt vervolgens omgezet in 4-trimethylaminobutyraldehyde (TMABA), waarna TMABA-dehydrogenase (TMABA-DH) TMABA omzet in 4-trimethylaminobutyraat (γ-butyrobetaine, γ-BB). De laatste stap is de omzetting van γ-BB naar carnitine door γ-BB dioxygenase (γ-BBD).
Om de carnitine biosynthese en homeostase te kunnen bestuderen, hebben we methoden ontwikkeld om TMLD, TMABA-DH, γ-BBD en CPTI activiteit en de concentratie van carnitine metabolieten in weefsels te kunnen meten. Deze methoden hebben we gebruikt om de carnitine homeostase te onderzoeken in twee muismodellen voor humane β-oxidatie defecten, te weten OCTN2 deficiëntie en zeer lang-keten acyl-CoA dehydrogenase (VLCAD) deficiëntie.
OCTN2 deficiënte (OCTN2-/-) patiënten en muizen hebben hele lage plasma en weefsel carnitine concentraties en lijden aan cardiomyopathie, hypoketotische hypoglycemie en blijven achter in groei. De behandeling van OCTN2 deficiëntie bestaat uit het dagelijks innemen van grote hoeveelheden carnitine. Dit vermindert de symptomen wel, maar leidt niet tot normale plasma en weefsel carnitine concentraties. Wanneer OCTN2-/- muizen echter γ-BB i.p.v. carnitine werd toegediend, steeg hun weefsel carnitine concentratie méér dan na toediening van carnitine. Dit suggereert dat γ-BB efficiënter wordt gebruikt dan carnitine. Experimenten in o.a. ratten en levercellen hebben aangetoond dat γ-BB goed wordt opgenomen door de lever via een specifieke transporter. Om deze transporter te identificeren hebben we transporters uitgezocht die (1) voorkomen in weefsels die γ-BB transporteren en (2) γ-BB-achtige stoffen transporteren. Door de γ-BB transport activiteit van deze transporters te meten hebben we SLC6A13 geïdentificeerd als γ-BB transporter. Daarnaast hebben we laten zien dat in de OCTN2-/- muis de biosynthese van carnitine verhoogd is en dat de expressie van SLC6A13 in de lever ook hoger is in de OCTN2-/- muis t.o.v. normale muizen. Dit suggereert dat SLC6A13 betrokken is bij de verhoogde omzetting van γ-BB naar carnitine in de OCTN2-/- muis.
Vervolgens hebben we het carnitine metabolisme onderzocht in het muismodel voor humane VLCAD deficiëntie. VLCAD is het eerste enzym in de mitochondriele β-oxidatie van lang-keten vetzuren en wanneer dit enzym defect is kunnen lang-keten vetzuren niet worden afgebroken waardoor ze ophopen in de cel. VLCAD deficiëntie wordt gekenmerkt door cardiomyopathie, hypoketotische hypoglycemie na vasten en plotseling overlijden. Voor ons

onderzoek hebben we de lang-keten acyl-CoA dehydrogenase deficiente (LCAD-/-) muis gebruikt omdat de symptomen van deze muis meer lijken op die van VLCAD deficiënte patiënten dan de symptomen van de VLCAD-/- muis. De carnitine concentratie in het hart van LCAD-/- muizen was normaal en er was slechts een milde stapeling van lang-keten acyl-carnitines. De acetyl-carnitine concentratie in LCAD-/- hart was echter zeer laag. Dit werd waarschijnlijk veroorzaakt door een zeer lage acetyl-CoA concentratie, hetgeen duidt op een aanzienlijk energie tekort. De cardiomyopathie in de LCAD-/- muis wordt dus waarschijnlijk veroorzaakt door energie tekort en niet door carnitine deficiëntie of stapeling van lang-keten acyl-carnitines.
Er is nog weinig bekend over de regulatie van de carnitine homeostase. Carnitine metabolisme wordt beïnvloed door Peroxisome Proliferator Activated Receptor α (PPARα), een transcriptie factor in de energie huishouding. Wanneer ratten en muizen vasten of PPARα-liganden innemen stijgt hun lever carnitine concentratie. Deze reactie blijft achterwege in muizen met een defect in PPARα (PPARα-/-). Dit suggereert dat dit effect tot stand gebracht wordt via PPARα. Wij hebben laten zien dat tijdens vasten de lever carnitine concentratie stijgt door zowel een verhoogde OCTN2 expressie in de lever, waardoor er meer carnitine geïmporteerd wordt, als ook een verhoging van de γ-BBD activiteit, waardoor er meer carnitine geproduceerd wordt. Deze effecten bleven achterwege in de PPARα-/- muizen, hetgeen suggereert dat OCTN2 en γ-BBD gereguleerd worden door PPARα.
Behalve de carnitine homeostase en regulatie hebben we ook de sub-mitochondriale localizatie van TMLD, het eerste enzym in de carnitine biossynthese, onderzocht. We hebben laten zien dat TMLD zich bevindt in de mitochondriale matrix. Omdat de andere biosynthese enzymen zich in het cytosol bevinden en TML en HTML niet zomaar door het mitochondriale binnen-membraan kunnen, moet er een transport systeem voor TML en HTML zijn. Dit transport systeem heeft waarschijnlijk invloed op de flux door de carnitine biosynthese. Dit wordt ondersteunt door het feit dat de snelheid van HTML productie geremd wordt wanneer TML eerst over het binnen membraan getransporteerd moet worden voordat het omgezet kan worden in HTML. Dit transport systeem is dus een extra stap in de carnitine biosynthese.

Het hier beschreven onderzoek verschaft nieuwe kennis over het carnitine metabolisme. Er zal echter nog meer onderzoek gedaan moeten worden om alle aspecten van de carnitine biosynthese en homeostase aan het licht te brengen.

Dankwoord

Pppffffoe! Het is af, na 4,5 jaar eindelijk uitgepromoveerd.
Dit was mij echter niet gelukt zonder de hulp en steun van vele……..

Ronald, natuurlijk wil ik jou bedanken voor jouw bijdrage (adviezen, ideeën, kritiek) aan mijn promotie onderzoek, maar meer nog voor je enthousiasme en vriendelijkheid toen ik kwam praten over een stage bij lab GMZ. Terwijl ik, na mijn eerdere stage, onderzoek niet echt meer zag zitten, wist jij mij binnen 15 minuten van het tegendeel te overtuigen en gedurende mijn hele stage heb je mij laten zien hoe leuk onderzoek kan zijn. Ik hoefde daarom ook niet lang na te denken over mijn AIO-plek bij GMZ. Heel erg bedankt.

Fred, jij bent ook zeker voor een groot deel verantwoordelijk voor mijn bovengenoemde 'herenthousiasmering'. Ik heb erg veel geleerd van jouw (soms wat chaotische) begeleiding. Heel erg bedankt, ik hoop dat je in de toekomst de mogelijkheid vindt om verder te gaan met het carnitine-onderzoek (en dat #@*$!-aldolase te pakken krijgt).

Femke en de MS-mannen, Albert, Arno, Henk van L, Henk O en Wim. Zonder jullie was dit een heel dun boekje geworden. Bedankt voor alle samples die jullie voor mij verwerkt hebben (waren het uiteindelijk meer cabios of meer acyl-carnitines?), hulp bij verschuivende retentie-tijden en het verwijderen van mysterieuze groene smurrie!

Sacha, Pedro en Judith, bedankt voor jullie hulp bij mijn muizen-proeven en DEC-protocollen. Gelukkig was het uiteindelijk niet nodig om Wy-14643-omeletjes te bakken!

Petra en Patricia, bedankt voor jullie geduld en hulp wanneer ik weer eens te laat bedacht had dat ik s'middags 20 grote bakken controle cellen nodig had.

Mirjam, jij bedankt voor al je hulp en het mee-opwerken van al die bakken cellen voor het valideren van het nieuwe CPTI-assay.

Rob en Jos, jullie wil ik heel erg bedanken voor al jullie goede ideeën en hulp bij de TMLH-localizatie en CPTI experimenten en jullie geduld als de COBAS weer eens gemeen tegen mij deed.

De DNA-dames: Janet K., Janet H., Wendy en Maaike, bedankt voor jullie hulp bij al mijn DNA/RNA-vragen.

Mijn (ex-) bench-genoten, Marjolijn bedankt voor het mogen stelen van je spullen en de gezellige gesprekken (zelfs als het af en toe over het P-woord ging).
Jeroen H, volgens mij ben jij de enige in Nederland die behalve alles over politiek ook alles over Paris Hilton weet!
Riekelt, bench- en gourmet-buurman, de andere helft van de 'groep-Vaz', bedankt voor het tolereren van mijn zooi, het stelen van je buffers en het weer aanzetten van de radio! Wordt het nou een huis of toch maar die baby?

Verder wil ik iedereen bedanken die achter de schermen lab GMZ draaiende houdt: Rally, Gerrit-jan, Susan, Margarethe, Jan en Desi.
Maddy, zonder jouw hulp met brieven, formulieren en vooral het opsporen en tackelen van Ronald had het heel wat langer geduurd voordat mijn boekje klaar zou zijn geweest. Heel erg bedankt.

Collega's zijn degenen die maken dat je met plezier naar je werk gaat. Daarom wil ik alle GMZ-ers bedanken voor jullie hulp, goede sfeer in het lab en gezellige praatjes tijdens de lunch, borrels of gewoon in de gang.

Ben, Karin en Guy, gelukkig zijn er ook buiten GMZ nog mensen die geïnteresseerd zijn in de carnitine biosynthese! Bedankt voor de interessante (helaas korte) samenwerking.

Dan alle (ex-) AIOs: Annemieke B., Hidde, Jasper, Linda, Marc, Marit, Robbert-Jan en Saskia, bedankt voor alle gezelligheid op het lab en vooral tijdens de AIO-etentjes. Ook al ben ik nu geen AIO meer, zijn jullie altijd welkom, ook namens de kat, om nog een keer te komen eten. Heel veel succes met jullie onderzoek of nieuwe baan!

Alle F0-115-2 bewoners, bedankt voor het aanhoren van al mijn promotieproblemen en jullie steun en goede raad.
Annemieke en Jolein, het is alweer een tijdje geleden, hopelijk zie ik jullie op mijn promotie en kunnen we lekker bijkletsen!
Lodewijk, de meester van de practical jokes, zonder jou zou er in onze kamer heel wat minder gelachen worden. Ik wacht nog altijd op dat telefoontje van de Young Einsteins!!!
Ference, vaak Lodewijk's 'partner-in-crime', maar tot genoegen van vele ook frequent grap-slachtoffer. Gelukkig heb je het dreigement om een nieuwe voetbal mee te nemen nooit ten uitvoering gebracht. Bedankt voor al je peptalks en gezellige onzin (van wie was ook al weer het geweldige idee om vissen te nemen?).
Roos, voor mij ben jij de personificatie van gezelligheid. Altijd kan je bij jou terecht voor een vrolijk gesprek, waarna het onmogelijk is om in een slecht humeur te blijven. Bedankt voor een luisterend oor en opbeurende woorden.
Carlo, bedankt voor je super enthousiaste (en een beetje chaotische) introductie in de wondere wereld van de vesicles. Het maakte niet uit hoe mysterieus mijn resultaten waren, jij wist er altijd iets positiefs uit te halen. Toch hoop ik dat jouw carnitine biosynthese experimenten meer opleveren dan mijn vesicle proeven!
Wouter, bedankt voor je hulp bij al mijn 'domme-biologen vraagjes', computer problemen, maar vooral voor alle leuke gesprekken over alles van "hyenas" tot "lichtgevende cola". O ja, $E \approx mc^2$.
Merel, bedankt voor de gezelligheid, het mij mee slepen naar lunch en vooral voor het aanbod om te helpen met mijn last-minute proeven! Heel erg lief, maar je moet ook aan je eigen project denken en nog veel belangrijker natuurlijk: niet te veel sporten!
Catia and Paula, obrigada for the gezellige conversations, PDF-help and especially the lessons in Portugese abusive words and questionable cocktails.
Malika, na ons eerste e-mail contact (niet reply all!) had ik niet gedacht dat het zo gezellig en lachen zou worden (ik denk niet dat ik het beeld van 'malika's monkey-ride'ooit nog uit mijn hoofd krijg). Bedankt voor al je steun en onze gesprekken over gezellige of frustrerende dingen. Ik vind het heel fijn dat jij mijn paranimf wil zijn en nu ik geen AIO meer ben, kunnen we onze eigen geheime etentjes gaan houden (dat zal ze leren!).

Beste Robert, bedankt dat ik bij jou foto's kon komen maken . Dankzij jou is de omslag van mijn boekje precies geworden zoals ik het in gedachten had.

Lieve Heleen, Eveline en Roos, bedankt voor het geduldig aanhoren van al mijn promotie-frustraties, jullie steun en goede raad (er gaat vóór 22 mei nog zeker iemand ge-GIGA-t worden!). Als het eigenlijk gelijk staat aan 3 zulke goede vriendinnen, wil iedereen wel "geen vrienden hebben". Alle biertjes die ik de afgelopen jaren niet met jullie heb kunnen drinken omdat ik de volgende dag weer braaf naar het lab moest, gaan we zeker inhalen!

Lieve I-tje, bedankt voor al onze 'ik wacht op de metro'-sessies, dat je zo'n lieve broer bent en natuurlijk dat jij mijn paranimf wilde zijn! Hopelijk word ik in de toekomst een keer jouw pastry-chef (ik beloof dat ik de boter niet op de grond zal laten vallen).

Lieve pap en mam, bedankt voor meer dan ik hier op kan schrijven en jullie onvoorwaardelijk vertrouwen in mijn promotie-capaciteiten (volgens mij zijn er weinig ouders die 3,5 jaar van tevoren al een promotie-kado in huis hebben).

Lieve Wietse, jij heb natuurlijk het meeste promotie-leed over je heen gekregen, met waarschijnlijk als hoogtepunt mijn hysterische pogingen om in de supermarkt Bureau-pedel aan de telefoon te krijgen, en alleen daarvoor verdien je eigenlijk al 'een half kantje'. Je weet dat ik erg slecht ben in 'dank-woorden' en niet het type om een half kantje lang aardig te blijven, daarom: Bedankt voor je steun en vertrouwen (en een schop onder m'n kont wannneer dat nodig was).
Ik ook van jou!

Naomi